POLITECNICO DI MILANO

School of Industrial and Information Engineering

Master Degree in Materials
Engineering and Nanotechnology

sp-Carbon chains by Pulsed Laser Ablation in Liquid: Synthesis and Stability

Supervisor: Prof. Carlo S. Casari

Co-supervisor: Sonia Peggiani

Candidate: Riccardo Alberto Lotti
Matr. 899585

Academic Year: 2018 - 2019

Abstract

In this thesis work, we investigate the possibility to optimize the Pulsed Laser Ablation in Liquid (PLAL) process for the synthesis of polyynes, which are linear carbon atomic chains. To achieve this aim we modified some laser ablation parameters, such as the ablation time, the laser fluence, the volume of the liquid and solvent in the synthesis is performed. In this way, we succeeded in improving the polyynes concentrations. In particular, the best result is achieved when organic solvents are used as liquid medium in which the PLAL process is carried out. In addition, we were able to synthesize both H-capped chains and methyl-polyynes. When acetonitrile is used, we also detected the presence of cyano-polyynes. The other aim of this thesis work is to study the degradation of polyynes and find a way to improve their stability. In order to do this, we performed several stability studies of the carbon chains under different environmental conditions, such as a decrease of the storage temperature, the addition of a surfactant to the polyynes solution and the different solvents in which the carbon chains are dissolved in. Only the addition of the surfactant (trisodium citrate) has no impact on the polyynes stability. Indeed, the decrease in the storage temperature slowed down the degradation rate with respect to the room temperature case. This is the same result achieved using organic solvents, which are able to improve the stability of polyynes with respect to the case of water . When acetonitrile and isopropanol are used, it is possible to detect polyynes signal up to 90 days from the synthesis. A Nd:YAG laser was employed to perform the PLAL synthesis, while to characterize the polyynes solution we used UV-Vis absorption spectroscopy, High Performance Liquid Chromatography (HPLC) and Surface Enhanced Raman Spectroscopy (SERS).

Sommario

Il carbonio esiste in molte forme diverse, come la grafite, il diamante, i nanotubi, i fullereni e il grafene. In tutte queste forme allotropiche, gli atomi di carbonio mostrano o la configurazione di orbitali ibridi sp^3 o quella sp^2. L'ibridizzazione sp non è invece presente in nessun allotropo conosciuto del carbonio. L'esistenza di un solido cristallino con quella particolare forma di ibridizzazione (chiamato carbyne) è ancora in discussione. Nonostante questo, è possibile sintetizzare catene lineari di diametro un atomo (dette Carbon Atomic Wires, CAWs), che possono avere due diverse strutture, a seconda del tipo di legami che esistono fra gli atomi della catena. Se i legami chimici sono sono tutti doppi, la catena che si ottiene è detta cumulene, se invece c'è un'alternanza di legami tripli e singoli, la specie prodotta è detta polyyne. L'ottenimento di una struttura invece dell'altra è legata sia alle distorsioni di Peierls sia al tipo di legame che il gruppo terminale è in grado di realizzare con la catena. L'interesse per questo tipo di materiale è dovuto alle straordinarie proprietà teoriche che lo caratterizzano, sia dal punto di vista meccanico che da quello ottico ed elettronico e che sono addirittura migliori di quelle del grafene. Il più grande limite all'utilizzo di questo materiale in applicazioni industriali è costituito dalla loro instabilità, che si traduce in una degradazione piuttosto rapida. Le cause di questa instabilità risiedono nella sensibilità delle catene all'ossidazione e al cosiddetto crosslinking, a causa del quale, se le catene interagiscono fra loro, gli atomi che le compongono perdono il loro carattere sp. Per via delle straordinarie proprietà delle catene atomiche di carbonio predette teoricamente, sono state sviluppate diverse tecniche per la sintesi di queste catene atomiche di carbonio. Esistono due tipologie di tecniche: quelle chimiche e quelle fisiche. La sintesi chimica è stata la prima ad essere impiegata per la sintesi delle polyynes ma, benchè consenta di conseguire ottimi risultati, come ad esempio la possibilità di ottenere catene stabili, non è scalabile a livello indutriale. Le tecniche fisiche, invece, non presentano questa limitazione. Pertanto nel corso degli anni si è investigata la possibilità di utilizzarle al fine di sintetizzare i

CAWs. In particolare, le due tecniche maggiormente usate sono la SADL (Submerged Arc Discharge), che sfrutta una scarica elettrica per formare un plasma in cui le polyynes si possono formare, e la PLAL (Pulsed Laser Ablation in Liquid), in cui la sintesi delle catene è possibile grazie al plasma generato dall'ablazione laser. La limitazione maggiore di queste tecniche è l'impossibilità (almeno per ora) di ottenere catene stabili. Per questa tesi come tecnica di sintesi si è utilizzata la PLAL.
In questo lavoro si sono indagati due aspetti. Il primo riguarda l'ottimizzazione del processo di ablazione laser per la sintesi di polyynes tramite la variazione di alcuni parametri del processo, come il tempo di ablazione, la fluenza del laser, il volume del solvente e il solvente stesso. Abbiamo dimostrato che è possibile ottenere una maggiore concentrazione di polyynes in soluzione sia riducendo la quantità di solvente utilizzata sia trovando il valore ottimo di fluenza o di tempo di ablazione. Tuttavia, un' eccessiva riduzione del volume o un valore troppo alto di fluenza o di tempo di ablazione hanno come conseguenza un incremento della degradazione delle catene durante il loro processo di sintesi. Maggiori concentrazioni sono state ottenute anche con l'utilizzo di solventi organici, tramite i quali è stato possibile anche ottenere catene con terminazioni diverse in concentrazioni significative. Il secondo aspetto che è stato investigato è la stabilià delle polyynes in diverse condizioni ambientali. Infatti, abbiamo conservato le catene a temperature più basse di quella ambiente, dimostrando che le basse temperature migliorano la stabilità delle catene, rallentando la loro degradazione. Un altro modo per variare la cinetica di degradazione delle polyynes consiste nel modificare il solvente in cui sono disciolte. I risultati dei nostri studi effettuati per indagare questo aspetto mostrano che l'utilizzo di solventi organici, specialmente acetonitrile e isopropanolo, migliora significativamente la stabilità delle catene. Infatti è stato possibile rilevare segnali di catene ancora presenti in soluzioni a 90 giorni dalla loro sintesi.

Introduction

Carbon exists in several different forms, some of which, such as diamond and graphite, are known since ancient times. The other forms of carbon were discovered over the last 30 years, giving a huge impulse to the arising of nanotechnology. In fact, these new forms are actually nanomaterials and they are fullerenes, carbon nanotubes and graphene, which have, respectively, three, two and one confined dimensions. In all the mentioned materials, the carbon atoms display the sp^3 or sp^2 hybrid orbitals configuration. There are no solid forms of carbon based on the sp hybrid orbitals. In fact, the existence of the so called carbyne is still under debate. However, there are compounds that shows only this type of hybridization. Those species are the Carbon Atomic Wires (CAWs), which have a linear geometry, due to the sp hybrid configuration. There are two possible structures: cumulenes, in which the bonds are all double bonds, and polyynes, in which there is an alternation of single and triple bonds. The occurrence of a structure with respect to the other is due to Peierls distortions and to the bonds the terminal groups can form with the carbon chains. The interest for CAWs arises from their extraordinary predicted properties even better than the ones of graphene, both from the mechanical and the electronic point of view. However, the main weakness of this material is its high instability, because it is sensitive to oxidation and crosslinking. Despite this limitation, several techniques were developed over the last decades in order to synthesize CAWs. There are two approaches: the chemical method and the physical ones. The chemical way was the first that was used to produce CAWs, and although it allows to obtain stable chains, the main limitation of this method is the difficulties of its use at industrial scale. Therefore, synthesis by physical methods was investigated as possible tool for CAWs production. There are two techniques that are used for carbon chains synthesis that are the Submerged Arc Discharge in Liquid (SADL) and Pulsed Laser Ablation in Liquid (PLAL). Both these techniques exploit the formation of a plasma to create the conditions in which polyynes can be synthesized. In the case of SADL, the plasma is generated by an electrical

discharge, while in the PLAL case the formation of a plasma is induced by the laser-matter interactions. The main limitation of these physical techniques are the difficulties in obtaining stable chains, that in fact have never been produced up to now.
In this thesis work, we investigated the synthesis of polyynes by PLAL process, trying to optimize it in order to achieve higher concentrations of the chains in solution and, possibly, new terminations. In addition, we studied the effect of different environmental conditions on polyynes stability, trying to find a way to improve it. This work is organised as follows:

- Chapter 1: a brief overview on structure and properties of all carbon allotropes is provided, followed by the discussion of CAWs structure, properties and synthesis methods.
- Chapter 2: presentation of the physics behind the PLAL technique and discussion of the effect of the process parameters. In addition, an overview about the state of art of polyynes synthesis by PLAL is provided.
- Chapter 3: description of the materials used for our experiments and of the experimental procedures followed for the synthesis and the characterization of produced chains.
- Chapter 4: the experimental results are described and discussed. In the first part of the chapter the results of the experiments, related to the change of process parameters, carried out to optimize PLAL m are presented . In the second part, we showed the results regarding the stability studies performed in different environmental conditions.

Contents

List of Figures

List of Tables

Chapter 1

sp-Carbon Atomic Wires

Carbon is one of the most abundant element in the universe and the fourth most abundant in our solar system, after hydrogen, helium and oxygen. On Earth it just represents the 0.2% of the mass of the planet crust, but although this carbon role is prominent in several fields, especially for life. Indeed, over 95% of all known chemical compounds contains carbon, making it the most versatile element [1]. This adaptivity comes from the ability of carbon to make single, double or triple bonds. To understand its peculiar chemical behaviour, we must look at its atomic structure. The carbon electronic configuration is given by the labelling $1s^2 2s^2 2p^2$, indicating that there are only two valence electrons in carbon ground state. But with only two electrons capable to make chemical bonds, there is not the possibility to explain the existance of species like methane, in which the carbon atom is able to form four different bonds. The theoretical frame that explains this apparent paradox is the Linear Combination of Atomic Orbitals (LCAO), which infers that the atomic orbitals of an atom can mix together to give rise to a new set of orbitals, the hybrid ones. According to this mechanism, the possible configurations are sp^3, sp^2 or sp hybrid orbitals, depending on the number of atomic orbitals that takes part in this process. The orbitals that are not involved in the hybridization remains unmodified and can be used to form double or triple bonds. The hybrid orbitals have a two-lobe asymmetric shape, with one lobe bigger than the other one. The shape of the orbitals is such that, when a bond is formed, there is strong overlap between the two orbitals involved, resulting in a strong bond. With the use of LCAO theory it is possible to predict the shape and the geometry of a molecule, as it will be clarified in the next sections [2]. For the moment, consider as examples of sp^3 configuration the methane molecule, for sp^2 ethylene and for sp acetylene. In case of fully carbon solids, orbital hybridization accounts for the so-called allotropy,

which is the ability of an element to exist in different physical phases. In case of carbon, for example, graphite and diamond are different allotropic forms (allotropes) of the same element. In this chapter, the focus is on the description of sp-carbon atomic wires, which are of great interest because of their outstanding predicted properties and potential applications [3, 4]. In order to give a clearer comprehension of this material a brief overview on the other carbon allotropes is provided.

1.1 Graphite

As mentioned in the introduction, due to allotropy, solid carbon exists in several different forms, some of which are known since ancient times. This is the case of graphite, which is the most widespread allotrope of carbon on our planet. In graphite, carbon atoms are in the sp^2 hybrid configuration, which means that the $2s$ and two $2p$ orbitals combine to give form to three hybrid orbitals, the sp^2 ones. In the sp^2 configuration, the resulting bonding geometry is the planar-trigonal one, with a bond angle of 120°. The last unmodified $2p$ orbital is orthogonal to the sp^2 orbitals plane and is used to form double bonds.

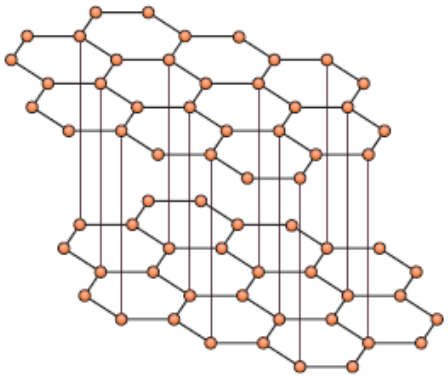

Figure 1.1: The structure of hexagonal graphite [5]

Graphite is a crystalline material, whose unit cell is a hexagonal one (as a result of the sp^2 hybridization) with a base of four atoms, two belonging to the same plane, the other two belonging to the lower and the upper ones. It is a layered material, in which each layer (called graphene) are composed by atoms disposed in a honeycomb array (see Fig.1.1). The stack of these layers can be of two different types, which are, namely, -ABABAB- and -ABCABC- , which corresponds to hexagonal and rhombohedral graphite.

An important aspect to point out is that while within a single layer the atomic bonds are covalent, the force that keeps all the layer together is the Van der Waals force. Therefore, due to this difference in the strength of the bonds, the material properties are anisotropic. An example of this is the electrical conductivity, which is strongly influenced by the direction (along a layer or inter-layer). This difference in the electrical behaviour is easily explained by the fact that the $2p$ orbitals not involved in the hybridization of all atoms of a layer, form a completely delocalized π orbital (while the sp^2 ones form localized σ orbitals). This results in a free motion of electrons along a single layer, while the electrons motion among the plane is more hindered due to the Van der Waals interactions. Looking at the band structure, it is revealed that graphite is a semimetal, which also explains the black colour characteristic of this material. In fact, in a semimetal the band gap is zero, so photons in the visible range are absorbed (noting that the colour is the complementary of what is absorbed). Because of its good electrical conductivity, graphite is used to produce electrodes. Another material property that is influenced by the structural anisotropy is thermal conductivity, which in the inter-layer direction is 200 times smaller than in the in-plane one. This is due to the different amplitude of vibrations in the diverse directions [6]. In addition to this, the presence of grain boundaries, lattice defects and other phonons can further reduce the thermal conductivity. Due to the presence of Van der Waals forces, the mechanical properties also significantly differ according to the different directions considered. In particular, again because of the weak inter-layer bonds, two adjacent layers can slide one on top of the other, which makes graphite a good material for lubricant applications.

1.2 Diamond

Diamond is the other carbon allotrope that has been known for centuries. It has been used only for decorative purposes, despite some of its properties are excellent. These extraordinary characteristics of diamond arises, once again, from the hybridization of the carbon atoms, which determines the geometry of the material. The hybrid form in the diamond case is the sp^3 one, which means that all the four orbitals of the outer shell of the atom combine to form four hybrid orbitals. The resulting geometry is a tetrahedral one, with a bond angle of $109° 28'$ and a FCC unit cell with two atoms per base, as depicted in Fig. 1.2. With respect to the case of graphite, diamond is an electrical insulator, due the lack of the delocalized π orbital.

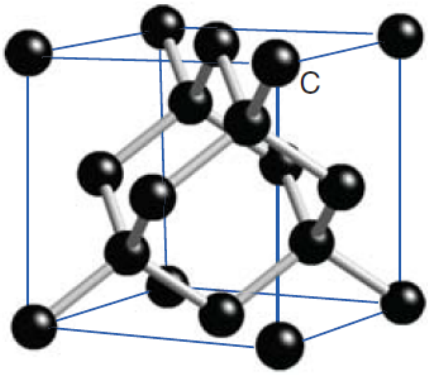

Figure 1.2: Diamond cubic structure [7]

This occurs because all the orbitals are involved in the hybridization mechanism, therefore there are no $2p$ orbitals left to form the delocalized π orbital. As a result, diamond is the widest band gap semiconductor, with a gap of 5.5 eV [1]. This characteristic is also the reason why diamond is transparent, because photons in the visible range cannot be absorbed. However, diamond can be both n and p doped. Considering, instead, the thermal conductivity, diamond is the best thermal conductor. Heat flow in this carbon allotrope is only due to lattice vibrations, so due to phonons flow. Because of the strong chemical bonds that keep carbon atoms together, this flow encounters few obstacles (namely, the atoms vibrations), so it can be very high. Presence of lattice defects, impurities and grain boundaries can reduce the thermal conductivity. Another excellent property that diamond has and that derives from the strength of its bond is its hardness, which has a value of 10 on the Mohs scale [1]. This makes diamond the hardest existing material. An interesting point of diamond is that it is not thermodynamically stable at room temperature and atmospheric pressure, being graphite the stable carbon allotrope in those conditions. So, diamond tends to transform into graphite, but because the process kinetics is very slow, the graphitization process takes a very long time.

1.3 Carbon-based nanomaterials

In the last decades, mainly by impulse of the arising of nanotechnology, new allotropic forms of carbon were discovered. The common feature of these new allotropes is the fact that they have at least one of the three dimensions confined at the nanometer level, so the properties they display are influenced by the consequent quantum confinement. The first to be

detected was fullerene, a molecule whose shape resembles the one of a soccer ball, in 1985 by Kroto, Smalley and Curl, who were awarded with by Noble prize in Chemistry [8]. This was followed by the discovery of carbon nanotubes, made by Iijima in 1991 [9]. Although the discovery of nanotubes is usually conferred to him, two Russian scientists, Radushkevich and Lukyanovich, published a paper in which images of carbon nanotubes are presented [10]. The last carbon allotrope to be discovered and isolated was graphene in 2004 thanks to the work of Geim and Novoselov [11]. Graphene, which is a one-atom thick carbon sheet, was theoretically predicted (and its band structure was calculated) since 1947, as attested by Wallace work [12]. The impact of these discoveries is so strong on material science that someone claimed that this is the "era of carbon allotropes" [13]. The efforts employed to discovery and synthesize these materials are justified by their incredible properties, which make these materials very appealing for several applications.

1.3.1 Graphene

As we have already said, graphite is a stack of several honeycomb layers, which are kept together by Van der Waals interactions. Each of this individual layer, when isolated, is called graphene. As in graphite, the atoms hybridization is the sp^2 one, which results in the planar honeycomb geometry of the graphene sheet. It is a crystalline material, whose unit cell is an hexagonal one with a base of two atoms. Graphene is thinnest ever observed material, having a thickness of just one atom. Due to this characteristic, graphene is considered the model of a 2D material. The very small thickness of graphene results on a strong quantum confinement, which accounts for the its properties. The huge interest that graphene was able to rise in the scientific community was due to its outstanding properties. Among the others, graphene has a very high electric conductivity, that comes from the presence of Dirac's cones in the material band structure (contact points between valence and conduction bands, making graphene a gapless material), and electron mobility [1]. Also its thermal conductivity has a high value, even higher than the diamond one. Moreover, the mechanical properties are very interesting, being, for instance, the Young modulus of $1\,TPa$ and it can sustain a deformation of 20% of its length [1, 14]. These characteristics, combined with the very large specific surface (i.e. $\sim 2630\,cm^2g^{-1}$) makes it really appealing to be used as filler for nanocomposites [14]. Other applications can be the in the electronic, biomedical or energy storage fields. In order to get a semiconductor material, necessary for some electronic applications, one possibility is to

increase the degree of quantum confinement. In this way what is obtained are graphene nanoribbons, that are just strips of graphene sheet. It is also possible, through a chemical way to get graphene oxide, which can be then chemically functionalized. Moreover, graphene properties are the starting point to discuss the properties of all the other carbon nanomaterials, being that carbon nanotubes and fullerenes can be thought, respectively, as wrapped and rolled graphene layer, as can be seen in Fig. 1.3.

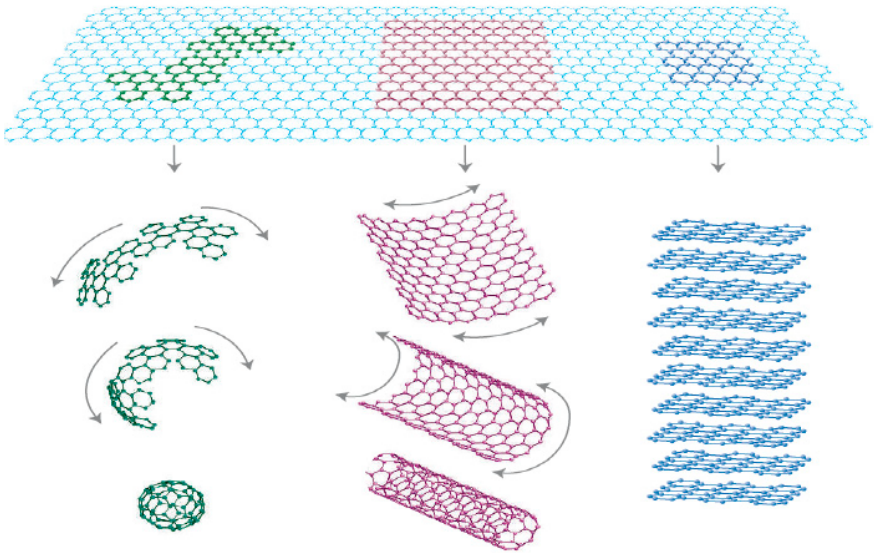

Figure 1.3: Structural deformations of a graphene sheet to obtain, respectively, fullerene, carbon nanotubes and graphite [1]

1.3.2 Carbon Nanotubes (CNTs)

Carbon nanotubes are the prototype of a 1D material, having they two of the three dimensions confined, and can be obtained just rolling a graphene sheet. The hybrid forms of atoms in this allotrope is mainly sp^2, although there is a certain degree of sp^3 hybrid orbitals, that is necessary to have a curved geometry. Nanotubes can be single or multi wall, depending on the number of graphene layer that are rolled up. In the case of multi-walled CNTs, a nanotube is co-axially inserted inside other nanotubes. In the following, just for the sake of simplicity, we will consider only single-walled carbon nanotubes. According to the way the rolling of the graphene layer is made, CNTs are divided in three structural classes: armchair, zig-zag and chiral, that are represented in Fig. 1.4.

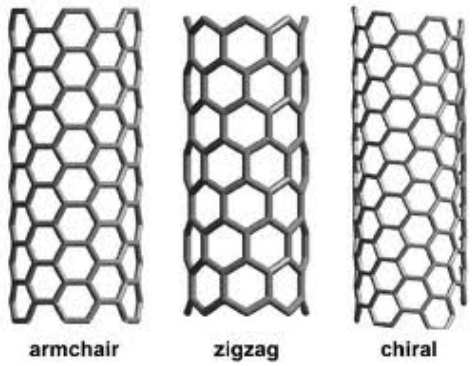

Figure 1.4: The possible CNTs geometries [15]

Obviously, the properties of the CNTs, especially the electronic one, are strictly correlated to the type of tube. An example is given by the electrical conductivity. In fact, if the nanotube is an armchair one it has a metallic behaviour, due to the presence in its band structure of the Dirac's cones. For those tubes, the electrical conductivity can be up to five times the one of copper [16].In the case in which, instead, it is a zig-zag tube only some of them are metallic, while the other are semiconductors [17]. Therefore, it comes out that the electrical properties of the CNTs can be finely tuned changing the tube geometry. Other properties relevant for applications are: the thermal conductivity (which is higher than the diamond one) and the mechanical one, especially the large specific surface and the elastic modulus (although these are smaller than the ones of graphene). Therefore, CNTs are a valid options for several applications, from electronics and optoelectronics to nanocomposites. Moreover, as in case of graphene, CNTs surface can be chemically functionalized to provide new properties to the material.

1.3.3 Fullerenes

Fullerenes were the first of the carbon nanostructure be synthesized and their discovery is a milestone in material science. They are a 0D system, because all their dimensions are confined and can be thought, in analogy for what we have said regarding carbon nanotubes, as a wrapped graphene sheet. In this allotrope, the main type of hybrid orbital is the sp^2 one, but due to the distortions needed to close the cage starting from a graphene sheet, a certain degree of sp^3 atoms are needed. Fullerenes are a large

family of cages, that can be made of different number of carbon atoms. The most stable fullerene geometry is C_{60}, which is a cage made by 60 atoms disposed in twenty hexagons and twelve pentagons. Pentagons represent the most distorted regions of fullerene. The structure of this allotrope is a truncated icosahedron (it is also called "*buckyball*"). Other common fullerenic systems other than C_{60} are made by 72, 76, 84, 100 carbon atoms. Some of the fullerene isomers are presented in Fig. 1.5. The smallest fullerene observed is C_{20}, which is composed by 12 pentagons. It is possible to entrap inside the fullerene cage a guest atom/compound, obtaining a so called endohedral fullerene. Another family of fullerenic compounds are the heterofullerene in which a carbon atom is substituted by an atom of a different element. These are two possible ways to modify the fullerene properties. Another method is the surface functionalization, through which we get the so called hexahedral fullerenes. Through surface functionalization, it is possible to improve some properties such as fullerene solubility, electrical conductivity and to make fullerene suitable for specific biomedical applications. Functionalized fullerenes have an application in organic solar cell where they can be used as electron donor material [13].

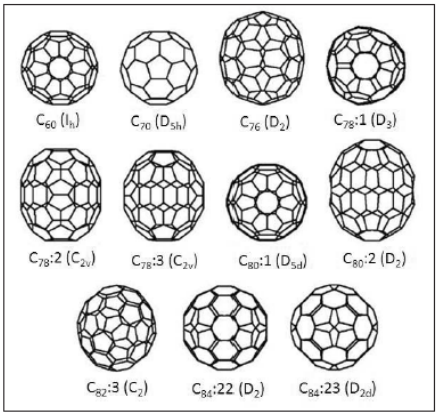

Figure 1.5: Some of the principal isomers of fullerene [18]

1.4 sp-Carbon atomic wires (CAWs)

In the previous paragraphs, we have presented a brief general overview about carbon allotropic forms. In all the materials that were discussed, carbon atoms are in the sp^2, sp^3 hybridization or a mix of the two, but there is not an allotrope of carbon in which the atoms are in the *sp* hybrid configuration, although materials in which *sp* hybridization is present exist

(e.g. acetylene). In the last decades, the interest for this "lacking" carbon allotrope increased due to all the research regarding the other carbon based nanomaterials, as well as astronomical observations (sp-carbon atomic wires are present in the atmosphere of some satellites and in the interstellar dust) [19]. With the name carbyne is intended an ideal infinite carbon atomic chain, which really is a 1D material, being a one-diameter thick wire, while the term bulk carbyne indicates the crystalline solid formed by *sp* carbon atoms. However, its existance is still under debate, due to the high instability characterizing this material. Considering the carbon chains, and not the crystalline solid, the first research about acetylenic compounds dates back to the end of 19^{th} century, as witnessed by the work of Bayer that was published in 1885. In 1963 a group of soviet scientists published a paper regarding the chemical synthesis of CAWs [20]. Several studies were published in the last years regarding the chemical production of CAWs. More recently, the attention of scientists drifted from chemical to physical methods, which are suitable for a industrial-scale prodution. All these efforts spent in trying to produce the "lacking allotrope" is mainly due to the incredibly properties CAWs are believed to have according to theoretical calculations.

1.4.1 Structure

CAWs have a linear geometry (bond angle 180°), which can be readily explained by the hybidization of the carbon atoms. In *sp* configuration, the $2s$ and one $2p$ orbitals combine to produce the two hybrid sp^2 orbitals, while the other two $2p$ orbitals not involved in the hybridization mechanism are available to form a triple bond or two double bonds. So, there are two possible isomers, that are represented in Fig. 1.6: polyynes, in which there is the alternation of single and triple bonds, and cumulenes, in which the bonds are all double. In polyynes, the triple bond is longer than it is expected, while the single is shorter. This peculiarity arises from the so called π-conjugation, which is due to the overlap between p orbitals. The main effect is the delocalization of π electrons, which makes conjugated materials good electrical conductors. Because of this orbital overlap, the system tends to have all equal double bonds. However, this is true just for an ideal chain, while in reality the equilibrium structure is the polyynic one, as clearly showed by Fig. 1.7. There are two reasons that can explain this: the first one is the onset of the so called Peierls distortions, which however is reasonable only for sufficiently long chains (more than 52 atoms connected); the second one is the role of terminations, that, especially in short chains, can induce a cumulenic or a polyynic geometry according to

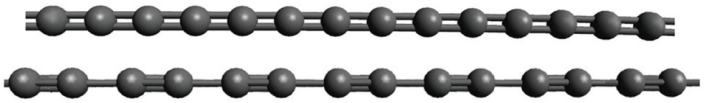

Figure 1.6: The two isomers of CAWs: cumulene (top) and polyyne (bottom) [21]

the type of bond the end-group is able to form with the carbon atoms of the chain [21]. If the capping groups can sustain a double bond, then the chain will be a cumulene, while if they can form a single or a triple bond the resulting chain will be a polyyne. A useful parameter that can discriminate between cumulenes and polyynes is the Bond Length Alternation (BLA), which is given by the difference between two adjacent bonds. Therefore, for cumulenes BLA=0 while for polyynes the BLA is not 0, and the value it assumes depends on the degree of conjugation, which influences the bond length.

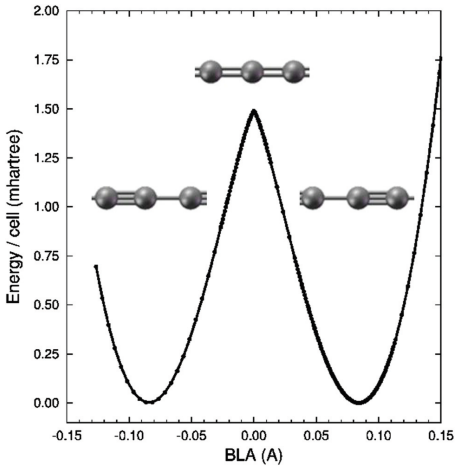

Figure 1.7: Potential energy surface of an isolated infinite CAW as function of the BLA [21]

As mentioned, the chain terminations have an important role in determining the structure of the CAWs. In the case of polyynes, the most common termination is the H atoms, but in literature are reported as terminations also N atoms, the methyl, the cyano and the phenyl groups [22, 23]. The possibility to change the chain structure (and therefore its properties) just changing the end-groups is an appealing feature for possible applications. In some papers, polyynes structures other than the linear one are reported. For instance, Tykwinski and co-workers showed the possibility to produce cyclic polyynes through chemical synthesis [24].

1.4.2 Properties

The predicted properties of carbon atomic wires are really outstanding. For instance, the theoretical mechanical properties are even better than the graphene ones. The Young modulus is estimated to be $32\,TPa$ [25] which makes CAWs the strongest material ever observed and makes them very interesting for mechanical applications (taking also into account the low mass of the material). Combining the elastic modulus with the incredibly high specific surface, carbon atomic wires are excellent candidates as filler for nanocomposites. As discussed in the previous paragraph, the CAWs are π-conjugated materials and the degree of conjugation (effectiveness of the π electrons delocalization) is a crucial parameter for the electronic properties of the chains. When the conjugation is maximum, which corresponds to case of cumulenes, the conduction band is half filled. This is the reason why cumulenes have a metallic behaviour. In the case of polyynes, instead, the valence band is completely occupied and the conduction band is fully empty, with a energy gap between the two. Therefore, polyynes are semiconductors [21]. The parameter that drives the metallic-semiconductive transition is the BLA.

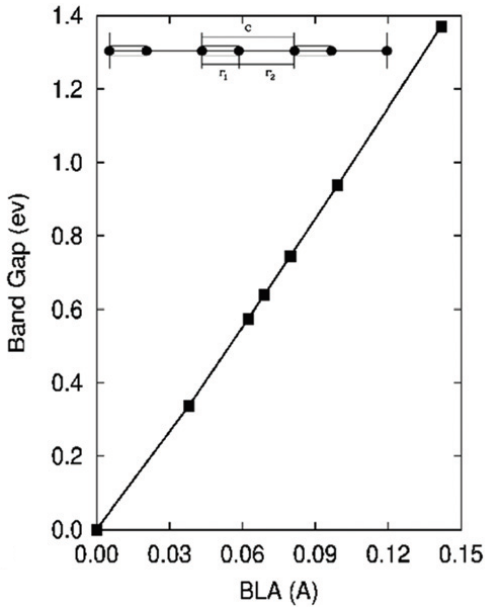

Figure 1.8: CAWs band gap as a function of BLA [21]

To a higher value of the BLA corresponds a higher value of the band gap, as showed by Fig. 1.8. On the other extremity, in the case of cumuelenes (BLA=0) the band gap is 0. A consequence of the dependence of the band

gap from the BLA is that BLA also influences the optical properties of the material, because a change in the band gap means a change in the photon energy that can be absorbed. Considering that the geometry of the chain is modified also by the terminations, we can engineer the electronic and optical properties of CAWs in a quite simple way. The thermal conductivity is another property in which CAWs excels, having a thermal conductivity value which is an order of magnitude higher than the graphene one. This incredibly high value is believed to be due to high phonons frequency and large mean free path, that leads to a ballistic heat transport along the chain [25].

1.4.3 Stability

The main aspect that limits the use of CAWs in commercial devices is their stability. In fact, they are very reactive and unstable systems. In addition, they are sensitive to a big variety of factors. The two main reasons for which polyynes degrade are oxidation and crosslinking. The oxidation-induced degradation is due to the interaction of polyynes with oxidizing agents, such as oxygen and ozone [26, 27], while the crosslinking degradation mechanism is activated by fact that polyynes can interact among themselves, thus leading to the loss of the *sp* hybrid form [25]. The products formed after a crosslinking reaction, in fact, are typically in the sp^2 hybridization. Due to this form of degradation, concentrated solutions of polyynes are not stable, and it is also this the reason why the solid form of this material is so hard to obtain. It is claimed that dilute solutions ($< 10^{-4}\ M$) of polyynes are stable for relatively long period of time [27]. Another mechanism of degradation is the polyynes hydrogenation, in which polyynes atoms lose their *sp* character, forming new bonds with H atoms. This process is initiated by a chemical reduction [28]. Other agents that can activate or accelerate the degradation process are light, acids, bases and, obviously, an increase in temperature [26, 27, 29, 30]. The main strategy adopted to enhance the CAWs stability is to try to cap the polyynes with appropriate terminations, such as for example phenyl groups. The insertion of a stabilizing termination is quite easy using a chemical synthesis method, while is way more challenging if a physical method is used. Another way is to embed the chains inside a solid matrix that can protect them. For instance, polyynes were embedded inside a PVA film, and their SERS polyynes signal was detectable up to 6 months [31]. In another case, the matrix chosen was made by a SiO_2 gel and this sample showed the SERS signal of polyyne up to 14 weeks [32]. Another remarkable work was done by Shi et al. who inserted a CAW inside a double-wall CNT, which was

needed to protect the chain from the environment. In this way, it was possible to obtain a chain made by more than 6000 carbon atoms [33]. However in that case, stability over time was not investigate.

1.4.4 Characterization methods

In this section, we will discuss the main characterization methods used to investigate CAWs, and in particular polyynes. The most commonly used techniques to characterize carbon wires are UV-Vis spectroscopy, Raman based techniques and High Performance Liquid Chromatography (HPLC). In the next paragraphs, a short presentation of each technique is given followed by the discussion of typical signals of polyynes, which are of interest for this thesis work.

UV-Vis spectroscopy

UV-Vis spectroscopy is a widely used technique which is based on the Bohr-Einstein relationship that correlates the difference in energy between two discrete atomic or molecular energy states with the frequency of the electromagnetic radiation. The other important law that gives the physical bases to this characterization method is the Lambert-Beer one, which establishes a linear relationship between the absorbed light (A, which is dimensionless) and the concentration of the absorbing species (c, in mol cm^{-3}) present in solution through the molar extinction coefficient (ε, in $cm^2\, mol^{-1}$) and the pathlength of the sample (d, in cm) (see 1.1). Note that the Lambert-Beer law is valid only for dilute solutions and for an incident radiation in the UV, visible and IR regions, which are the frequency ranges in which electronic transitions in molecules occur. Another intereresting aspect to take in consideration is the fact that the molar extinction coefficient is not only peculiar of each system, but it depends also on the solvent in which the compound is dissolved.

$$A = \varepsilon c d \tag{1.1}$$

From an UV-Vis absorption measure we obtain an absorption spectrum in which are depicted some peaks. These peaks indicates that the wavelength at which they occur is able to excite an electronic transition characteristic of the molecule. Therefore, from the peaks positions, we can get information regarding the structure of the molecule. Another information we can gain from the spectrum is the concentration of the species present in solution. This information is related to the peak height. In the case of polyynes, the absorption spectrum is quite peculiar, as shown in the Fig. 1.9. In

fact, it is characterized by three main peaks, in which the most intense is the one at longer wavelength, and by a series of secondary peaks at longer wavelengths.

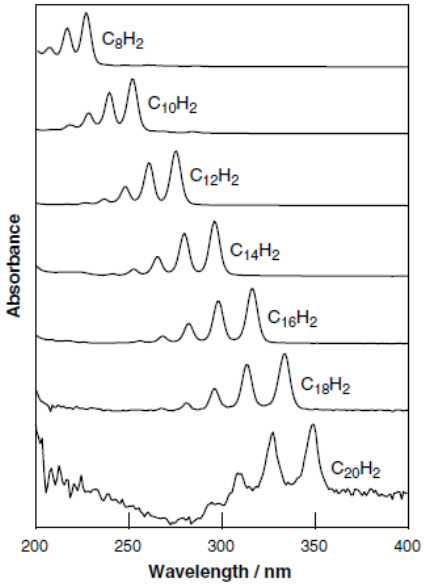

Figure 1.9: UV-Vis absorption spectrum of polyynes [31]

Another peculiar characteristic is that the longer the chain, the more red-shifted are the absorption peaks. This feature, that enables us to distinguish polyynes with different lengths, comes from π conjugation. The more a molecule is conjugated, the lower is its HOMO-LUMO gap, which however cannot reach zero because of the Peierls distortions. Longer polyynes show a higher conjugation with respect to the shorter ones because there is a high number of $2p$ orbitals that can contribute to the π molecular orbital. Therefore, the longer the polyyne the smaller is the HOMO-LUMO gap and thus the more red-shifted are the absorption peaks. In addition, is possible to distinguish polyynes with the same length but with terminations different from the H atom one, due to the fact that the absorption peaks are shifted (as in the case of the methyl-capped polyynes) or have a slightly different shape (as for instance in the case of the cyano-capped polyynes [23]). If the analysis is performed on a solution containing polyynes with different length and terminations, the peaks displayed in the spectrum are the main of the most concentrated species.

Raman based techniques

A very useful characterization technique, especially for carbon based materials, is Raman spectroscopy, which is based on inelastic scattering of light. Due to interaction with light, the molecules of the sample are excited to a virtual state and then they relax to a vibrational state different from the original one. Relaxation process can occur because of the emission of a photon that will have a different energy with respect to the energy of the incident photon. If the emitted photon has a lower energy, the process is called Stokes, if it is higher the process is called anti-Stokes. The anti-Stokes mechanism requires a initial energy level higher than the final one, meaning that the molecule at the beginning must be in a vibrational excited state. Therefore it is less probable than the Stokes process. The energy difference between the incident and the emitted photons is related to the vibrational energy of the molecule in the final vibrational state. It is important to note that, because of the nature of the process, the Raman signal is a sort of fingerprint of the molecule (each functional gruop has its own characteristic frequencies). In addition, with Raman spectroscopy only the vibrational transitions with at least one non-zero component of the transition polarizability tensor are detectable.

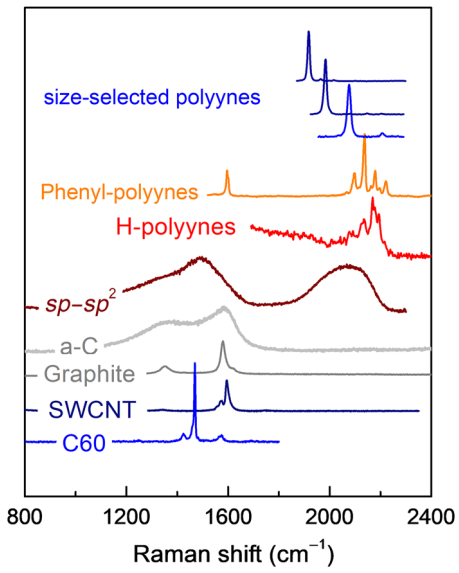

Figure 1.10: Raman spectra of different C allotropes [25]

As previously mentioned, the Raman spectroscopy is quite useful for carbon based materials, because this technique is very sensitive to the different carbon allotropes, as can be seen by Fig. 1.10. For instance, the Raman

peak of diamond is at 1332 cm^{-1} while the characteristic one of graphite is at 1580 cm^{-1} (the so called G peak). With this technique we are also able to distinguish monolayer graphene from multi-layer graphene. In the case of polyynes, the stretching of a carbon-carbon triple bond falls in the 1800-2200 cm^{-1} region, where there is no signal coming from other carbon allotropes. The Raman spectrum of polyynes shows a first and more intense peak at higher frequencies (called α peak) and another less intense peak at lower frequencies (the β peak) (see Fig. 1.11a).

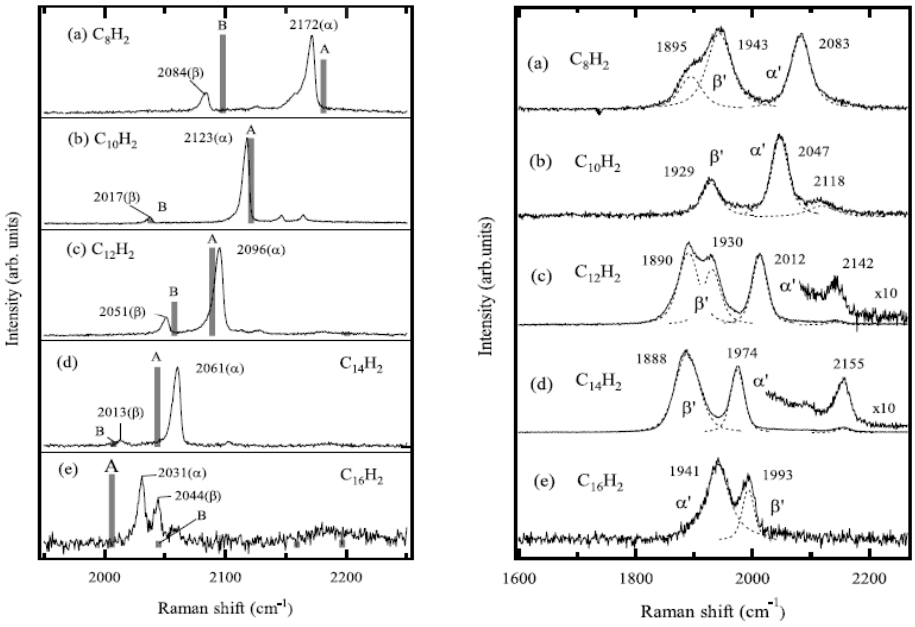

Figure 1.11: The Raman (a) and SERS spectra of polyynes with different length [35]. The bar named A and B represents the simulated Raman peaks

With a Raman measure it is possible, also, to distinguish the polyynes according to their length, knowing that shorter chains have their peaks at higher frequencies. However, when the species to analyse are in too low concentration ($< 10^{-3}\,M$), there is no possibility to detect those species by Raman spectroscopy. Therefore, there is the need for the Surface Enhanced Raman Spectroscopy (SERS), in which we utilize metallic nanoparticles (or metallic substrates) to improve the Raman signal. The enhancement is due to the generation of a localized surface plasmon on the metal nanoparticle (where the plasmon is a collective excitation of the electrons). There are two mechanisms that contribute to the enhancement, the electromagnetic effect

and the chemical one. The first arises from the localization of light on the metal surface, it is considered a long-ranged interaction and is independent on the molecule to analyse, while the latter comes from the molecule-metal interaction and it has a short range. The major contribution to the enhancement of the signal is due to the electromagnetic effect and the signal improvement can be up to a factor of $\sim 10^6$ [34]. The main disadvantages consist in the peaks shift to lower frequencies and the formation of new peaks, both due to the interactions with the metal nanoparticles. These effects can both be seen comparing the graphs in Fig. 1.11.

High Performance Liquid Chromatography

HPLC is commonly used in chemical and pharmaceutical laboratories to determine the products purity. A part of the sample solution is withdrawn and injected in a porous column, which is the responsible for the separations of the different species present in solution. The column is a cylindrical tube filled by small spherical particles, which usually are made of porous silica. However, columns can be made by different materials, such as polystyrene, zirconia, alumina, titania or graphitized carbon. The selection of the proper column depends on the species that have to be analysed and it affects the effeciency of species separation. The column is also called stationary phase, in contrast to the mobile phase, which is the liquid solution that flows inside the column and makes the elution of the molecules from the column possible. Inside the column, the separation of the different species proceeds, exhibiting two different behaviuors: differential migration and molecular spreading. The first is essential for the chromatographic separation and as a result of this mechanism, the different species are eluted at different times; the latter is due to the fact that the molecules can move inside the column, occupying a larger volume of the column defining a so called band. When a band is eluted, a chromatographic peak is recorded. The elution time gives the identity of the chromatographic peak [36]. Typically, inside the HPLC system is included another characterization system, such as a UV-Vis spectrophotometer or a mass-spectrometer. In the case of polyynes, usually the HPLC technique used is the so called Reversed-phase, in which the column is made of a non-polar material and the mobile phase is a mixture of water and an organic solvent (such as acetonitrile or methanol). The longer the carbon chains, the higher is the elution time, due to the fact that shorter chains can be more easily eluted because of their smaller interactions with the column. In addition, chains with same length but different terminations are eluted at different times, due to the different interactions each group has with column. Another interesting aspect

is that with this technique is possible to collect each chromatographic peak corresponding to chains with the same length, thus obtaining a sample of size-selected polyynes, that can be therefore investigated by other techniques.

1.4.5 Synthesis methods

Chemical Synthesis

As already mentioned, the interest for polyynes goes back to the end of 19^{th} century and the first to be interested in *sp* carbon materials were chemists. Therefore, the first synthesis methods used were the chemical ones. During the years, more sophisticated experimental procedures were developed with the main aim to synthesize polyynes in a single step, as attested by the works of many authors [37–39]. The main advantages that a chemical synthesis has are the fact that is possible to produce polyynes in very high concentrations (much higher than the ones achievable with physical methods) and, moreover, it is relatively easy to obtain chains with terminations different from the H atom one. It is also possible to cap the chains with bulky groups, such as phenyl or dinaphthyl groups, making polyynes stable over time [37, 38]. In addition, the longest polyyne produced was synthesized by a chemical technique and it was 44-atoms long, with bulky groups able to stabilize the molecule [40]. Obviously there are drawbacks, such as the difficulty to find suitable chemical reactions and the need for a purification step after the synthesis, to eliminate unreacted reagents. Another problem is the big difficulties to use this method for an industrial production.

Physical methods

To overcome the problems of chemical synthesis, other production methods were investigated, and two physical techniques arose as the most relevant: Submerged Arc Discharge in Liquid (SADL) and Pulsed Laser Ablation in Liquid (PLAL). In Fig. 1.12, the typical apparatus for both SADL and PLAL are reported. Between the two, SADL was the first to be used for polyynes production. In this method, two electrodes, that for polyynes production are usually made of graphite, are placed close to each other to make an arc discharge occur. From this, a plasma is formed and part of the material of the electrodes is removed. With the growth of the use of lasers for productive processes, laser light was also used to try to produce *sp* carbon wires.

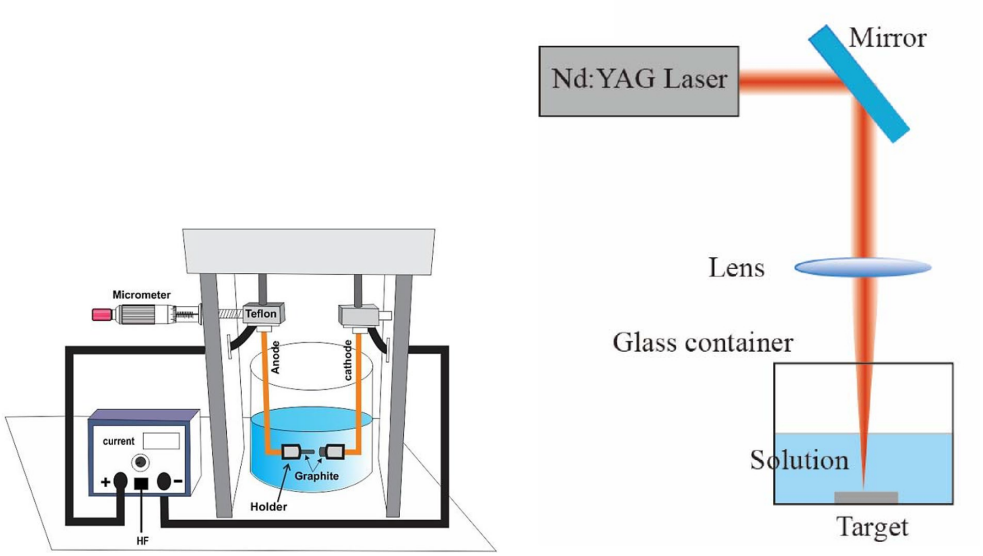

(a) (b)

Figure 1.12: Typical experimental apparatus for, respectively, SADL (a) [41] and PLAL (b) processes [42]

In a PLAL process the laser light is focused on a target, typically made of graphite, and due to the high energy density that is achieved, a plasma is formed. Because of the formation of plasma, the conditions needed to physically synthesize CAWs are obtained. The liquid in both the SADL and PLAL case accomplishes two functions: the plasma confinement and the collection of all the material produced during these processes. Another common feature of both the techniques is the importance of the solvent for polyynes production. In fact, when an organic solvent is used, the amount of generated chains is much higher, due to the fact that the solvent provides additional carbon atoms. The physical methods are faster, easier and require less material than the chemical ones. Moreover, they are suitable for an industrial-scale production. A disadvantage is the formation of a lot of non-*sp* carbon materials, especially in the SADL process, which make more complex the data analysis [43]. In the next chapter, PLAL process will be analysed in more detail.

Chapter 2

Pulsed Laser Ablation in Liquid (PLAL)

To produce nanomaterials there are two types of fabrication strategies, the top-down one, in which the starting point is a bulk material and part of it is removed (e.g. litography), and the bottom-up one, through which the nanostructures are built starting from the atomic or the molecular level (e.g. self-assembling). From this statement, it is quite clear that laser ablation, during which material is removed due to laser-matter interaction, is a top-down technique. The interest for possible applications of laser in productive processes arose immediately after the invention of the ruby laser in 1960s [44]. The choice of laser is justified by the process rapidity and by the high intensity of the laser beams that makes their use suitable for all kinds of materials. The major application of laser ablation is Pulsed Laser Deposition (PLD), which is a process that allows to obtain thin films on a solid substrate. In contrast to the PLAL one, the environment of PLD contains a gas, usually inert, or it is vacuum. The first work on laser ablation performed in liquid dates back to 1987. In this study, Patil et al. employed laser ablation in liquid to synthesize iron nanoparticles in a water environment [45]. Then, other works were done to try to exploit this new technique. In particular, PLAL studies received great impulse due to the possibility to produce noble metal nanoparticles with size control if the ablation is performed in an aqueous solution of surfactants [46]. Another interesting application of PLAL, which is more relevant for this thesis, is the possibility to produce carbon nanostructures, such as for example carbon nanotubes [47]. Moreover, in the last years, great efforts were done to investigate polyynes synthesis, as it will be shown in the last part of this chapter. Before that, a description of the physical process of PLAL is given, followed by the discussion of its main parameters.

2.1 PLAL physics

In PLAL process a focused laser beam irradiates a target, which is located inside a container that is filled by a liquid. Due to the very high energy density, peculiar of laser, material can be removed from the target and therefore, because of the unusual conditions that are created, nanomaterials (such as metal nanoparticles) are formed. According to the used laser parameters, the ablation mechanisms that are activated can be quite different. Therefore, in the following, we will focus just on nanosecond-pulse laser ablation, which is the type of ablation used in this thesis work. In this case, the pulse duration is bigger than the electron-lattice thermalization time, which allows the presence of thermal processes that are not active for shorter pulses (i.e. *ps* and *fs* pulses) [48]. The main steps PLAL process is composed by are depicted in Fig.2.1.

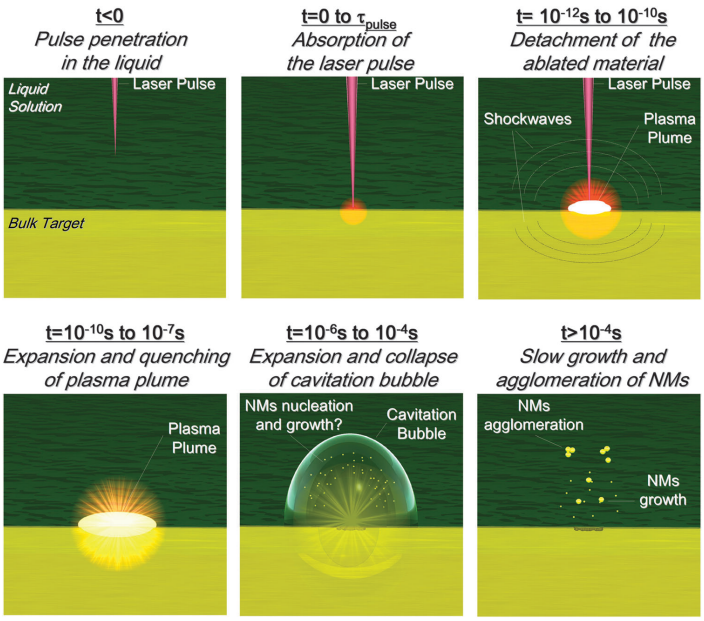

Figure 2.1: Sketch of the main stages of pulsed laser ablation in liquid [48]

2.1.1 Phenomenological description

Before reaching the surface target, the laser beam has to pass through a liquid layer that can partially attenuate its energy due to absorption phenomena. Because the absorption coefficient depends on the wavelength of the laser, we can select a liquid that is transparent to the wavelength chosen for the ablation. In this way, all the energy of the beam is delivered

to the target. In any case, even if part of the laser energy is absorbed by the liquid, it is generally accepted that this is not a crucial issue for nanomaterial synthesis due to the fact that the energy absorbed by the target is orders of magnitude higher than the one eventually absorbed by the liquid. Another aspect to take into account is the possibility that, above a certain fluence threshold, non-linear optical processes (e.g. multi-photons absorption) can be activated, leading to undesired degradation of the liquid [49]. Moreover, we must also avoid solvent optical breakdown, which can be easily prevented working in defocusing conditions (for pulses longer than picosecond) [48].
Once the beam reaches the target surface, linear and non-linear optical mechanisms are involved in absorption of the laser pulse [50]. Non-linear optical processes are activated because of the high electromagnetic field intensity, which is proportional to the ratio between the fluence and the pulse duration. The shorter is the pulse the higher is the intensity (keeping the fluence constant) and so the more relevant are the effects of non-linear phenomena that lead to localized photoionization. The thickness of material involved in the beam absorption is in the order of the so-called material skin depth, which is the level from the material surface that determines the region in which most of the electric current flows [51].
As already mentioned, in the case of nanosecond-pulse ablation, in addition to photoionization, the material can be ablated by thermal processes, such as thermoionic emission, vaporization, boiling and melting of the target. The role of these mechanisms is determined by the pulse duration that, in nanosecond-ablation, is longer than the electron-lattice thermalization time. It is important to underline that those thermal processes, because of their intrinsic nature, affect a bigger volume than the skin depth and a surface larger than the laser spot area (being skin depth and laser spot area, respectively, the volume and the area affected by photoionization) [48]. The absorption of the laser light induces local space-charge fields and electrons-ions collisions, that are responsible for the detachment of ablated material. Moreover, the heating of the material, which is due to the transfer of kinetic energy of the excited electrons to the lattice, favours the material removal. Because the temperature difference between the irradiated spot and the rest of the target is quite high, the material detachment occurs in a region that basically corresponds to the laser spot area. The properties of the nanomaterials produced by PLAL are strongly influenced by the properties of the ablated material and an important role is also covered by the ablation mechanisms, whose complete description is still lacking due to the complexity of the process.
From thermodynamic considerations, however, we can distinguish mainly

three types of ablation mechanisms, which are: vaporization, normal boiling and explosive boiling. The activation of one of these modes is determined by the ablation parameters and especially by the pulse duration. For nanosecond-pulse laser ablation, the main ablation mechanism is believed to be the explosive boiling. This phenomenon, also called phase explosion, occurs when solid matter is rapidly superheated up to the thermodynamic critical temperature, at which the spinodal decomposition in vapor and liquid in the irradiated material occurs by homogeneous nucleation [48]. Another mechanism, the Coulombic explosion can contribute to fragmentation of detached particles. Coulombic explosion occurs when, after the emission of electrons from the particles by thermoionic effect, the electrical repulsion becomes so strong to induce the fragmentation of the particle itself [52].
Simultaneously to ablation, the recoil pressure of the ablated material generates two shockwaves, one propagating in the target and the second propagating specularly in the liquid (which sometimes is also called simply acoustic wave). The presence of a shockwave, which moves with supersonic velocity, means a sudden discontinuity in density and temperature along its front. Moreover, the wave propagation heats liquid and target, thus promoting a further material detachment from the crater. An interesting aspect of the shockwave is that the energy needed to generate it is about $10-50\%$ of the absorbed energy, so it is a way the system has to relax part of its energy [48]. The ablated material contains highly ionized species due to high temperature and direct photoionization, therefore it can be considered as a non-equilibrium plasma plume. Plasma plume can reach a temperature of $10^3\ K$, a pressure of $10^9 - 10^{10}\ Pa$ and a density of $10^{22} - 10^{23}\ atoms\ per\ cm^3$ [48]. It has a lifetime of tens of nanoseconds with an evolution kinetic very fast due to the alternation of the heating caused by the laser and the cooling due to the plume expansion and heat transfer with the solvent. The plume is a non-equilibrium plasma because it can contains melted drops and, sometimes, solid fragments, therefore the thermodynamic equilibrium is not reached [48, 53]. Another factor that influences the plume expansion is the presence of the liquid, which acts as a buffer that strongly confines the plume in space. This confinement slows down the cooling at the interface between ablated material and the target, because the ablated material in the plume can deliver thermal energy to the target surface. As a consequence, the ablation yield is higher than the one in a gaseous environment because a larger portion of the target reaches the energy threshold for detachment (this effect is sometimes called plasma etching) [48].
Once the plasma plume is extinguished (after about $10^{-8} - 10^{-7}\ s$ from

the pulse generation), its energy is released to the surrounding liquid inducing the formation of the so called cavitation bubbles. There are two mechanisms that can induce the bubbles formation. One is explosive boiling, during which the temperature of the liquid is increased close to the kinetic limit of superheat, the other is called cavitation, which occurs when the liquid pressure drops below the tension strength of the liquid [54].

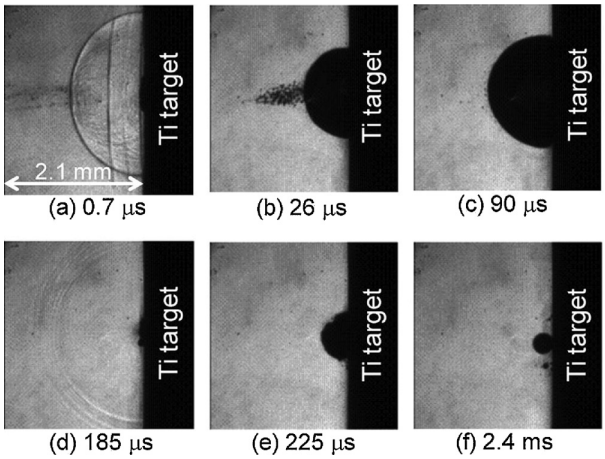

Figure 2.2: Snapshots of the cavitation bubbles [54]. In these photographs, it is possible to observe the shockwave due to recoil pressure (a), the expansion (b, c) and the collapse of a cavitation bubble that generates a second shockwave. In (e) and (f) we can see the start of a new cycle.

These bubbles travel at a supersonic speed in the liquid ($> 10^3\, m\, s^{-1}$), for a maximum distance of few millimetres [48]. During their expansion, the temperature and pressure inside the bubbles drop to values below the ones of the surrounding liquid. At this point, the bubbles collapse emitting a shockwave, the second one from the start of the ablation process. In Fig.2.2 are reported the main stages of a cavitation bubble lifetime. The emission of the second shockwave is the last physical process related to the laser ablation in liquid. Some authors claim that already formed nanomaterials can travel in front of the expanding cavitation bubbles [48], while some others suggest that nanomaterials are formed inside the bubbles during their expansion. According to this theory, the species present inside the bubbles are in higher energetic states due to the high temperature [55, 56]. The temperature gradient at the bubble-liquid interface would promote the nucleation and condensation of the nanomaterials. In addition, when the bubbles collapse, temperature and pressure reach, in the collapse point,

values similar to the plasma ones. This can induce the occurrence of phenomena such as aggregation or phase transitions of the nanomaterials [48]. As stated by Yan et al. [54], bubbles nucleate on the target surface and form a foamy layer on top of it. Then coalescence occurs, so only one bubble is left and during its expansion it can leave the target surface. The bubble dynamics oscillates between its expansion and collapse from which a shockwave is emitted. In another work, it is proved that viscosity of the liquid is crucial for bubble lifetime because at higher viscosities the expansion-collapse frequency is smaller and so the bubble lifetime increases [57]. After the shockwave generated by the collapse of the cavitation bubbles, the system reaches the physico-chemical steady state. In this step, the nanomaterials can undergo minimal modifications due to the condensation of ablated atoms and molecular clusters that still survive in solution [48]. If the nanomaterials solution that is obtained is not stable, aggregation may start, possibly resulting in precipitation on a long timescale (in the order of several minutes).

2.2 PLAL parameters

As comes out from the previous section, the physics behind the PLAL process is quite complex and, in some points, not fully understood. This complexity is mainly originated by the fact that PLAL depends on a large number of factors that can be divided in laser parameters (e.g. pulse energy, laser wavelength, pulse duration, repetition rate, pulse number) and materials parameters (such as target material, solvent and eventual solute present in solution). All of these factors have an impact on the produced nanostructures and on their properties. In the next paragraphs, the most interesting and important parameters will be discussed, following the distinction above mentioned between laser and materials parameters.

2.2.1 Laser parameters

Laser wavelength

The laser wavelength is a crucial parameter for laser ablation because it determines the energy provided by each single photon. The typical range for the choice of the laser wavelength for a PLAL experiment is from the UV and to the NIR. The wavelength chosen for the ablation must be the one at which not only the solvent is transparent, but one that also is not absorbed by the nanomaterials formed after the ablation. If this last condition is not satisfied, the already formed nanomaterials can be

modified or even destroyed by the laser beam. An example of this is the photofragmentation of Au nanoparticles, that takes place simultaneously to ablation if the beam wavelength is 532 nm or 355 nm [58]. Another interesting point to note is that the absorption coefficient is dependent on the laser wavelength. Indeed, the shorter is the wavelength, the higher is the absorption coefficient of solid materials. Moreover, multiphotons absorption and photoionization are more probable at shorter wavelength, having effects on the temperature, pressure and ionization of the plasma plume. In addition, when a short-wavelength is used, more reactive species are present in solution [48].

Pulse energy

Another parameter of paramount importance in PLAL is the energy of a single laser pulse, which, once the wavelength is selected, determines the number of photons per pulse. The amount of energy delivered by a single pulse is proportional to the quantity of material ablated at the same time. A larger amount of energy per pulse results not only in a larger amount of ablated material, but it implies also a higher concentration of species in the plume, which can explain the increase in the size of nanoparticles reported in literature when the pulse energy is increased [59]. It is also important to note that, increasing the pulse energy, multiple mechanisms of material detachment (such as fragmentation, phase explosion, boiling and vaporization) are simultaneously possible [48].

Pulse duration

The duration of a single laser pulse has significant effects on the structure and composition of the final products. This is because, keeping the same fluence but increasing the pulse duration, thermal mechanisms of ablation predominate with respect to the photoionization ones. Thermal processes are present for ps pulses and longer ones because their duration is of the same order fo magnitude of the electron thermalization process. A consequence of the occurrence of thermal ablation mechanisms is the shape of the crater, which has sharp borders only if thermal processes are not active (i.e. fs pulses). When considering ns pulses, there is an additional phenomenon that occurs, which is plasma shielding. Due to the duration of its lifetime, the laser pulse coexists for relatively long time with the plasma plume. Because of this temporal overlap, part of the laser beam energy is transferred to the plasma plume and in this way the plasma temperature, pressure and lifetime increase [48]. Another effect of laser-

plasma interaction is the higher homogeneity of the plasma due to this interaction. Plasma shielding is identified as the cause for ablation rate saturation that occurs at high laser irradiances [54].

Spot area

The main effect of a change in the spot area size is a change in the productivity of the nanomaterials. Indeed, keeping constant the fluence, an increase in the irradiated area results in a higher amount of material that is ablated. Consequently, a higher concentration of material is present in the plume, yielding, in the case of ablation of a metallic target, larger nanoparticles [48]. It is important to underline that, as already discussed in other sections, when more energy is delivered to the target multiple ablation mechanisms can occur at the same time, which usually results in a broadening of size distribution of the nanoparticles.

Repetition rate

The repetition rate is determined by the time interval between two successive laser pulses. The higher the repetition rate, the smaller is obviously the time interval. An increase of the repetition rate corresponds to an increase in the nanomaterials productivity, for time intervals longer than the cavitation bubbles lifetime, which is in the order $10^{-4} - 10^{-3}\ s$ [60]. If, instead, it is shorter than bubbles lifetime the ablation is less effective because the bubbles represents a discontinuity of the refractive index, thus causing scattering of the laser light and therefore less energy can reach the target [48]. In addition, during the expansion of the bubbles the ablation takes place in a hot, low density gas, so the plasma confinement is less efficient, making less efficient the plasma etching of the target [60]. Another point to note is that, increasing the repetition rate, the local concentration of nanomaterials increases, inducing their aggregation and coalescence [48].

Number of pulses

The number of pulses is proportional to the ablation time through the repetition rate. The amount of ablated material obviously increases with an increase in the number of pulses, as reported by Mafunè et al [61]. However, in long-times ablations it can occur that already formed nanomaterials may undergo compositional or morphological modifications (or both) due to the interaction with the laser light [48]. A way to partially prevent this phenomenon is to select a laser wavelength that is not absorbed by the

ablation products, taking also into account the other constraints on the wavelength that were discussed above.

2.2.2 Materials Parameters

Target material

The target is the only source of matter for the formation of nanomaterials, even if, in some cases, species dissolved in the liquid, or the liquid itself, can provide atoms to build up the nanostructures. Because of this, the choice of the target material is quite important and has great influence on the final product. In literature, several different materials are used as ablation target. Because the most popular use of PLAL is for the production of nanoparticles, the most widespread target are the metallic ones, such as the ones made of Fe, Cu, Ag, Au and others [62]. The use of noble metals is justified by the possibility to obtain nanoparticles for particular applications, such as an enhancement medium for SERS analysis. It is interesting to note that the nanoparticles obtained via PLAL have a polycrystalline structure. Other used targets are semiconductors, doped oxides or metal alloys [63–65]. The main critical issue regarding this last type of target is the lack of control on the stoichiometry of the final nanomaterial. Another commonly used target is graphite, whose ablation leads to the formation of amorphous carbon and, of great interest for this thesis, polyynes. Moreover, at very high fluences, it is also possible to synthesize nanodiamond, due to the high temperature and pressure generated during the ablation in liquid [48].

Solvent

The main role the liquid has in PLAL, apart from the collection of the material produced during the ablation, is to confine the plasma plume. Because of plasma confinement, the amount of material that can reach the energy threshold to be ablated is bigger, due to the additional energy transfer from plasma to the target . Naturally, the properties of the liquid, such as viscosity and density, affect the confinement at which the plasma is subjected. Consequently, the produced nanomaterials properties, especially the structure, are influenced by the solvent [48]. In addition, during the ablation the liquid can degrade and so the composition of the final products can be different from the expected one. An important aspect to take into consideration is the liquid layer thickness. Indeed, it is reported that there is an optimal value of liquid thickness for which the ablation rate is

maximum [66]. Moreover, Kim and co-workers found that the presence of a liquid layer increases the ablation rate and lowers the ablation threshold of the target material [67]. This last result is in contrast to what was found by Starinskiy et al., whose findings reveal an increase of the ablation threshold in the case of a laser ablation in liquid with respect to the dry case [68]. This inconsistency may be due to the different type of target used (Al foils in the first case, noble metal bulk targets in the second).

2.3 PLAL for polyynes synthesis

As discussed in the first chapter, polyynes synthesis was first developed by chemical methods. Although this, in last decades, physical techniques were investigated as possible methods for polyynes production. To our knowledge, the first paper discussing laser ablation as synthesis technique for polyynes dates back to 1987 [69]. In that study, however, Heather et al. used laser ablation in a gas environment, which is the same technique used by Kroto, Smalley and Curl to synthesize fullerene. It is noteworthy to underline that fullerene discovery happened during a set of experiments whose aim was to investigate the synthesis of long carbon chains, i.e. polyynes [8]. One of the first PLAL experiments performed using a graphite target is the one of Wakisaka et al., in which a graphite target was irradiated in benzene to study the formation of C_2 carbon cluster [70]. The typical experimental setup used for polyynes synthesis consists of a nanosecond-pulse laser, optical components to focus the laser beam, an organic solvent and a bulk graphite target. However, since this field is relatively new and there is not a consolidate procedure, there are several studies performed using a completely different apparatus. An important aspect to underline is that from a laser ablation the chains that are obtained are of different length and, depending on the solvent used, may have different terminations. An hypothesis regarding the growth of polyynes states that it proceeds by the successive coupling of C and C_2 radicals. This process is in competition with the termination mechanism, which is due to the formation of a chemical bond between a carbon radical and, typically, an hydrogen radical [71]. Although this theory has received support by many authors, another hypothesis was proposed by Zaidi and co-workers who claimed that the chain growth is an ionic one [72]. The longest polyynes detected after a PLAL synthesis is C_{30} and was obtained by Matsutani and co-workers ablating a graphite rod in decalin [73]. Although the length of this chain is much less than the longest synthesized by a chemical method, it was possible to achieve this result because of the solvent viscosity, which is

believed to suppress the C_2 diffusion [74]. In this way, the concentration of that species is higher and the termination reaction is less probable. In the following, we will present a brief overview on laser ablation in liquid for the synthesis of polyynes, focusing our attention to the effect that the main parameters have on the production of linear carbon chains.

Pulse wavelength

The most popular wavelengths used in PLAL experiments for the synthesis of polyynes are 532 nm and 1064 nm, even if other wavelength were used, such as 800, 355 and 266 nm [75, 76]. The choice of these two wavelengths is related to experimental findings, which prove that the longer wavelengths produce a larger amount of polyynes and also longer chains, as showed by Fig.2.3. This result can be explained by the fact that shorter wavelengths can be scattered by impurities present in solution way more easily than longer ones, therefore the ablation process is less effective. It is also worth noting that shorter wavelength can be absorbed by the solvent, which reduces the energy that reaches the target, and by previously formed polyynes, causing their degradation [77]. Both these effects decrease the ablation yield. Despite many works of different authors support the higher efficiency of longer wavelengths for polyynes synthesis, it is reported in literature a work which states the opposite [71]. Since the experiments of the two experiments taken in considerations were not performed in the same exactly conditions, this may have had an impact on the experimental results. Especially, it is probably that the target-solvent coupling is the factor that determines if shorter or longer wavelength is more effective. Moreover, the fact that PLAL is relatively novel technique and is even more recent its application for the synthesis of carbon chains may explain the lack of a consistent literature.

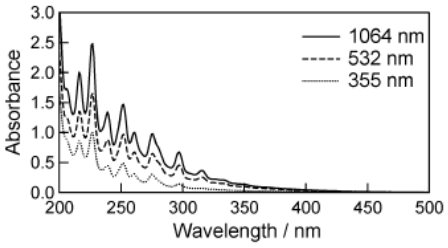

Figure 2.3: UV-Vis spectra of n-hexane solutions after laser ablation at different wavelength of graphite pellets [77]

Pulse energy

As it can be expected, a higher energy per pulse results in a higher polyynes concentration in solution, because at higher energies a larger amount of material is ablated at the same time. However, the increase of polyynes concentration is not valid for polyynes of all lengths. Indeed, the longer polyynes are present in less amount when the energy of the laser beam is increased (see Fig.2.4a). This effect is probably due to the degradation of the longer chains induced by the laser itself, because they are less stable than the shorter ones. Therefore, it is possible that in the conditions that are established at higher energies, longer polyynes are even less favoured than in a low pulse-energy case. It is reported a case in literature, in which the concentration of both short and long polyynes increase and this occurs when the laser wavelength is 1064 nm [78], as can be seen in Fig.2.4b.This apparent paradox may arise from incomplete understanding of the polyynes growth in under PLAL conditions.

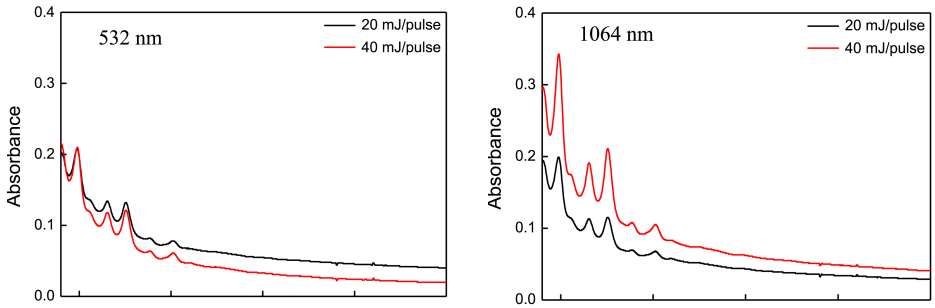

Figure 2.4: UV-Vis spectra of laser ablation of graphite target in deionized water performed at different pulse energy and different laser wavelength [78]

Repetition rate

The typical repetition rate for a polyynes synthesis via PLAL is 10 Hz, as reported in almost all the papers. Santaga et al. studied how the ablation products change according to a variation of repetition rate from 10 Hz to 1 kHz. The experimental results showed that higher repetition rates favour the formation of diamond. The explanation for this effect is that at higher pulse repetitions the conditions for diamond formation (high pressure and high temperature) are fulfilled. However, even when diamond is produced, polyynes are still formed, as can be seen in Fig2.5 [79]. No study, instead,

was done to investigate the effect that different pulse durations may have on polyynes synthesis. Despite it, there are papers in which the laser pulse duration is in the order of fs, ps [69, 70, 81]. It is possible to note that ns pulse lasers are the most widespread in the field of PLAL for carbon chains synthesis.

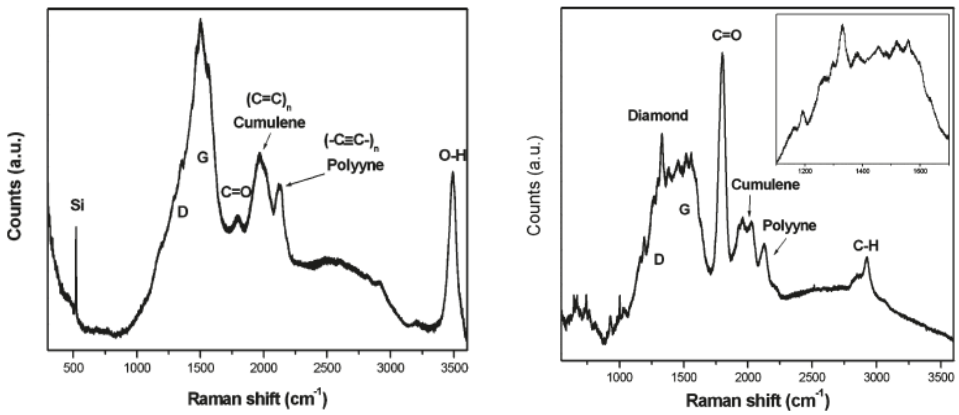

Figure 2.5: SERS spectra of species produced by PLAL with repetition rate of 10 Hz (a) and 1 kHz (b) [79]

Ablation time

Regarding the effect on the increase in the ablation time, there is no accordance among the authors. In fact, there are two opposite results. Some authors, such as Park and co-workers, sustain the idea that longer ablation times lead to the formation of a larger amount of polyynes and to longer ones, although for some wavelength this is not rigorously true, as can be seen in Fig.2.6 [76]. Shin and co-workers, instead, claims that after 30 minutes of ablation there is a saturation of polyynes production [80] (see Fig2.7). This, however, is in contrast with the experimental results of other authors, considering as example the fact that Matsutani and co-workers were able to produce C_{30} after an ablation of 52.5 min. It is important to note, in this frame, that in that paper the ablation time for which it was possible to get such a long chain is called an "optimized ablation time" [73]. Therefore, it is quite probable that an increase in the ablation time has not always the same effect on polyynes formation, but it depends on the other factors, such as the laser wavelength, the pulse energy, the target material and solvent properties.

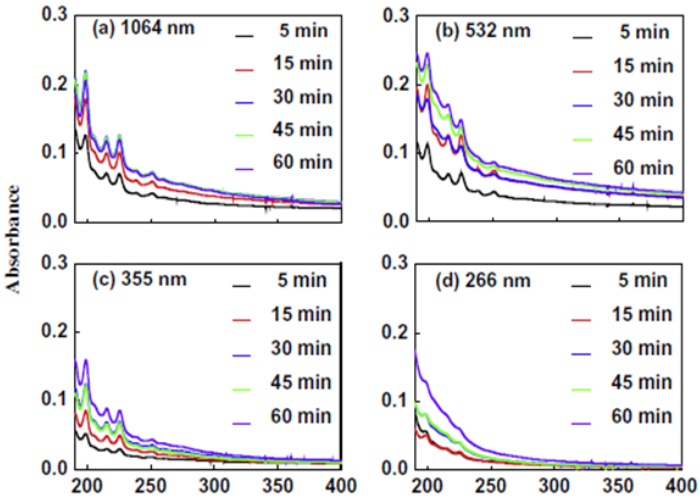

Figure 2.6: UV-Vis spectra of polyynes produced using different laser wavelength and different ablation times [76]

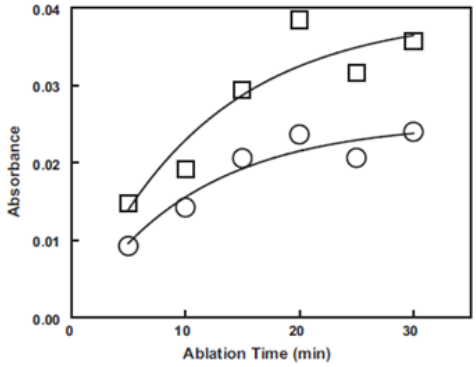

Figure 2.7: Polyynes synthesis saturation after 30 minutes of ablation [80]

Target

In the literature, there are several works in which the target material for the ablation is different from bulk graphite, which was the first to be used and it is still nowadays the most used one. For instance, all the other allotropic forms of carbon (except graphene) have been used as targets for PLAL experiments [81, 82]. Other solid targets utilized are PTCDA pellets [77], which are dye molecules, and even films of solid hexane [83] and solid methane (in appropriate conditions) [84].
Clearly, some of the above mentioned targets are not bulk materials, such as for example carbon nanotubes and fullerene, so they must be dispersed in the solvent. Because the target consists, in those cases, in dispersed

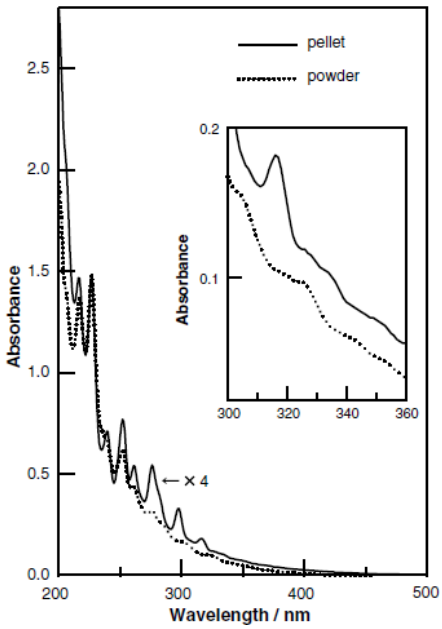

Figure 2.8: UV-Vis spectra of polyynes produced from graphite pellets or powders [85]

particles, there is more material which is simultaneously ablated and each of the ablated particle acts as a nucleation site for the carbon chains. Due to the presence of a higher number of nucleation sites than in the bulk target case, the amount of produced polyynes is larger. However, when particles or powders are irradiated by the laser, the diffusion of C_2 is increased, resulting in shorter chains [85]. This statement is confirmed by an experiment performed used a graphite rod and graphite pellets (see Fig.2.8) [73]. In this way it was possible to assign the difference in results to the different size of the targets, being them of the same material. In some other papers, the target was not present and the laser was focused either on the air-solvent interface or inside the liquid. Due to the absence of a target and therefore to the absence of all the phenomenon typical of the ablation, these studies should be considered as laser irradiation rather than PLAL experiments. The solvents used for laser irradiation are organic ones because they have to provide all the carbon needed to form polyynes. They include alkanes, alcohols, acetonitrile (ACN), acetone, benzene and toluene [72, 85–88] . Although laser irradiation is not properly PLAL, the experimental results are encouraging, as can be seen in Fig.2.9.

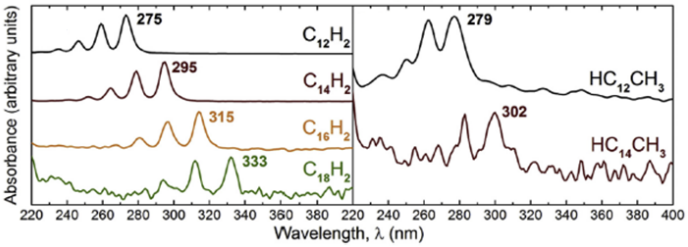

Figure 2.9: UV-Vis spectra of polyynes produced from a laser irradiation of toluene [75]. On the left are shown the absorption spectra of hydrogen terminated chains and on the right the spectra of the methyl-capped ones

Solvent

As there are reported in literature many different targets for laser ablation, there are also many works that investigate the effects of different solvents on polyynes growth. We will consider the case of an ablation in deionized water as reference case, due to the fact that in this case the target is the only source of carbon. Water is simple to handle and is very cheap but it allows only the formation of short polyynes [76, 89, 90]. Therefore, many authors investigated the use of organic solvents such as alcohols, alkanes, acetonitrile and decalin [30, 31, 73, 74, 80, 85, 89, 91–95]. In Fig.2.10 the UV-Vis spectra of PLAL experiments performed in some solvents are displayed. The reason to use organic solvents lie on the hypothesis that this type of solvent would act as a secondary source of carbon, being the main one the carbon target. Indeed, when organic solvents are used, the chains are longer and produced in a larger quantity. The hypothesis that also organic solvents is a source of carbon was confirmed by Wakabayashi et al., that were able to demonstrate through Nuclear Magnetic Resonance (NMR) that atoms of the solvent participate in the formation of polyynes [23]. This is also an indirect experimental evidence of the fact that organic solvents degrade under PLAL conditions. Another reason to use solvents different from water is to synthesize carbon chains with terminations different from the H atom one.
At the moment the only alternative terminations that were possible to obtain using PLAL are the methyl and cyano groups and the deuterium atoms. This last capping agent is observed in deuterated water [80]. While the methyl group was detected in different solvents [75], the cyano one was observed only when the solvent used was acetonitrile [23, 80]. Note that the polyynes detected with this two groups have only one end terminated in that way, while the other one is a H atom. However, in literature are

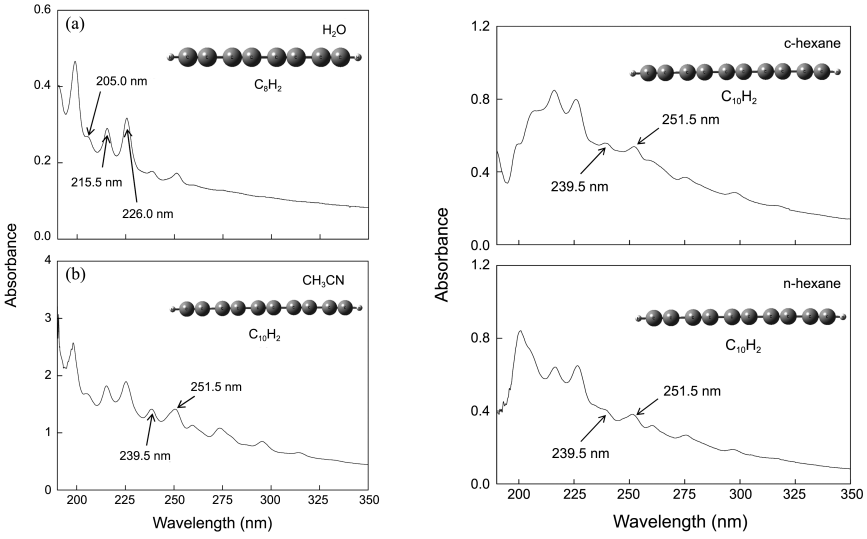

Figure 2.10: UV-Vis spectra of PLAL experiments in different solvents [80]

reported few papers in which it is claimed that some chains have both ends terminated by nitrogen atoms [95, 96]. Other studies were conducted considering some properties of the solvent, such as the pH and the viscosity. If the solution in which the ablation is performed is acidic, the termination of the chain is more probable due to the higher concentration of H^+ ions and this results in shorter polyynes [80] (see Fig2.11).
Regarding the viscosity, experiments demonstrated that for high viscosity solvents, such as decalin, the produced polyynes are longer [73]. This can be explained by the fact that in highly viscous liquids the diffusion of growing species, so the growth of the chain is favoured and the synthesized polyyne are longer [74].

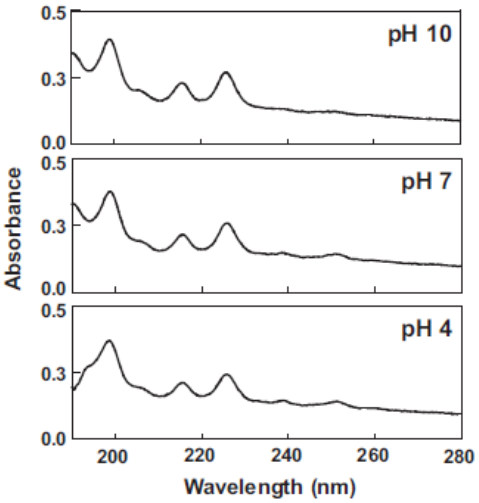

Figure 2.11: UV-Vis spectra of polyynes produced in solutions withe different pH values [80]

Chapter 3

Materials and Experimental Methods

This chapter is divided into two sections: in the first, we present a description of the materials, both targets and solvents, used to perform the experiments of this thesis work, while in the second part, the focus will be on the experimental proceedings used for the polyynes synthesis via PLAL, the characterization analysis and the stability studies of polyynes in solution that were conducted. Moreover, when possible, a discussion of the reason behind each choice will be given.

3.1 Materials

3.1.1 Target

For all the experiments conducted for this thesis work, the target used in PLAL synthesis of polyynes were made of bulk graphite. Although the material was always the same, two different types of target were used. The first is a graphite disk, with a diameter of 8 mm and a thickness of 2 mm, while the second one has a cylindrical shape, whose diameter is 6 mm and the length is about 1 cm. A picture of both targets is presented in Fig. 3.1. The need of two targets with different size and shape relies on the fact that part of the experiments were performed in 10 mL of solvent, while the other part in only 2 mL (the motivation for this choice will be discussed in the next chapter). Therefore, to ensure an easier and more precise placement of the target under the laser light, different containers were used. Moreover, the containers used were chosen in order to limit the motion of the targets during the ablation. In fact, when the target is hit by

the laser light, it tends to move a little inside the container, especially the cylindrical one. When the 2 mL configuration was used, the target selected was the disk one, while in the other condition the cylindrical targets were utilised. It is important to note that, being the material the targets are made of the same, no differences in the ablation behaviour can be ascribed to the different targets used.

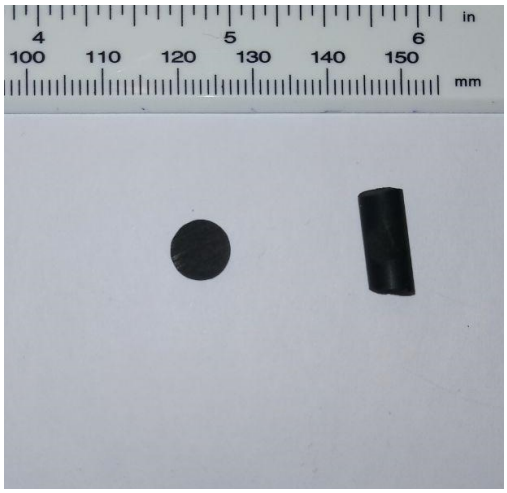

Figure 3.1: Targets used for PLAL experiments

3.1.2 Solvents

Several different solvents were used as liquid media for the ablation. A summary of their most relevant properties for our interest is reported in Tab 3.1. The solvents used include deionized water and many organic solvents, which are methanol, ethanol, isopropyl-alcohol (IPA), acetonitrile (ACN) and toluene. The chemical structures of the solvents used are reported in Fig 3.2. The reason to use water was to have a reference sample that can be used as comparison with the other solvent. Moreover, it must be easy to handle, non-toxic and non-flammable. The use of organic solvents, instead, is motivated by the fact that it was proven that organic solvents, due to their degradation during the PLAL process, are secondary sources of carbon atoms for the polyynes growth [23]. Therefore, in those cases it is possible to produce a higher amount of chains and with bigger length. Regarding ACN and toluene, there is an additional reason, which is the possibility to obtain chains with terminations different from the hydrogen atom, which are for ACN the cyano and the methyl groups, while for toluene the phenyl and the again the methyl ones.

Solvent	*Density* (gcm^{-3})	*Boiling point* ($°C$)	*Refractive index*
Water	1	100	1.333
Methanol	0.792	64	1.326
Ethanol	0.789	78	1.359
Isopropyl alcohol	0.786	82	1.375
Acetonitrile	0.782	81.6	1.342
Toluene	0.867	110.6	1.494

Table 3.1: In this table are reported selected properties of the solvent used [97]

We chose these organic solvents due to the fact that many of them was already used as liquid for laser ablation, while others, namely IPA and toluene, were never used for that role. All the solvents used were HPLC grade, which means that their purity was guaranteed to be $\geq$99%. It was chosen to select solvents with this high purity due to the fact that one of the analysis performed on the sample was HPLC, which is very sensitive to any impurity present in the solvent. HPLC analysis imposed another constrain on the selection of the solvent, which the solvent compatibility with our HPLC system aand with the mobile phase we employed for the analysis. Another reason to have a highly pure solvent in which perform the laser ablation was to have no impurities that can interfere in the polyynes growth. As mentioned in the previous paragraph, two configurations were used, in which the solvent volume was 10 or 2 mL.

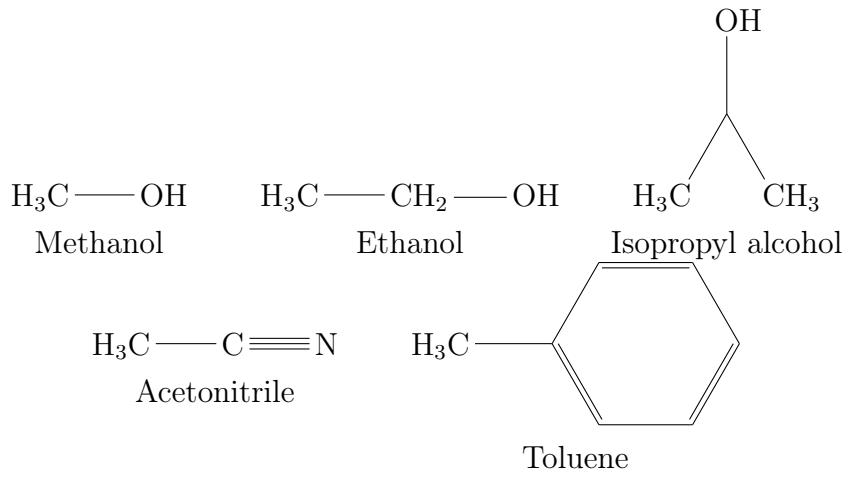

Figure 3.2: Chemical structure of the organic solvents used

The solvent volume determines the thickness of the liquid layer over the target that has consequences on the focalisation of the laser beam on the target, as it will be discussed later. When working with just 2 mL of liquid, to avoid the evaporation of the solvent,the container with the solvent and the target was immersed in a beaker filled with water, in order to cool down the solvents and reduce the evaporation. In particular, the cooling of the solvent was necessary for the organic ones, due to their quite low boiling point and for safety issues, due to their flammability.

3.1.3 Solute

Another way to provide the chains different terminations, apart from using particular solvents, is to dissolve in the selected liquid an appropriate solute. With this aim we dissolved 3 mg of 4-bromobenzonitrile in 2 ml of IPA (therefore the molar concentration of this molecule was approximately $8{\cdot}10^{-3}$ M). The 4-bromobenzonitrile structure, displayed in Fig. 3.3 allows to suppose that, from its dissociation during the ablation, it is possible to obtain chains with cyano or phenyl groups. However, this is not the only reason to dissolve a species in the solvent. Another motivation may be trying to improve the polyynes stability in solution, adding to the solvent a surfactant. Although there is no work in literature regarding this topic, there are several studies regarding the improved stability of other carbon nanostructures, such as carbon nanotubes or fullerene, after the addition of a surfactant. For this reason, we decided to dissolve trisodium citrate (TSC) in water, which is widely used as surfactants for metal nanoparticles, in three different concentrations that are 10^{-1}, 10^{-3} and 10^{-6} M. Two set of experiments were conducted using TSC, due to the fact that the addition of the surfactant was made once before the laser ablation and the other time after it.

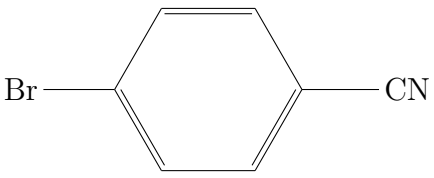

Figure 3.3: 4-Bromobenzonitrile structure

3.2 Experimental Methods

3.2.1 PLAL

The experimental apparatus used for the PLAL synthesis utilised in this thesis is showed in Fig. 3.4. The laser is a Quantel Q-switched nanopulsed Nd:YAG laser with a repetition rate of 10 Hz. In all the experiments performed the selected wavelength was 532 nm, although other wavelengths, such as 1064 and 355 nm, were available. We decided to work with this wavelength because 532 nm is one of the most used wavelength for polyynes synthesis via PLAL. Using that wavelength the pulse duration is 5 ns and the maximum energy per pulse is 300 mJ. However, due to the presence of a beam attenuator, it is possible to regulate the pulse energy from 300 down to 7 mJ.

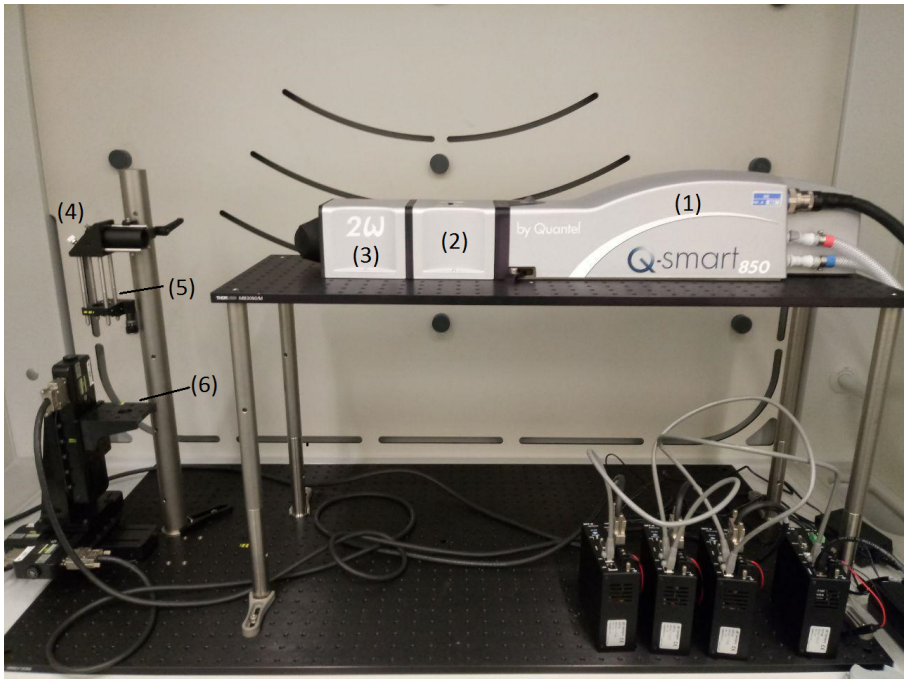

Figure 3.4: PLAL experimental setup, which is composed by the laser head (1), the beam attenuator (2),the second harmonic generation module, needed to get the 532 nm wavelength (3), the mirror (4), the focal lens(5) and the x-y-z stages (6)

Once the beam leaves the apparatus, it has a diameter of 9 mm. Then it propagates until reaches a mirror inclined at 45°, whose role is to deviate the laser beam and send it first to a focal lens and then to the target. Note that

we never worked in perfectly focusing conditions, but in defocusing ones because of splashes generation when the lens-target distance approaches the same value of the focal length. The origin of these splashes is the too high laser fluence easily achieved in fully-focusing conditions. Three lenses with different focal lengths (15, 20 and 25 cm) were used for our experiments. It is important to underline that at each lens change we modified the lens-target distance in order to have always the same spot area on the target. This was necessary to keep constant the laser fluence (if the beam energy is maintained constant). However, sometimes it was not possible to keep the same fluence due to the generation of splashes during the ablation. In those cases, we either moved to even further defocusing conditions, decreasing the lens-target distance and thus obtaining a larger spot area, or decreased the laser pulse energy. In both cases, the laser fluence resulted decreased. When considering at which distance from the lens the target must be placed, we have to take into account two different phenomena: the light focalisation due to the presence of the lens and the light refraction caused by the liquid layer. This last phenomenon results in an increase of the focal length when a liquid is present with respect to the case in which there is no liquid, as it is depicted in Fig 3.5.

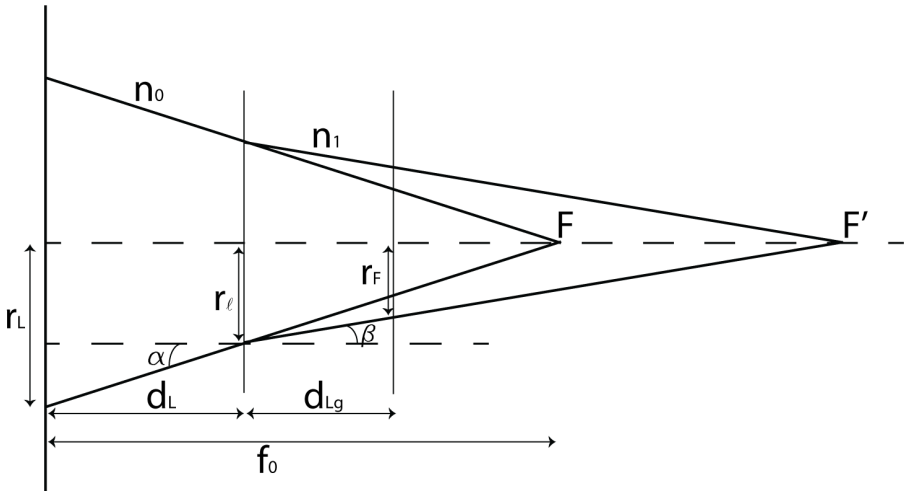

Figure 3.5: In figure it is displayed the scheme used to derive Eq. 3.1. It also shows, qualitatively the change in focal lenght when the laser beam moves from a lower refractive index medium (air) to a higher refractive index one (any of the solvent used).

$$r_F = r_L - (h - d_{Lg})\frac{r_L}{f_0} - d_{Lg}\tan\left[\arcsin\left(\frac{r_L}{n\sqrt{r_L^2 + f_0^2}}\right)\right] \tag{3.1}$$

In Eq. 3.1, it is reported the formula used to calculate, considering the geometrical optics, the laser spot area on the target (r_F). All the parameters that appears in the expression of r_F are known or easily measurable and they are the beam radius at the lens (r_L), the lens-target distance (h), the liquid layer thickness (d_{Lg}), the lens focal length in air (f_0) and the liquid index of refraction (n). It is relevant to stress the fact that the effects of the refraction depends on both the thickness of the liquid layer and the index of refraction, so on the solvent used. The last point to discuss regards the target motion which is possible in our system through to a stage able to move in the three directions of space. Moreover, we were able to move our target in a spiral way because each translator is connected to a controller that can be programmed by the computer, in particular we use a Matlab code. In this way, the target could be ablated more uniformly preventing its ageing. However, it was possible to use this motion system only with the disk target, while there was no way to use it with the cylindrical ones, due to the curvature and small size of their lateral surfaces (which were the ones that were ablated).

3.2.2 UV-vis spectroscopy

The first characterization analysis after one laser ablation was UV-Vis absorption spectroscopy, because it can give us both qualitatively (which species were present in solutions) and quantitatively (from the absorbance given by the spectrophotometer is possible to calculate the concentration of the species through the Lambert-Beer law). The instrument used in this thesis work was a Shimadzu UV-1800 spectrophotometer with two lamps, a halogen one and a deuterium one. Although its measurement wavelength range is between 190 and 1100 nm, the typical range of our measurements was from 190 to 350-400 nm, according to the solvent used for the ablation. To perform an analysis in this region, just few minutes are required. The choice of using a relatively small wavelength range relies on the fact that the signals associated to polyynes, especially to the short ones, are in the UV region. However, once it was performed an analysis with a much larger range (190-700 nm) to detect signals of species produced during the ablation other than polyynes. However, it was not possible to detect any signal at all in the region beyond 350 nm. In order to perform this analysis, the solution is put in quartz cuvette with a light path of 10 mm. This information is needed to calculate the species concentration using the Lambert-Beer law. One of the disadvantages of this characterization method is related to the solvents cut-off, which is the wavelength below which the absorption spectrum is no longer reliable due

to the light absorption by the solvent. Fortunately, most of the solvents used in this thesis has a cut-off quite low, close to 200 nm. The only exception is toluene, whose cut-off is at 285 nm.

3.2.3 High Performance Liquid Chromatography

HPLC analysis were performed to better understand which species were produced during the laser ablation. Our system. which is presented in Fig. 3.6, is composed by an autosampler, a liquid chromatograph, an oven, a photodiode array detector and a fraction collector. The column is a C8 one (made by silica particles to which 8 carbon atoms, which form the alkyl ligand chains, are attached), with a length of 25 cm and an inner diameter of 4.6 mm.

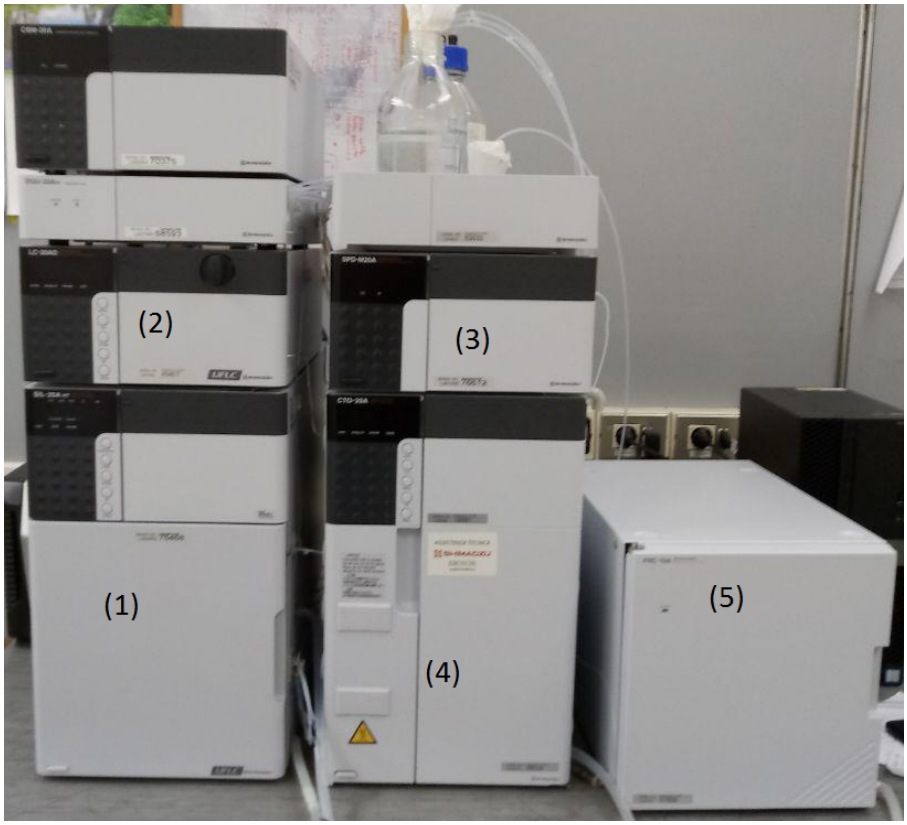

Figure 3.6: HPLC apparatus that is composed by the auto sampler (1), the liquid chromatograph (2), the diode array detector (3), the column oven (4) and the fraction collector (5)

The silica particles, instead, have a diameter of 5 μm. The photodiode has two lamps, a tungsten one and a deuterium one and its wavelength

measurement region is between 190 and 800 nm. The mobile phase utilised in all the analysis is a solution of water and acetonitrile, whose exact composition depends on the analytic method used. In HPLC analysis there are two types of methods: the isocratic one, in which the composition of the solution is kept constant, and the gradient one, in which the composition changes as the analysis proceeds. In our case, both these techniques were used, according on the solvent in which the ablation was performed. If it was water, the employed method was an isocratic one, with a concentration of acetonitrile of 80% and a duration of, typically, 10 minutes. If the PLAL experiment was conducted in an organic solvent, instead, the isocratic method is not suitable, because there is no separation of the chromatographic peaks, so it is not possible to clearly understand the species that are present in solution. Therefore, we used the gradient approach. Two gradient methods were used, the 50-80 one and the 50-90 one (where 50 is the initial ACN concentration and 80 and 90 are the final ones). The way in which the concentration changes over time in both the methods is reported in Fig. **??**.

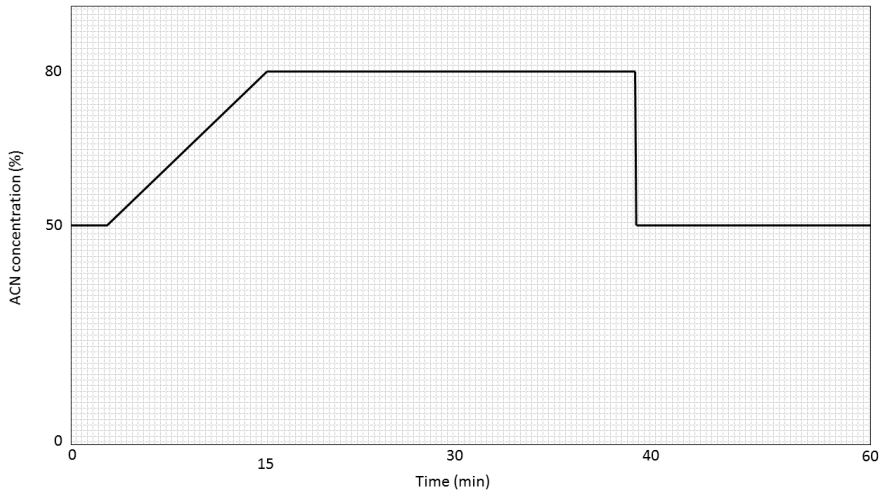

Figure 3.7: ACN concentration variation in gradient 50-80 method

The main disadvantage of these two methods is the quite large amount of time requested (1 hour). Our HPLC system is also able to collect a desired chromatographic peak, due to the presence of a fraction collector as mentioned above. So that the species present in that peak can be analysed individually and with other techniques. It is important to note that because of the working principle of the apparatus, the collected species are partially diluted with the mobile phase, therefore their concentration

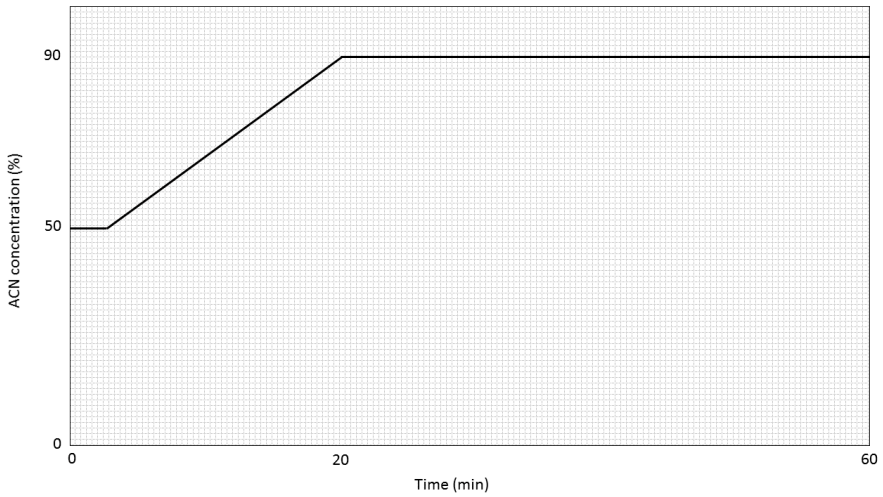

Figure 3.8: ACN concentration variation in gradient 50-90 method

is not the one of the original sample.

3.2.4 Raman and SERS analysis

The Raman analysis were conducted using a Renishaw Raman microscope, which has two available wavelength that are 514.5 and 457 nm. The power of the laser depends on the wavelength selected and , indeed, the max power is 50 mW for the green light and 20 mW for the blue one. Despite this, the power used are usually much lower, about 10 mW. As mentioned in the first chapter, the concentration of polyynes produced via PLAL synthesis is quite low, so it is not possible to detect any Raman signal. Therefore, we had to move to SERS analysis, for which we need to add to our sample a colloidal solution of Ag nanoparticles, whose role is to enhance the signal of the species present in solution. The Ag colloid was prepared using a chemical procedure. In most of our analysis we used the 514 nm ligth. The reason to use this wavelength is that the employed Ag nanoparticles showed a higher enhancement with the green light than with the blue one. This is caused by the interaction of the polyynes interactions with the nanoparticles, that induces an enlargement in the width of the Ag nanoparticles plasmonic peak (which is the responsible for the signal enhancement). The main disadvantage of SERS analysis is the fact that is not trivial to determine the amount of Ag nanoparticles to add to our sample in order to have the enhancement. In our case the difficulties are even more due to the fact that the polyynes concentration is different in each ablation. However, we found that good polyynes to

colloidal nanoparticles ratio that worked well are from 1:1 to 1:3.

3.2.5 Stability studies

As discussed in the first chapter, the main limitation to the use of polyynes is the instability of this material at room temperature and in contact with air. Therefore, a study regarding the degradation of polyynes is quite interesting. We decided to investigate polyynes stability using either UV-Vis spectroscopy or HPLC. Typically, UV-Vis spectroscopy was used when the laser ablation was performed in 10 mL of solvent, while in the case of 2 mL there was not enough amount of solution to perform this analysis. The time interval at which all the solutions were checked was always the same, independently of which technique was employed to investigate the chains stability. The checks were made after 9, 18, 30, 45, 60, 90 and for some cases even 120 and 150 days. All the samples selected for the stability studies were kept in the same conditions, i.e. under neither direct nor diffuse light and at room temperature. To investigate the temperature effect on polyynes degradation, the samples were put once at 5°C and in other two cases the temperature was -13°C. In two sets of experiments, the effect of trisodium citrate (TSC), a commonly used surfactant was investigated. The addition of TSC to the solution was done both before the ablation and after it.

Chapter 4

Experimental results

In this chapter we present the results of the conducted experiments. In particular, in the first part we will show the experiments performed to optimize the PLAL process for the synthesis of polyynes. To achieve this aim, different PLAL parameters were changed, such as the ablation time, the pulse energy, the solvent and so on. In the second part of the chapter, instead, we will present the stability studies results. As in the first part of the chapter, the results will be discussed according to the factor affecting the polyynes stability we were investigating in each experiments, e.g. the temperature, the presence of surfactant etc.

4.1 PLAL optimization

The experiments, whose results are shown in this paragraph, were conducted with two aims. The first is to better understand PLAL process for polyynes production, while the other is to get a higher concentration of polyynes in solution. Therefore, we tried to optimize the ablation in liquid process, evaluating the effect of some parameters on polyynes formation. The investigated parameters are the ablation time, the pulse energy, the solvent volume and the type of solvent. It is important to underline that, in order to evaluate correctly the impact of each of these factors, only one paramter at time is changed.

4.1.1 Ablation time

In literature there is no agreement on the effect of ablation time on polyynes formation (as discussed in chapter 2), therefore it is interesting to investigate it. However, we decided to do it in a different way with

respect to the one followed by all the other works. In fact, we decided to conduct our experiments inserting some breaks during the ablation process, while in the studies reported in literature the PLAL process is performed without. The choice of making breaks during the laser ablation relies on the hypothesis that, in the pauses, the already formed polyynes may diffuse in the liquid. In this way, the probability that the chains are degraded by the laser should be reduced. We performed two sets of experiments, one in 10 mL of deionized water and the other in 10 mL of an aqueous solution of isopropyl alcohol at 40%. Not only the solvent volume is the same for all the experiments, but we also kept constant the laser fluence so that the observed differences among the results can be attributed just to the change in the ablation time. The breaks also allowed us to manually rotate the targets to avoid their ageing, due to the fact that we used the cylindrical one and so it was not possible to move them automatically (as discussed in chapter 3). Considering the case of deionized water, the selected ablation times were: 15 minutes, 30 minutes with a break of 2 minutes in the middle, 35 minutes with breaks of 5 minutes each after the 5, 15 and 25 minutes of effective ablation and, lastly, 4 hours with a break of 30 minutes after the first 2 hours of ablation.
The UV-vis spectra of the solutions obtained with these laser ablation times are reported in Fig 4.1. The lowest concentration was achieved in the 15 minutes ablation, which was taken as reference to compare the effects of breaks, while the highest one was obtained in the 15+15 minutes one. This result is quite expected, due to the fact that in one case the ablation time is the double of the other one and all authors sustain that ablation yield increases for increasing times up to 30 mimutes, [76, 80]. More interesting are the results of the other two PLAL experiments. Considering the 35 minutes one, if only the total ablation time has an impact on polyynes formation, we should expect that the obtained concentration would be higher than the one achieved after 30 minutes of PLAL. However, this is not the case, so we can deduce that the number and the duration of the breaks affect the final result. An hypothesis may be that, too many pauses produce a high dispersion of the growing chains that, once they have left the ablation region cannot grow anymore. This hypothesis may explain why, with respect to the experiment with just one break that is only 2 minutes long, the yield of the 35 minutes PLAL with three breaks of 5 minutes each is smaller. However, the diffusion of the growing chains is accompanied by the diffusion of the already terminated chains, that leaving the spot area, cannot be destroyed by the laser light. We decided to perform the last experment in water is the 4h one with a break of 30 minutes. The reported spectrum is the one obtained after a 1:1 dilution,

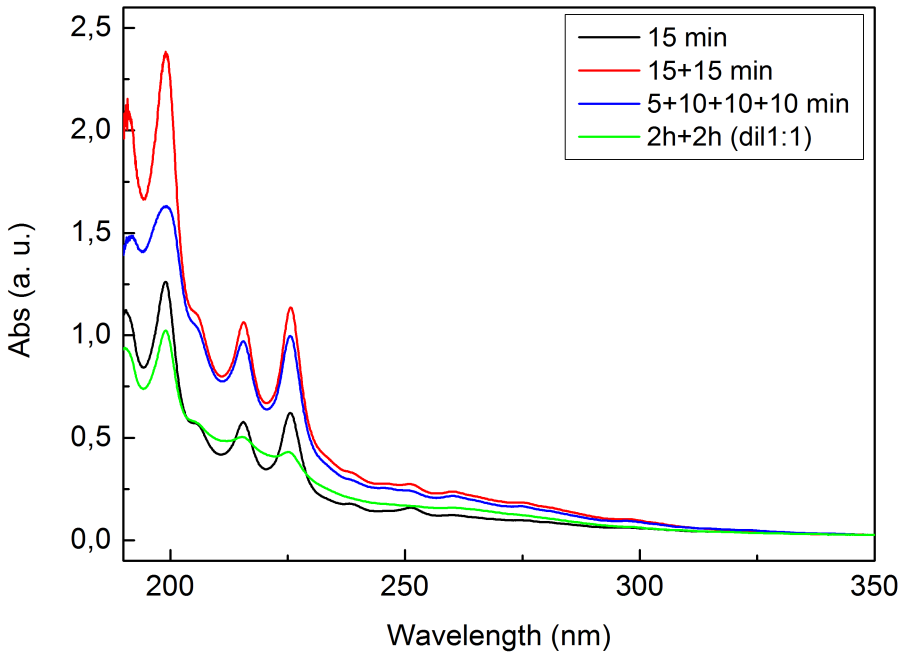

Figure 4.1: UV-Vis spectra of polyynes solutions in water obtained using different ablation times. The spectrum of the 4h PLAL experiment is reported diluted because the non-diluted one was saturated and no peaks were visibile. This effect was probably due to the presence in the liquid of carbon particles able to scatter light.

so the real absorbance is double the diluted one. Therefore, the absorption in this case is above the blue curve but still under the red one. This fact can again be explained by the presence of two phenomena: the diffusion of both the growing and already formed chains and polyynes degradation due to the laser. In this case, the occurence of the break is after much longer time than in the 35 minutes PLAL, so the pause has a beneficial impact, because the diffusing species are mainly the already terminated chains and not the growing ones.

The second set of experiments conducted to investigate the effect of the ablation time on polyynes formation was performed using as liquid for PLAL an aqueous solution with a water to IPA volume ratio of 60:40. The choice of using this particular solution was to increase the amount of polyynes produced with respect to the case of pure water,due to the presence of isopropanol, avoiding the generation of splashes, which would occur if the liquid is an organic solvent even at relatively low pulse energies. This effect is related to the lower boiling point of the organic solvents with respect to the water one. Three ablations were performed using, as

ablation times: 10 minutes, 30 minutes and 35 minutes with three breaks of 5 minutes each (in analogy with what was done with pure water).

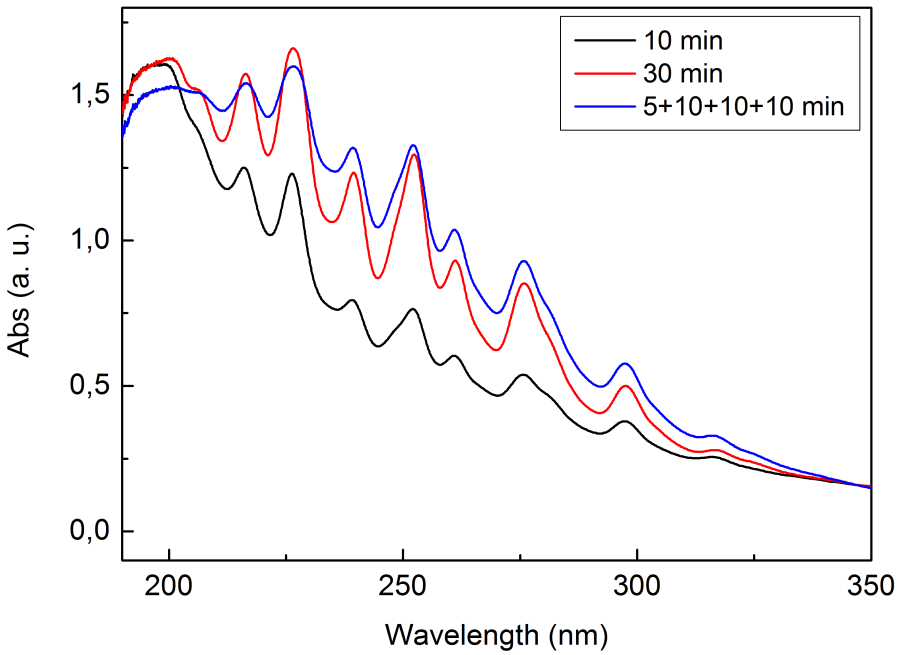

Figure 4.2: UV-Vis spectra of polyynes solutions in IPA aqueous solution obtained using different ablation times

The results, showed in Fig. 4.2, reported, once again, that better results are achieved inserting breaks during the PLAL process. Despite this, the differences among the results are less marked than when pure water was used as medium for PLAL. A possible explanation can be that the presence of an organic solvent (even if it is in solution with water) favours a higher production of polyynes, so we can get a relatively high concentration of carbon chains even for short ablation times (i.e. 10 minutes). If the only effect of breaks during the PLAL process is to allow the diffusion of the species present in solution, then we can suppose that a stirring of the solution (through, for instance, a magnetic stirrer) would have, maybe, a similar effect. It was not possible for us to test this hypothesis, due to the limited space in our experimental apparatus and the low amount of solvent we used. Although the stirring of the solution is used in several works present in literature, no one described its possible effect [30, 76, 80].

4.1.2 Laser fluence

Another interesting PLAL parameter to investigate is the laser fluence, which is defined as the ratio between the pulse energy and the laser spot area on the target and its typical unit of measure is J/cm^2. Also in this case we performed two series of experiments, employing for both cases deionized water as medium in which perform PLAL but with two different volume. Indeed, in one case we used 10 mL while in the other 2 mL. At first sight it seems we can compare all the obtained results because the solvent is the same and because we are considering the fluence we are not constrained by spot area, which depends on the target -lens distance and on liquid layer thickness and so ultimately on solvent volume. However, we cannot do it because, being the volume different, also the degree of confinement of the plasma produced during the ablation is different. As a consequence, the PLAL process is not exactly the same in both the situations and therefore we may expect some differences on the formation of polyynes. So we will discuss each series separately.

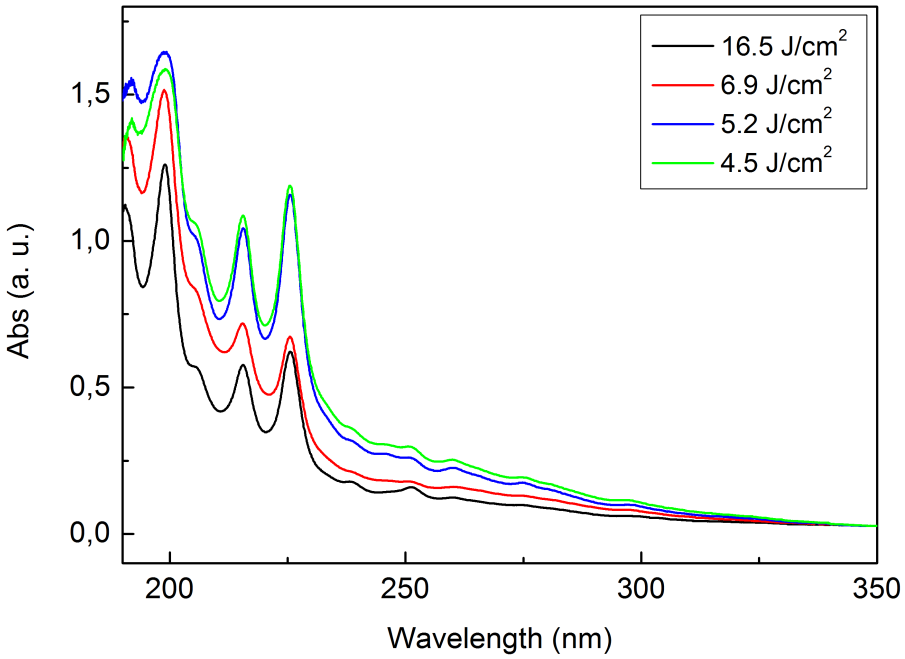

Figure 4.3: UV-Vis spectra of polyynes solutions in 10 mL of deionized water obtained using different laser fluences

In the 10 ml case, we select four different fluences, which are 16.5, 6.9, 5.2 and 4.5 J/cm^2. These values were obtained changing the lens-target distance, thus achieving a larger spot area on the target, keeping constant

the pulse energy at the value of 300 mJ. The UV-Vis spectra of the polyynes mixtures obtained are showed in Fig. 4.3. As can be seen in the figure, the highest concentration of polyynes is reached when the fluence is the lowest (4.5 J/cm^2). This result can be explained considering that, even in the case of lowest threshold, the laser energy is sufficiently high to ablate the graphite target. But if the laser is able to ablate graphite if the fluence is 4.5 J/cm^2, then all the energy in excess, with respect to this value, is not necessary and can lead to the degradation of the chains during their synthesis. A proof that may sustain this hypothesis is the fact that the lower is the fluence used, the higher is the absorbance obtained, up to a level in which it does not matter if there is further reduction of the laser fluence (see in Fig. 4.3 that there is almost no dfference between the spectra obtained at 4.5 J/cm^2 or the one got at 5.2 J/cm^2). However, this is not the only hypothesis that can explain the trend found in the experiments. In fact, there are two ways to decrease the laser fluence: reducing the pulse energy and increasing the laser spot area. Therefore adopting one way or the other is not indiferrent, although both leads to a decrease of the fluence. If the spot area is increased mantaining the same pulse energy, then a larger area is irradiated, thus increasing the amount of material that can reach the energy level to be ablated. Instead, if the pulse energy is decreased and the spot area is kept constant, the amount of material that can be ablated is slightly. Therefore, due to the way the experiment was conducted up to now, we can only infer that a decrease in fluence, caused by an enlargement of the spot area, results in a higher ablation yield.

In order to understand if a decrease in the laser fluence, caused this time by a decrease of the pulse energy keeping the same spot area on the target (i.e. 5.41 mm^2), is beneficial for polyynes synthesis via PLAL, we conducted another set of experiment. This time we also used just 2 mL of water. The chosen fluences were, in this case, 5.6, 2.8, 1.84 and 0.15 J/cm^2. We selected those values because it is reported in literature that when the target is made of graphite if the fluence exceeds 2.4 J/cm^2 there is the emission of C_2 radicals [98], which are supposed to be needed for the growth of the chains. Therefore, we decided to use as fluence a value that is slightly above 2.4 J/cm^2 and one slightly less than it. The other two values, namely 5.6 and 0.2 J/cm^2, were selected because they corresponds to, respectively, the maximum and the minimum pulse energy available in our system. The UV-Vis spectra of the produced polyynes mixtures are displayed in Fig. 4.4. Looking at the reported spectra, it is quite evident that laser fluence has a significant impact on the polyynes formation. In particular, the highest concentrations were achieved in the 5.6 and 2.8

J/cm^2 cases. This is because in those situations, the threshold to produce C_2 radicals was overcome. However, also in the 1.8 J/cm^2 case there is a significant production of polyynes. This is probably due to the fact that we considered as threshold for polyynes formation the fluence above which there is the emission of C_2 radicals found by Sasaki and co-workers [98].

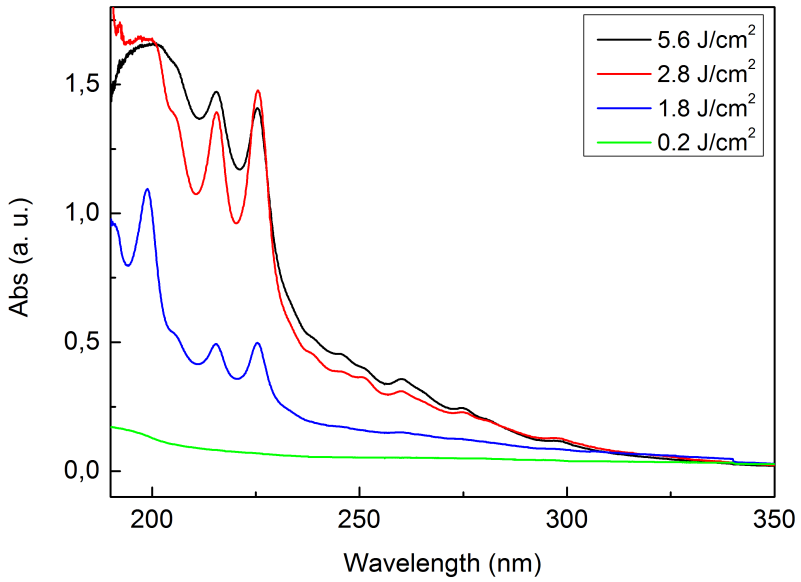

Figure 4.4: UV-Vis spectra of polyynes solutions in 2 mL of deionized water obtained using different laser fluences

However, this value was found using 1064 nm as laser wavelength and, even more important, the experiment was carried out in vacuum, while in our case the target is immersed in a liquid. The effect of a liquid layer on the fluence needed to form the C_2 radicals is not known. Despite this, it is highly probable that 1.8 J/cm^2 is above that fluence threshold. From our results we can deduce that an increase of the fluence is beneficial for polyynes synthesis (see the 2.6 J/cm^2 case). However, a too high increase is instead detrimental, due to the fact that there is probably a sort of dynamic equilibrium between the formation and the degradation of polyynes and a change in the laser fluence can shift the equilibrium more on the degradation or more on the synthesis of the chains. It is quite difficult to establish which fluence, between 5.6 and 2.8 J/cm^2, allows to get the best result just considering the UV-Vis spectra reported. So, a HPLC analysis was performed using the isocratic method described in the previous chapter. In Fig. 4.5 the UV-Vis spectra got from the DAD of HPLC system of C_8 and C_{10} were presented.

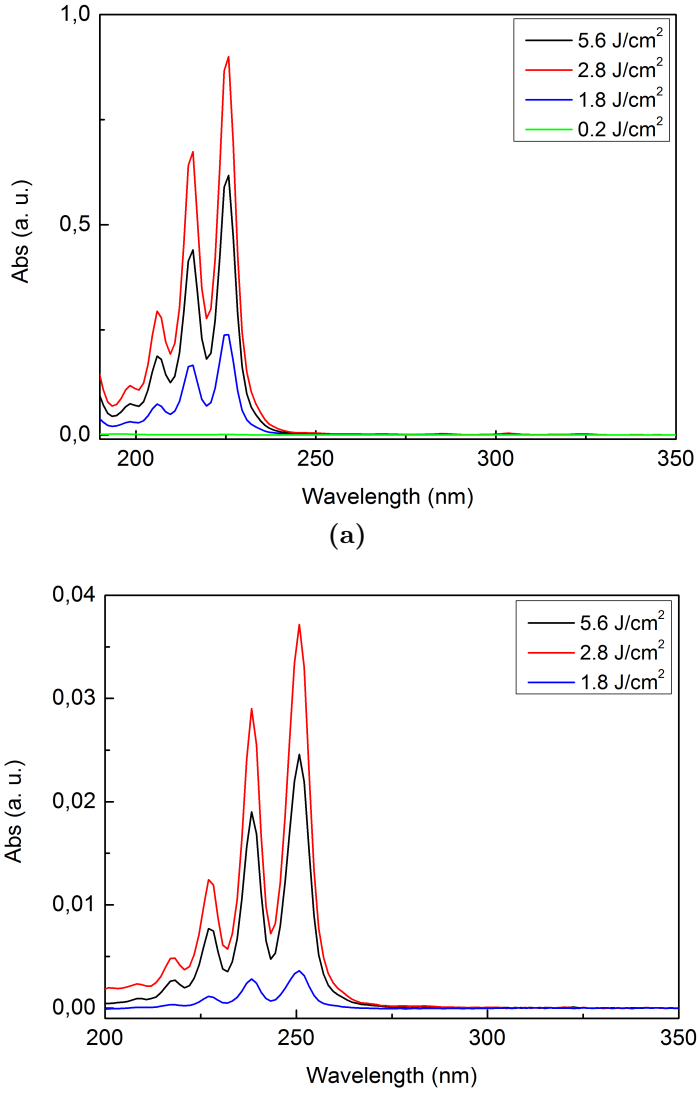

Figure 4.5: UV-Vis spectra of C8 (a) and C10 (b) obtained from the DAD of HPLC apparatus at difference fluences. In the C10 graph, there are only three curves because at very low fluence no C10 was formed

We decided to present only the spectra of these two species because are the most relevant in terms of concentrations and their absorption spectra falls in the wavelength range above 190 nm. Using HPLC technique, we are able to confirm that when the fluence is closer to the threshold value considered (i.e. 2.4 J/cm^2), the obtained polyynes concentration is higher for all the chains length. However, from an HPLC analysis we can make only qualitatively considerations, not quantitavely ones because the absorption obtained by the diode array detector inside the HPLC system is relative and not the absolute one. Anyway, this is not an issue, being our interest just to understand the effect of laser fluence. It is interesting to note that both the experiments performed in 10 mL and the ones conducted in 2 mL, show the same trend, although, as discussed at the beginning of the paragraph, no direct comparison should be made between them.

4.1.3 Liquid volume reduction

As discussed in the second chapter, the choice of the solvent in which perform the ablation is crucial, bacause the solvent may act as a source of carbon atoms. In this section, we will focus on the amount of solvent used, while in the following paragrah we will discuss different types of solvent. The volume of the solvent affects the laser spot area (that is influenced by the liquid layer thickness) and the confinement of the plasma plume. So, a variation in the volume of the solvent may have significant consequences in the synthesis of carbon chains. In addition, even if the amount of produced polyynes will be the same, the obtained concentration should be higher if the volume is reduced. Therefore, we performed four PLAL synthesis changing only the liquid volume employed. Specifically, we decided to conduct these experiments in 10, 2.5, 2 and 1.5 mL of deionized water. We chose water as medium for PLAL because it is easier to detect any difference in the achieved polyynes concentration. The UV-Vis spectra of the four solutions are showed in Fig. 4.6. Note that in all cases, except the 10 mL one, the peak related to C_6 (the one placed at 198 nm), is saturated. Therefore, the displayed concentration is not the real one, which is higher. This feature of the spectrum is due to the instrument, which is not able to detect a too high concentration
A way to avoid this is to dilute the polyynes mixture, so that the spectrophotometer can give us a real measure of the concentration. However, because we are interest in a general overview we did not performed the diluted analysis. Comparing the UV-Vis spectra, we can immediately notice that the worst result is achieved in the 10 mL case. This is quite expected just because the volume is much bigger than in the other cases,

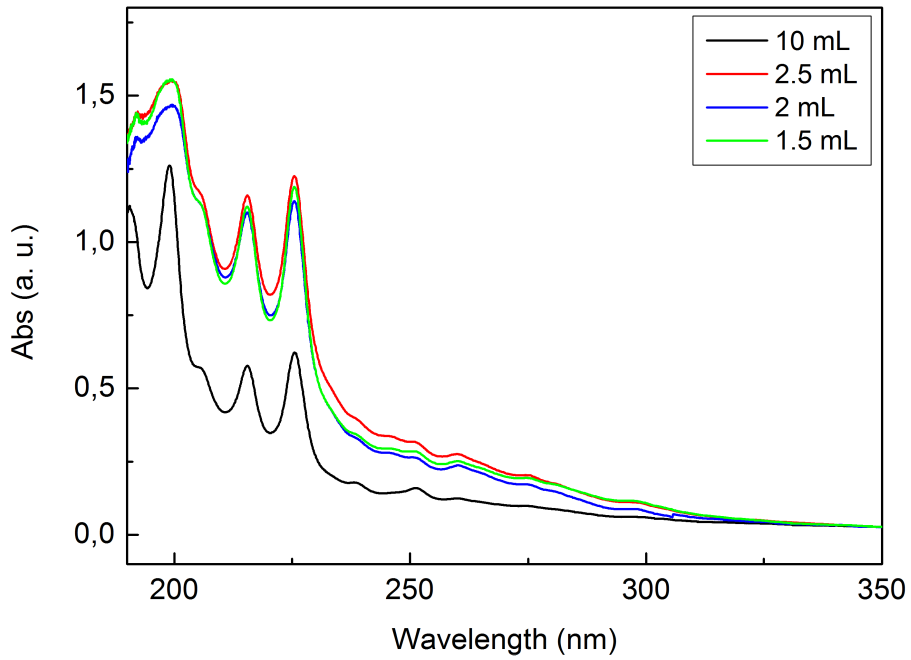

Figure 4.6: UV-Vis spectra of polyynes solutions produced in different volumes of deionized water

therefore the obtained polyynes solution will necessary result more diluted than the other ones. However, the fact that in so small volumes we were able to get relatively high concentrations is not so trivial. In fact, in so small volumes the polyynes present in solution may suffer much more a degradation due to laser or plasma heating. This can be the cause of the very small differences that exist among the spectra of 2.5, 2 and 1.5 mL solutions, although in the latter two cases the volume is further reduced by, respectively, 20 % and 40% with respect to 2.5 mL. Moreover, as stated many times in this thesis, a higher polyynes concentration means also a higher degradation of the chains during their synthesis due to the laser action. The improved polyynes concentration achieved just reducing the liquid volume is an important result because it allows us to get a better result with a low consumption of solvents.

4.1.4 Solvent

The last set of experiments was designed to investigate in which way the solvent used can affect the polyynes synthesis via PLAL. So, we decided to use water and some organic solvents, such as acetonitrile, methanol, ethanol, isopropyl alcohol, and toluene. Some of these solvents were already

used as medium in which carry out PLAL synthesis of polyynes, while some other, i.e. isopropyl alcohol and toluene, were never investigated. All the experiments proposed here were performed using just 2 mL of solvent to achieve a higher concentration. We did not use a smaller volume in order to avoid overheating, which is detrimental for polyynes stability and a safety issue when working with flammable solvents such as the ones selected. The pulse energy varies a little in each ablation but it is kept quite low (such that no differences can be attribuited to the different fluences adopted), to avoid both the generation of splashes that could reach the focalising lens and the occurence of flames.

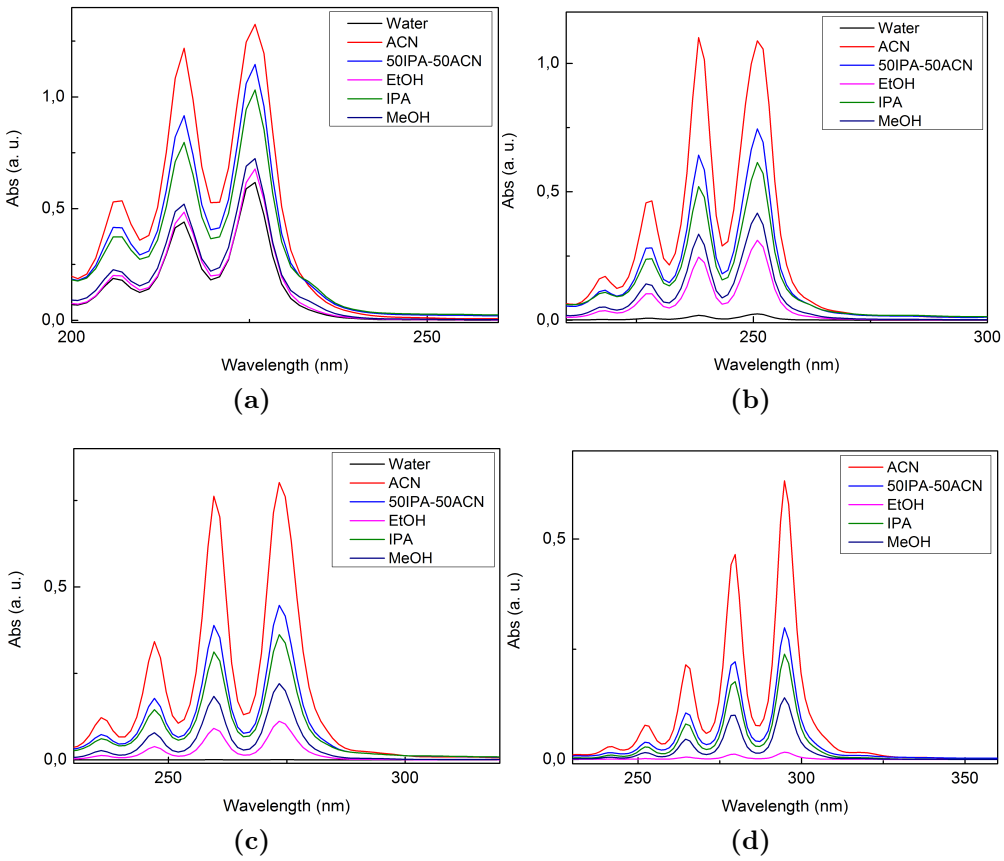

Figure 4.7: Comparison of UV-Vis spectra of C8 (a), C10 (b), C12 (c) and C14 (d) obtained from the DAD of HPLC apparatus in different solvents. In the C12 graph, there are only four curves because C14 is not formed in water.

In order to better understand which species are formed during the ablation, we executed an HPLC analysis on all the samples. It is noteworthy to

underline that, despite for all the organic solvent samples the HPLC method used was the 50-90 gradient one, while the water one that was analysed using the isocratic method, the injected volume in the chromatographic column is the same for all the samples (i.e. 100 μ L). Therefore, we can compare directly the results obtained in the different solvents. Only toluene is left apart, because for the experiments conducted in that solvent a separate discussion is needed.
In Fig. 4.7, the comparison of UV-Vis spectra of some polyynes (C8, C10, C12 and C14) are reported. From those graphs we can clearly notice that the highest concentration of chains of all length is achieved using acetonitrile as medium in which perform the ablation. Isopropyl alcohol is, among the alcohols used, the one that allows to reach higher concentrations. It is interesting that using ethanol the amount of polyynes that are formed is less than the one produced using methanol. Further investigations need to be done in order to understand the reasons why ethanol is not as good as methanol. The causes may be related to the physical properties of the solvent or to the not adequate working conditions. Water is, as was expected, the worst liquid in which perform a PLAL synthesis to produce polyynes, due to the fact that in this case the only source of carbon is the graphite target. However, there are several relevant aspects to discuss regarding our results of polyynes PLAL synthesis in water. The first is that, as can be seen in Fig. 4.7a, the C8 concentration in water is not so different from the one obtained using, for instance, ethanol. However, the difference in the concentrations increases significantly when considering longer chains, noting that C12 is the longest chain we were able to form using water. The ability to produce polyynes up to C12 via PLAL in water is a remarkable result. In fact, there is only one paper in literature in which C12 is formed in water using PLAL as synthesis method [95]. The third and last aspect to underline of our PLAL in water results is that we were able to detect signals not only of hydrogen-terminated polyynes but also of the methyl-capped ones. In particular, we detected the presence of $C8CH_3$ (where not specificated the end-capping agent is an hydrogen atom in the formula, so with the label CH_3 we mean a chain with endgroups an H atom and a methyl group). The UV-Vis spectrum of this species is reported in Fig. 4.8. To our knowledge, there is no study in literature in which methyl-capped polyynes were produced in water.
With respect to C8, $C8CH_3$ shows a shift of 4 nm to longer wavelength of the absorption peak. Indeed, while the C8 peaks are at 206, 216 and 225 (the last one is the highest peak), the $C8CH_3$ are at 210, 220 and 229 nm. The amount of formed methyl-capped polyynes is, however, very low. An indication on this can be deduced by calculating the ratio between the

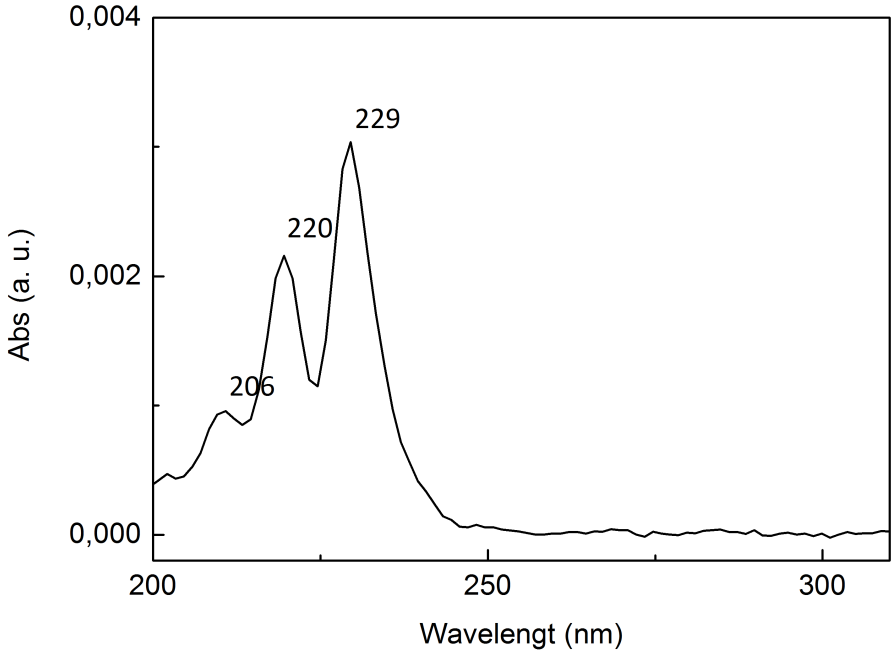

Figure 4.8: UV-Vis spectra of $C8CH_3$

area of the chromatographic peaks related to C8 and $C8CH_3$, noting that the area of a chromatographic peak is related to the amount of species eluted (and therefore present in solution). The result of that ratio is about 205, meaning that the C8 is over 200 times more abundant than $C8CH_3$, considering the case of a PLAL in water. The mechanism of formation of methyl-capped polyynes is quite unknown, due to the fact that also the growth mechanism of hydrogen-capped chains is not fully understood. The presence of the methyl group after a laser ablation in water can only be explained by its formation during the ablation. Assuming that the polyynes growth proceeds by the addition of monoatomic or biatomic carbon radicals, the methyl group can only form if a monoatomic radical binds itself to three hydrogen atoms and then forms a bond with a growing chain. However, this is just a supposition with no experimental data able to support it. Considering now the organic solvents, it is quite evident from Fig. 4.7 that the amount of produced polyynes is higher than in the water case, as one should expect, because in those cases there is an additonal carbon source that is the solvent. However, there are significant differences among the results of the different solvent used in terms of obtained concentrations.Despite this difference, in almost all the experiments conducted we were able to achieve the formation of polyynes

up to C22, whose UV-Vis spectrum is showed in Fig. 4.9. To our knowledge one of the few cases in which C22 or longer chains are obtained is when decalin is used as solvent for the laser ablation, if the target is made of graphite [73, 74]. Another case in which C22 can be formed is when the target are CNTs dispersed in methanol [81]. When Compagnini et al., such as Shin and co-workers, used the same solvents and target we employed, the maximum length they achieved is C16 [80, 89]. The only case we were not able to detect C22 is when ethanol was used. Moreover, the case of ethanol was the one in which we obtained the shortest chains when using an organic solvent. In fact, only polyynes up to C16 were detected, which is, anyway, a result confirmed by other studies [93].

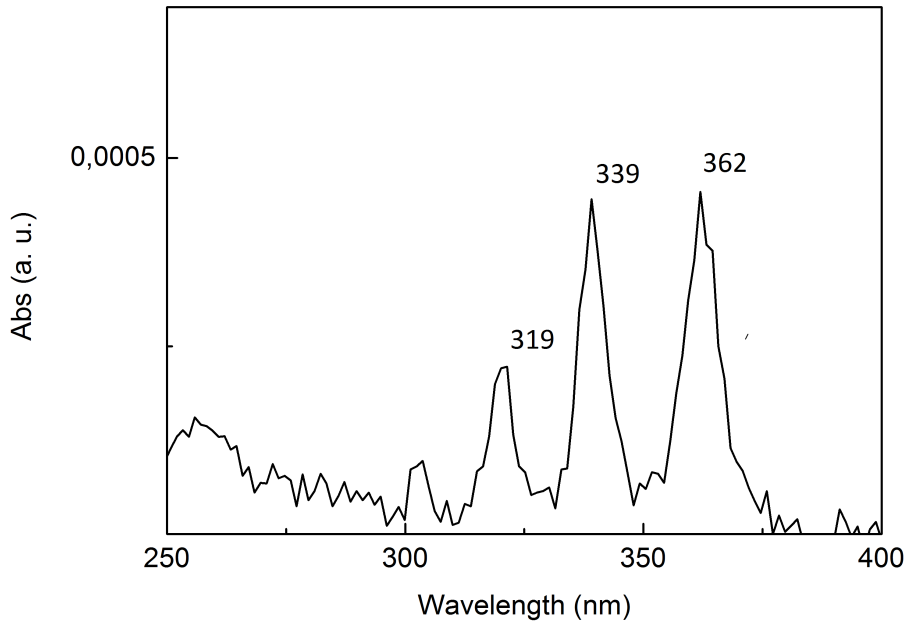

Figure 4.9: UV-Vis spectra of C22 obtained from HPLC DAD

The use of solvents different from water can be motivated by the will to obtain terminations different from the usual hydrogen atom. Due to the solvents molecular structure, we expected that in all the solutions there would have been methyl-capped polyynes. Indeed, we were able to detect this class of polyynes up to $C16CH_3$. In the Fig 4.10, we show the different concentrations of methyl-capped polyynes obtained in the different solvents. The solvent that allows to get the higher amount of methylpolyynes is isopropanol and this can be justified by its molecular structure, that has two methyl groups.
A separate discussion is needed for two other species that we believe to

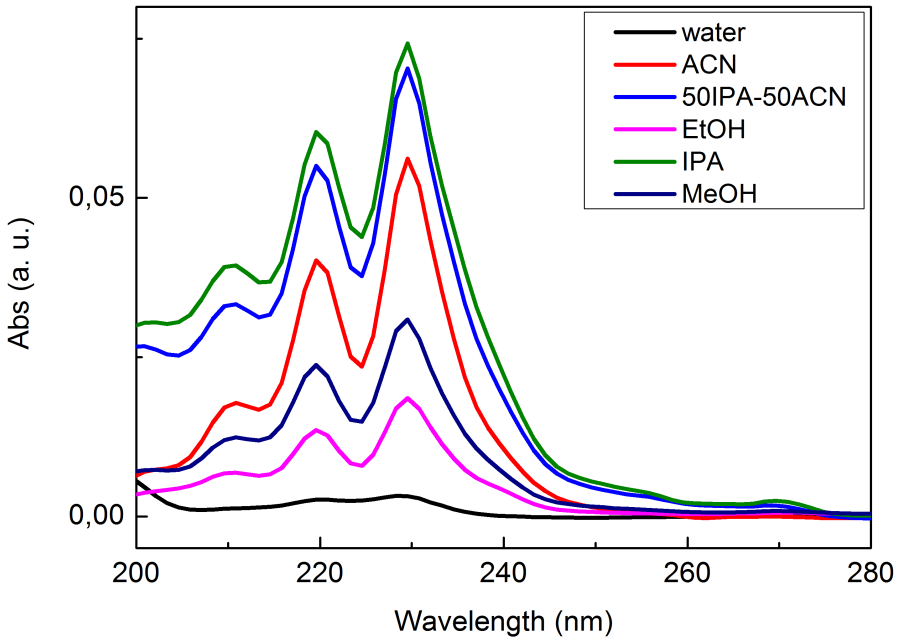

Figure 4.10: UV-Vis spectra of $C8CH_3$ concentrations obtained by HPLC DAD

be methylpolyynes. We display their UV-Vis spectra in Fig 4.11. We believe that those compounds are $C6CH_3$ and $C18CH_3$, which were never found in any previous work. There are two reasons that make us suppose that those two species are methyl-capped polyynes. The first is given by their elution time from the chromatographic column. The order of elution, considering three chains with the same length but different terminations, is that the first to leave the column are the H-capped chains, followed by the cyano-polyynes and the last to be eluted are the methyl-capped ones. Both the supposed $C6CH_3$ and $C18CH_3$ follow this empirical order. It is important to underline that this elution order is valid with our column and mobile phase and that can change according to the specific HPLC system used. The second evidence that makes us believe that the compounds in exam are methyl-capped polyynes is that the chains terminated with one methyl group show a redshift in the absorption peaks with respect to their parent hydrogen-capped polyynes. This shift becomes smaller and smaller as the chains becomes longer, because as the chain length increases the end-groups effect becomes less relevant. The positions of H-capped and CH_3-capped chians is reported in Tab. 4.1. In our case, both species satisfy these empirical observations. In addition, their spectra are very similar to the one of polyynes, which have a peculiar shape made of three absorption peaks. For the believed $C6CH_3$ it is possible to see just the first

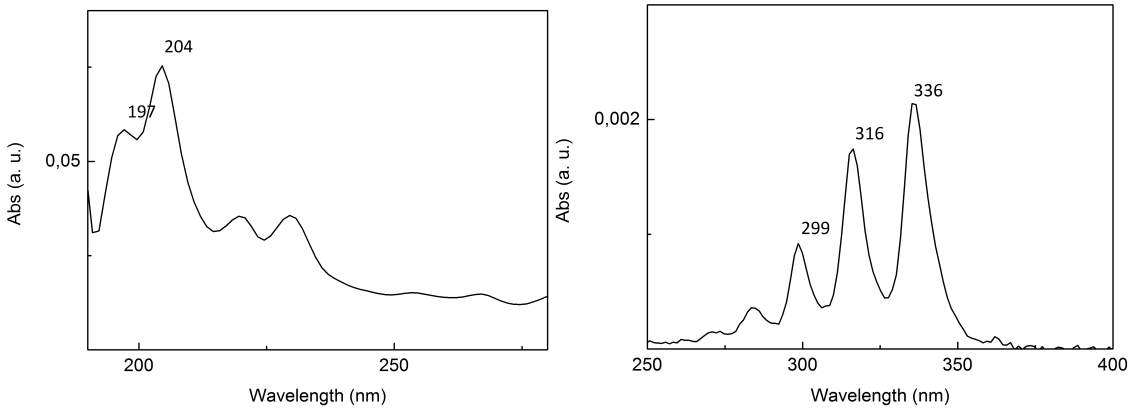

Figure 4.11: UV-Vis spectra of $C6CH_3$ (a) and $C18CH_3$ (b) obtained from the DAD of HPLC

n	HC_nH	HC_nCH_3	HC_nCN
6	// // 198	not found	200 206 216
8	206 216 225	210 216 229	210 216 229
10	228 239 251	231 242 256	231 242 25
12	247 260 274	251 264 278	251 264 278
14	265 279 295	268 283 299	not found
16	281 297 314	285 301 318	not found

Table 4.1: H-capped, CH_3-capped and cyanopolyynes peak positions (in nm). The double bar for C6 states that we do not know the postion of the other two peaks because are not detectable by our system (tehy are below 190 nm)

two, due to the fact that the third is below the instrument limit (190 nm). We tried to separate and collect those species through HPLC, however their concentrations were too low even to be detected using SERS analysis. Therefore, there is no ultimate experimental proof that can sustain our hypothesis. The last termination we succeeded in obtaining is the cyano end-group, which was obtained when acetonitrile was used. An interesting feature of the UV-Vis spectra of CN-capped chains is that their peak position is redshifted of about 15 nm, in a similar trend followed by the methyl-capped polyynes. The peak positions of H-terminated polyynes and of CN-capped chains are reported in Tab. 4.1.

The cyanopolyynes that were detected using HPLC were long maximum

13 carbon atoms (C12CN). We are not sure if longer cyanopolyynes were formed but not detected because, when the ACN concentration in the mobile phase reached 90%, the chromatographic peak related to the cyano-capped chains was closer and closer to the H-capped polyynes peak. The peaks of H-capped chains and of CN-terminated ones were so close that the cyanopolyynes peak was a shoulder of the hydrogen-capped polyynes peak. Therefore, we are not sure that we did not detect cyanopolyynes longer than C12CN because they were not formed or because their peaks in the chromatogram were covered by the one of H-capped polyynes. In order to get rid of this problem, we should improve the chromatographic method, probably changing the mobile phase.

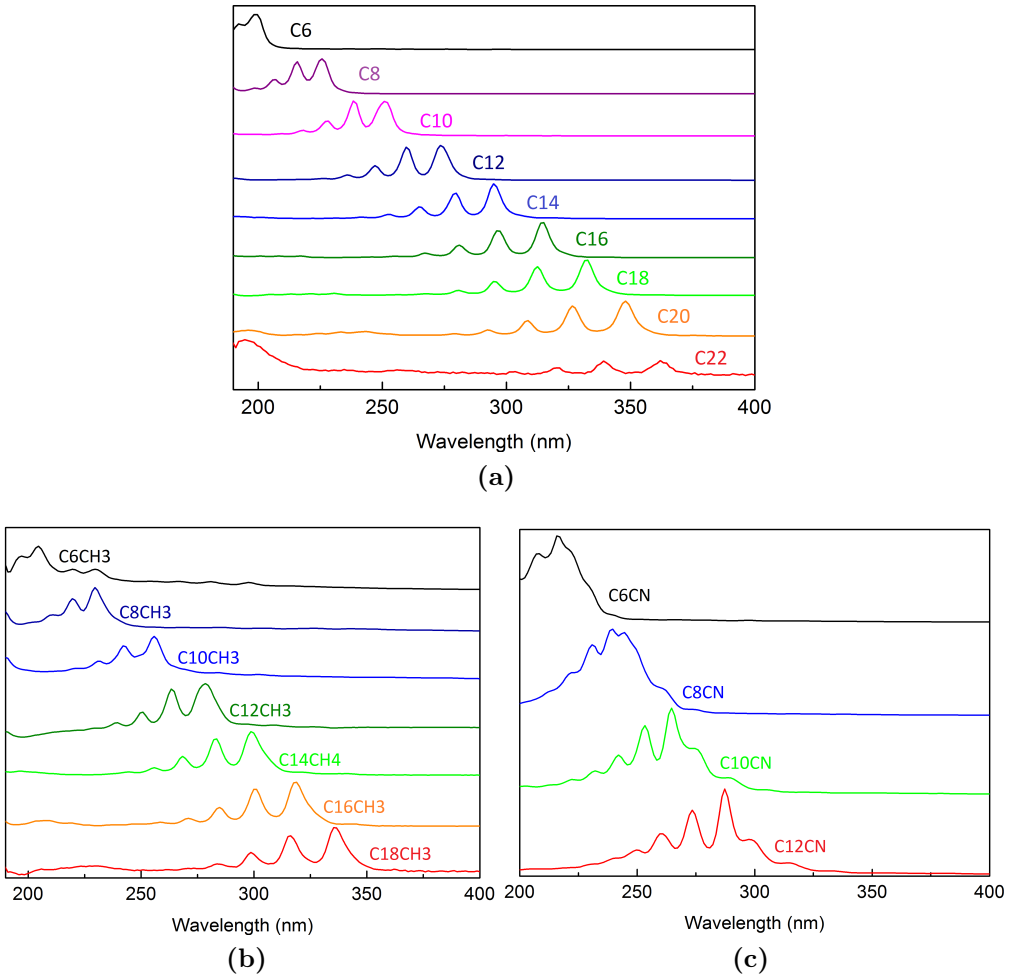

Figure 4.12: UV-Vis spectra of H-capped (a), methyl-capped and (b) cyano-capped polyynes (c) from HPLC DAD

However, we preferred to investigate the solvent effects on polyynes formation keeping unmodified the chromatographic analysis. In addition, we were not able to detect any signal related to dicyanopolyynes (namely NC_nN). As summary, we report the UV-Vis spectra of all the polyynes we were capable to synthesize via PLAL in Fig. 4.12.
Another interesting aspect to study is the relative abundance in which polyynes with different terminations occur in the solvents. In order to investigate this aspect, first we made the ratio of the chromatographic peaks area of the H-capped polyynes and of the methyl-capped ones. The result is showed in Fig. 4.13. As displayed in the graph, the H-capped polyynes are always way more abundant than the methyl-ended ones. However, there are some differences according to the different solvents used. For instance, IPA is the best solvent, among the ones we employed in our experiments, to use to obtain the larger amount of short CH_3-capped chains (the hydrogen-terminated polyynes are just 10 times more abundant than the CH_3-capped ones). The worst for methyl-capped polyynes is ethanol, in which, considering the best situation, the C10 concentration is about 30 times the $C10CH_3$ one. A feature common to almost all the solvents is that the longer is the chain, the less is the amount of CH_3-polyynes fomed.

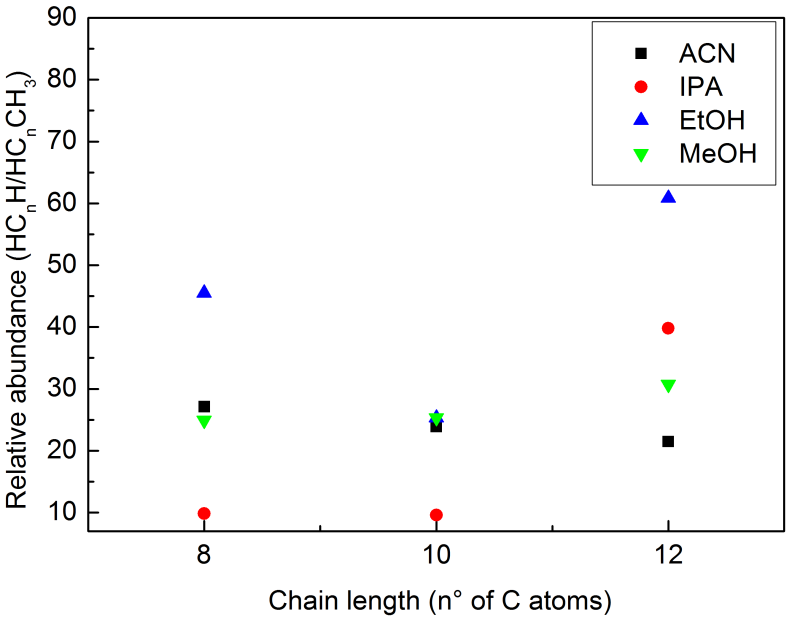

Figure 4.13: Relative abundance of H-polyynes with respect to CH_3-polyynes in ACN

This is probably due to the fact that methyl-capped polyynes are less stable than the H-ended ones and this, combined to the lower stability of

longer chains, leads to lower formation of this type of polyyne. However, the data regarding ACN is in opposition with what stated. The case of acetonitrile is worth to be analysed further because this is the only situation in which we detected the presence of both cyano and methy-capped polyynes. Considering the molecular structure of this solvent, which is composed by a cyano group bonded to a methyl one, we would expect that, if the dissociation of the solvent occurs, the amount of formed CN-capped chains and the of methyl-polyynes should be similar. Instead, what is observed is that, doing the same procedure described before for the comparison of abundance of H-polyynes with respect to the CH_3 ones, the difference between cyano and methyl polyynes even for short chains (i.e. C8 and C10) is significant. Indeed, CN-polyynes are more than four times more concentrated than the methyl ones. The results are displayed in Fig. 4.14.

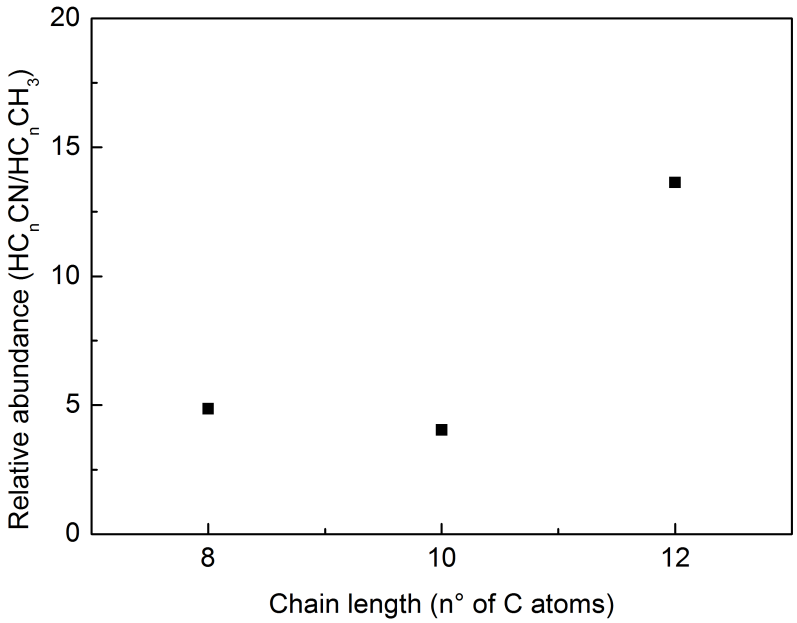

Figure 4.14: Relative abundance of CN-polyynes with respect to CH_3-polyynes in ACN

This effect can be due to either a higher instability of the methyl-capped chains (which will be, that results in a lower amount of formed polyynes of that type, or to the higher probablity of dissociation of the methyl group during the ablation with respect to the cyano one. An evidence that sustains this last hypothesis is that, in the cyano group, the carbon atom forms a triple bond with nitrogen, therefore there is the need of a high

energy to break it. In the methyl group, instead, there are just three single C-H bonds, which are easier to disrupt. Therefore, we believe that in this difference in the strength of bonds in the cyano and in the methyl groups lies the reason for the higher in formation of cyano and methyl-polyynes.

Toluene

A separate discussion must be done for toluene, which was chosen as solvent for PLAL experiments for the possibility that, after the dissociation during the laser ablation, phenyl groups may attach to a growing chain, leading to the formation of stable chains. A first experiment was conducted with 2 ml of toluene and the laser pulse energy was very low, in order to avoid flames occurence. The UV-Vis spectra of the solution after the abalation was quite useless, due to the fact that the toluene cut-off is at 285 nm and so no polyynes signal was detected in that analysis. From HPLC we were able to individuate H-terminated polyynes up to C20, but polyynes with other terminations were not detected.

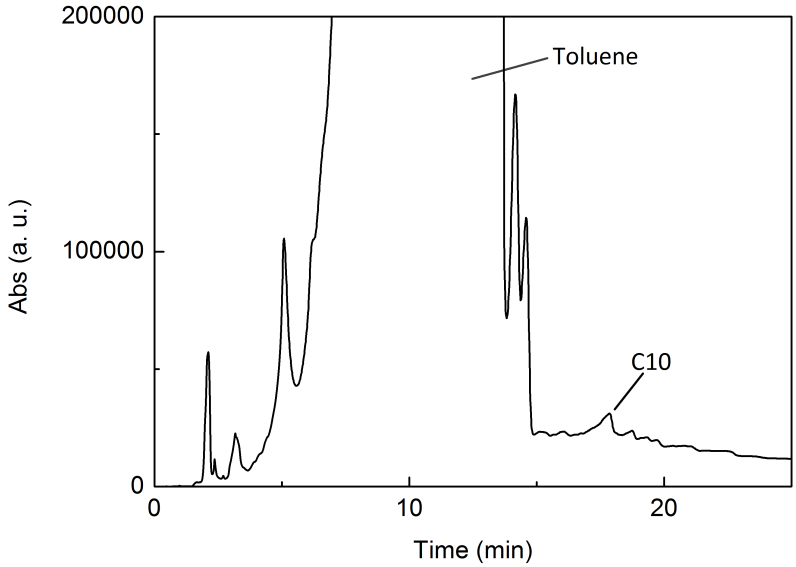

Figure 4.15: Section of chromatogram of 100% toluene. Due to the presence of this large toluene peak, the first polyyne that can be see distinctly is C10

We must underline that in the chromatogram of this anlysis, there is a very large peak related to the elution of toluene (for approximately 10 minutes all the peaks were covered by the toluene, as can be seen in Fig. 4.15). To

solve this problem we tried to inject less volume than the initial 100 μL, but in that case it was no longer possible to see any signal of polyynes. Therefore, for the next experiments we decided to use an aqueous solution of toluene at 2.5% in volume. The results also in this case were satisfying because we were able to obtain H-capped polyynes up to C16, but, as in the 100% toluene case, no CH_3-terminated chain was detected. However, we found that, after about 13 minutes from the beginning of the HPLC analysis phenylacetylene (PA) was eluted. We cannot know if this species is present also in the 100% toluene case, due to the fact that in that case PA signal was covered by the toluene peak. We can infer that it is PA because that species was eluted at a time at which PA should leave our column (in our specific chromatographic conditions) and because the UV-Vis spectrum of this species (that is reported in Fig. 4.16) is exactly the one of phenylacetylene.

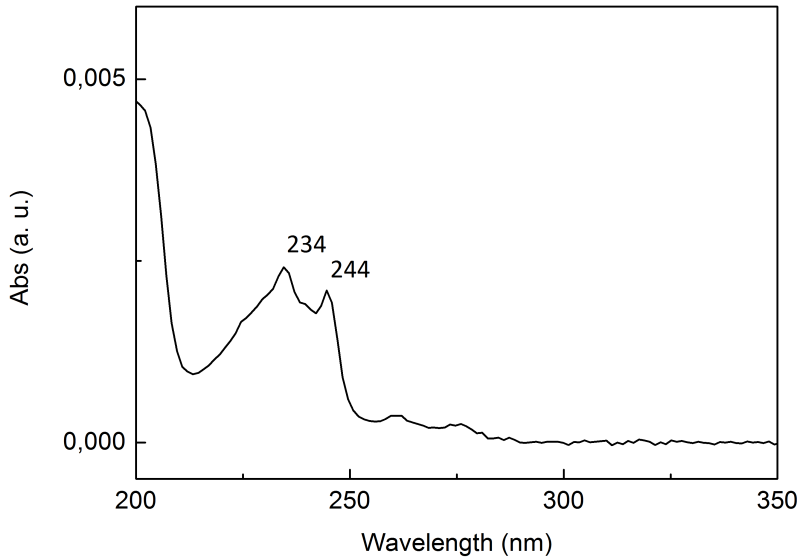

Figure 4.16: Phenylacetylene UV-Vis spectrum from the 2.5% toluene aqueous solution

Although we know that UV-Vis absorptions are not molecule fingerprints (as are Raman peaks), we believe that it is quite difficult that a molecule could have the same exact UV-Vis spectrum of another one (despite it should be theoretically possible). Therefore, we succeeded in attaching a small chain to an aromatic ring, so it seems possible to exploit PLAL as method to produce polyynes with one ended capped by a phenyl group. However, further investigations are needed to clarify if it is really possible. We tried also another way to produec phenyl-capped polyynes with respect

to PLAL in toluene. Indeed, we dissolved 3 mg of 4-bromobenzonitrile in 2 mL of isopropanol. We decided to use IPA instead of water, because in the alcohol we were able to dissolve a much higher amount (one order of magnitude more) we could dissolve in water. However, from the HPLC analysis we cannot detect any signal related to PA or phenyl-capped polyynes.

4.2 Stability

In chapter 1 we discussed the high instability of polyynes that is the main obstacle to their use at industrial level. The degradation of sp-carbon chains is mainly due to the exposure to oxdizing agents and to the interaction of polyynes among each others. We studied the effect of some factors, the ones considered the most relevant, on the stability of the carbon chains. These factors are: the temperature, the presence of a surfactant and the solvent. In the next paragraphs the results of conducted studies will be presented.

4.2.1 Temperature

It is well known that temperature is crucial for the kinetic of every chemical or physical process and this is true also for the degradation of polyynes. Therefore, we decided to perform several studies investigating its impact on the stabiity of the carbon chains. Obviuosly, because we are interested in increasing the polyynes stability, all the studies were performed putting the samples at temperatures lower than the room one. Part of the solution is always kept at room temperature in order to have a reference sample for comparison.
The first investigation was done placing part of the polyynes mixture at 5 °C. Checking the solution periodically (as described in the third chapter), we can see the temporal evolution of the mixtures (both the one keep at low temperature and the one kept at room temperature as reference). The UV-Vis spectra of the solutions at different times are reported in Fig. 4.17. As displayed in the graph, in the sample kept at room temperature there are no peaks related to polyynes after 30 days, while considering the sample kept at 5 °C polyynes signals are detected up to 60 days after the synthesis. A misleading feature of these spectra is that the UV-Vis absorption curves recorded after weeks from the ablation seems to have a higher absorption than the one obtained just after the synthesis but with less resolution. This effect is probably due to the degradation of the chains that involves

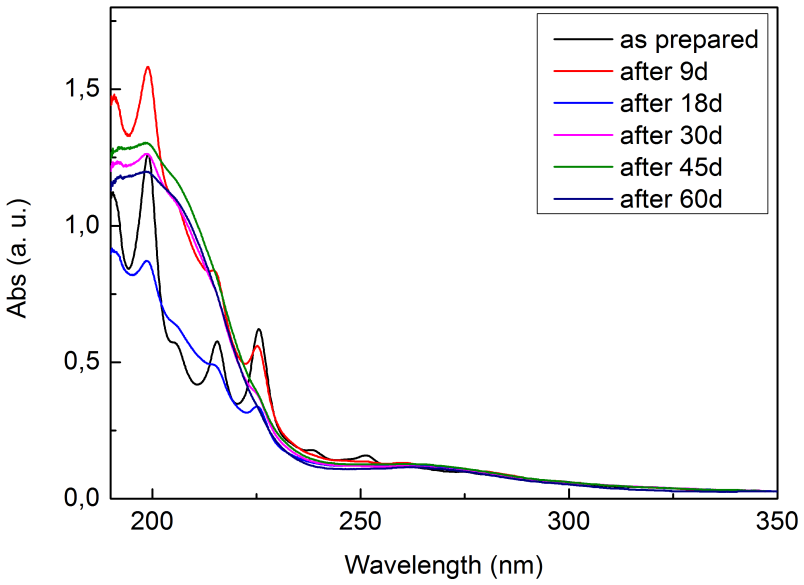

(a)

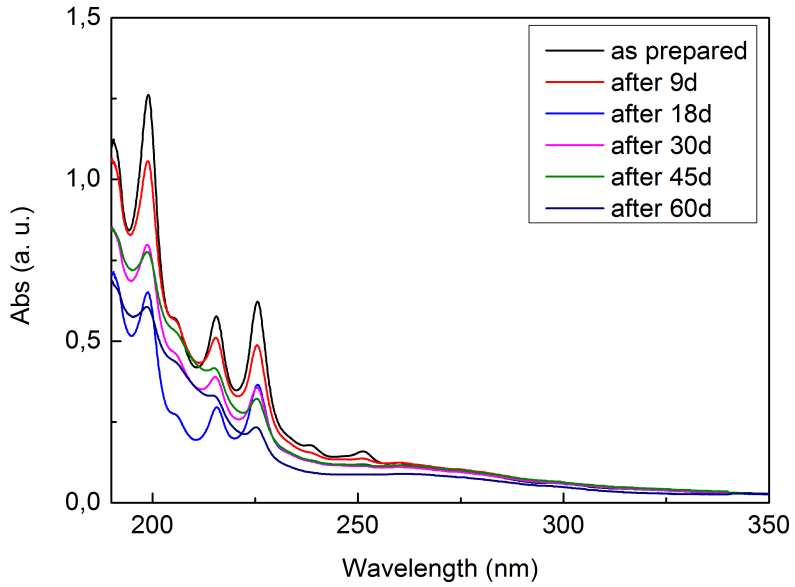

(b)

Figure 4.17: UV-Vis spectra of the sample kept at room T (a) and of the one kept at 5°C (b) at different times

the formation of some byproducts, which creates a sort of background that makes the peaks higher. This hypothesis is confirmed by the fact that because the samples are kept at different tempeatures their degradation kinetics were different and so the formation of these byproducts occured at different times. In fact, the raising of the absorptions curves happened at different times, respectively after 9 days for the sample mantained at room temperature and after 45 days in the other case. The correct way to interpret these data is to consider the peak to valley distance and in that case we found that the polyynes concentration always decreases in both the samples, even if this occurs with different rates. While after 30 days polyynes are completely degraded if kept at room temperature, if the temperature is decreased to 5 ° polyynes are found after 120 days from their sythesis, as reported in Fig. 4.18. Therefore, we demonstrated that a decrease in temperature enhances the polyynes stability.

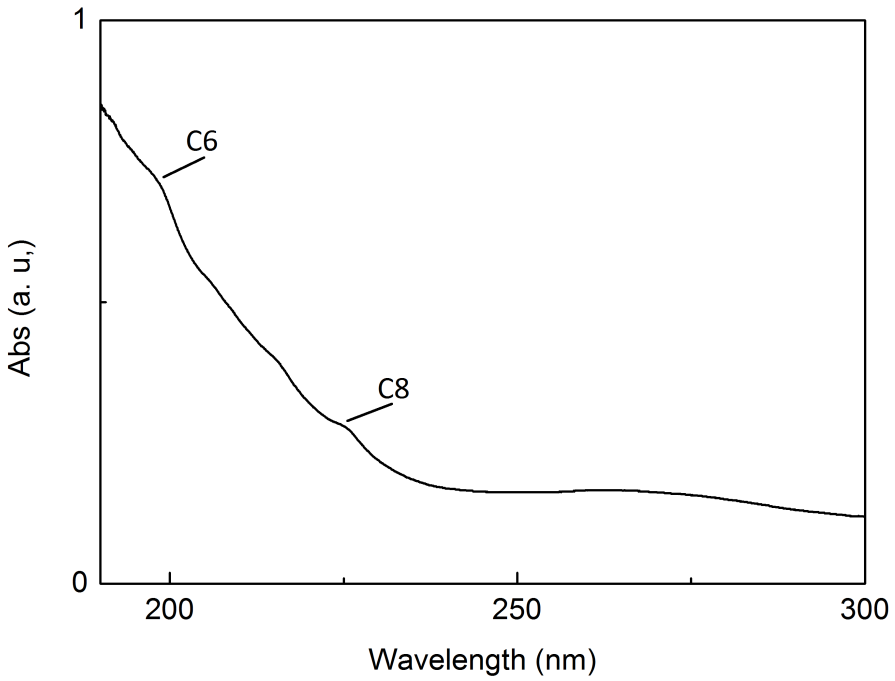

Figure 4.18: UV-Vis spectrum of polyynes solution in water in 5 °C after 120 days

In order to try to improve the result obtained decreasing the temperature at 5 °C, we conducted another study but this time the sample was put at -13 °C. Because the solvent used was water, the idea was that, due to the fact that the temperature was below its melting point, ice would have formed, encapsulating polyynes inside itself and thus preventing their degradation.

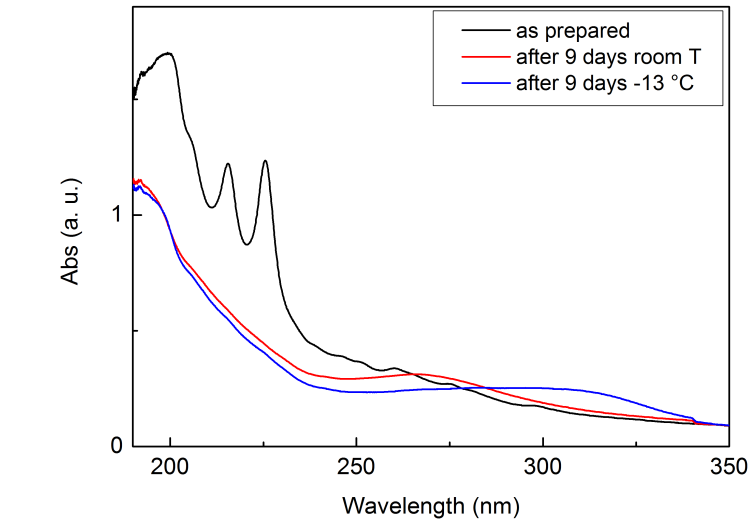

(a)

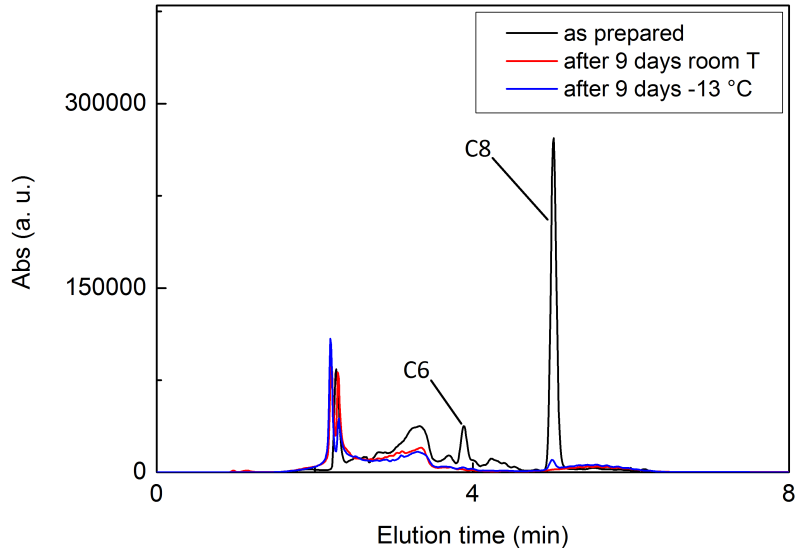

(b)

Figure 4.19: UV-Vis spectra (a) and chromatogram (b) of the sample kept at room T and of the one kept at -13 °C after 9 days. The chromatogram was taken at 225 nm

However, polyynes in the frozen sample degraded at a very high rate. We suppose that, even if assuming that the water solidification would cause no harm for the chains (we have no experimental proof regarding this), the melting of the ice accelerated their degradation.

In Fig. 4.19 are reported both the UV-Vis spectra and the chromatogram

(taken at 225 nm) of the solution just after the laser ablation and after 9 days for both the room temperature reference sample and the one kept at low temperature.
Because the unsuccess of the further improvement of polyynes stability was probably due to the freezing of water, we decided to repeat the experiment keeping constant the temperature (-13 °C) but changing the solvent. The solvent used the second time was isopropyl alcohol, due to its very low melting point (-89 °C), so that no solvent freezing was possible. We report in Fig. 4.20 the trend over time of the chromatographic peaks of some selected polyynes, both short and long ones.

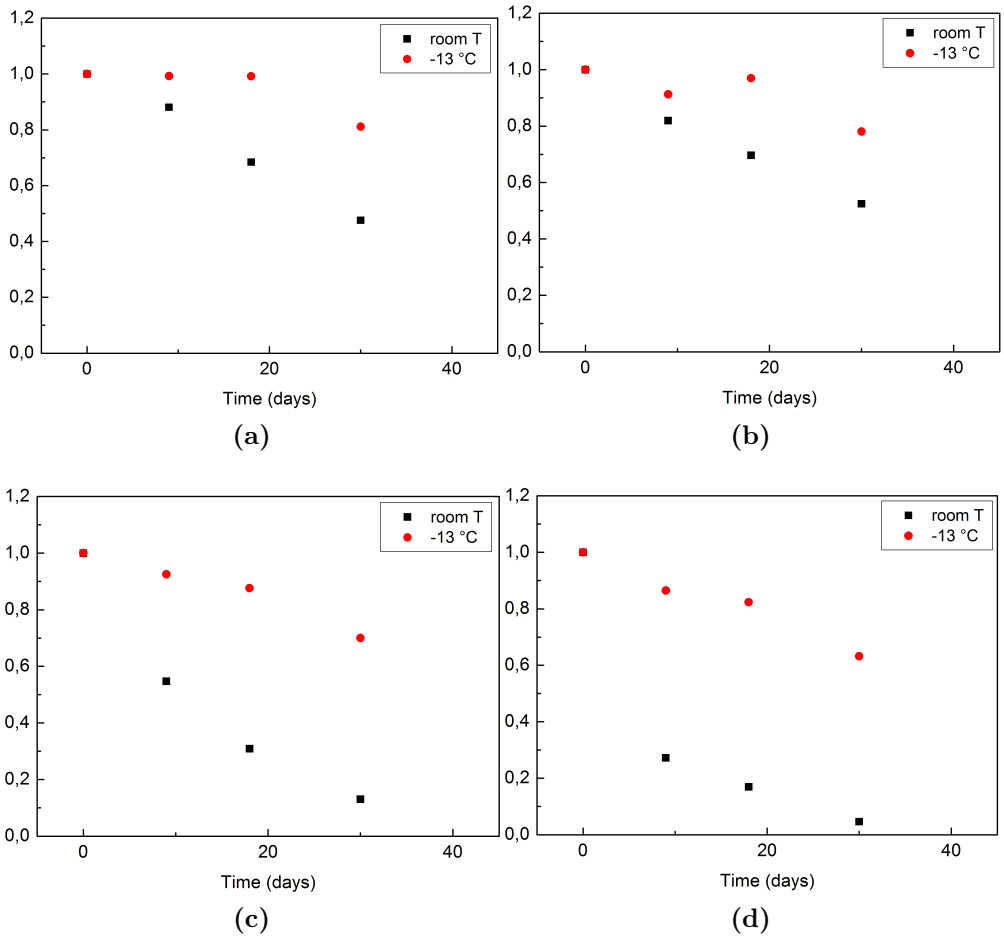

Figure 4.20: Temporal evolution of the chromatograohic peaks area of C8 (a), C10 (b), C18 (c) and C20 (d)

As can be seen in reported graphs, there is a significant difference between the sample kept at room temperature and the one kept at low temperature.

For instance, the concentration of C8 is practically unchanged up to 18 days. However, the bigger difference is observed for the longer chains, namely C18 and C20. While in the cooled sample the concentration decreases are smooth and way linear, in the sample kept at room temperature there is a drop in the concentration after the first 9 days. An hypothesis of this behaviour is that those long chains are incredibly sensitive to degradation due to interaction with other chains. As the concentration of polyynes is high (as in the first days after the ablation), the probability they interact with other chains is high and this results in a fast degradation. As the degradation proceeds, the concentration of the chains decreases therefore there are less interactions among the chains. Consequently, the degradation rate slows down.

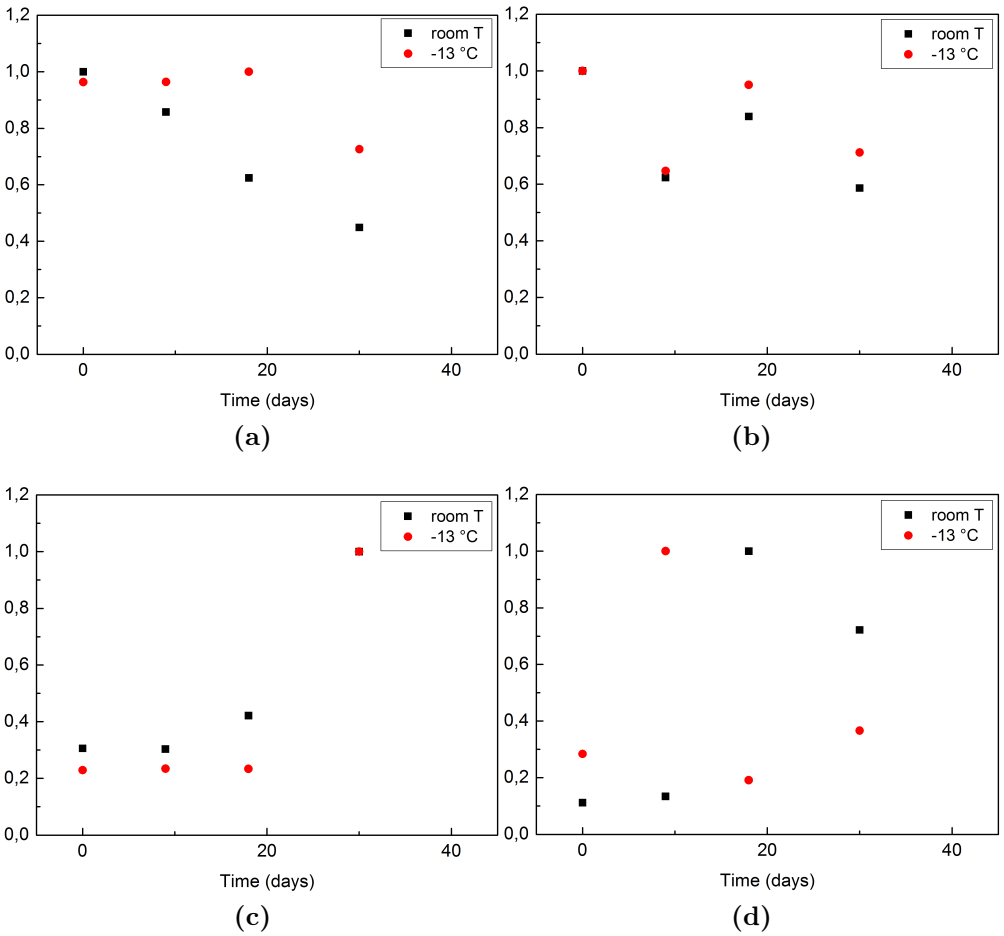

Figure 4.21: Temporal evolution of the chromatographic peaks area of $C8CH_3$ (a), $C10CH_3$ (b), $C12CH_3$ (c) and $C14CH_3$ s(d)

In the sample mantained at low temperature, this phenomenon does not occur because at that temperature polyynes have much less kinetic energy, so the probability that chains interact is rather low. In Fig. 4.20b, there is an increase in the concentration from 9 to 18 days after the synthesis. This phenomenon is observed in the C10 case (the only species that shows this behaviuor among the H-capped chains) and in almost all the methyl-capped polyynes, as showed in Fig. 4.21. This phenomenon is observed in the C10 case (the only species that shows this behaviuor among the H-capped chains) and in almost all the methyl-capped polyynes, as showed in Fig. 4.21.

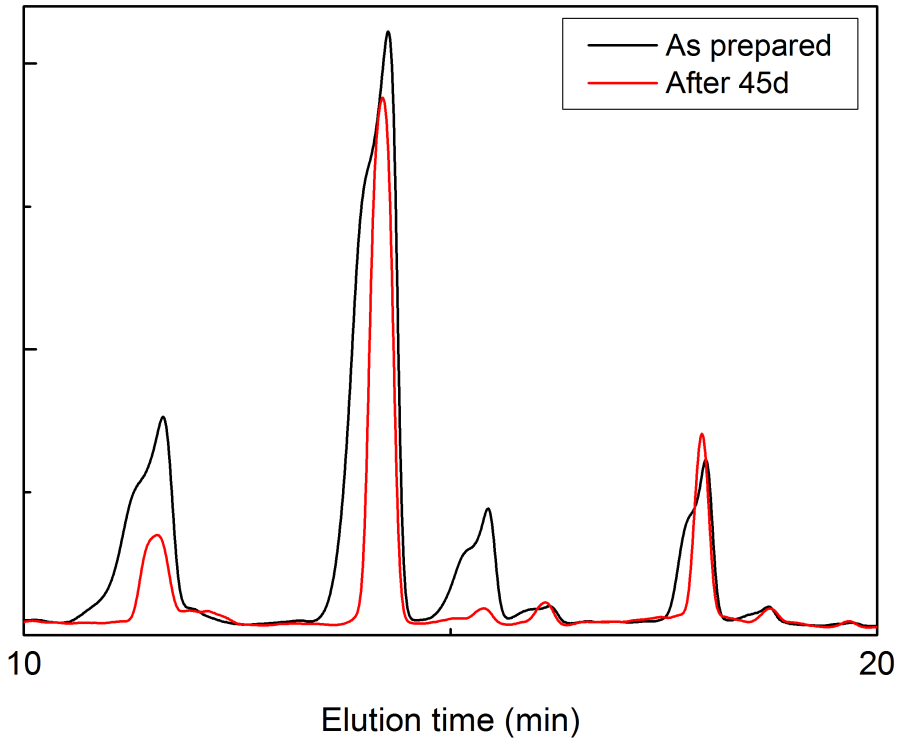

Figure 4.22: Chromatographic peaks variation over time

A possible explanation is related to the variation over time of the shape of the chromatographic peaks. In fact, as showed in Fig. 4.22, the shape of peaks changes significantly and this may affect the evaluation of the peaks area. The chromatographic peaks of the analysis performed just after the polyynes synthesis have not a good shape. They are asymmetric and have a quite big shoulder. The cause of this effect relies on the injection volume that was always 100 μL. A high injection volume means a high amount of material that must be eluted by the column and this can lead, in some

cases, to the column overload that results in an enlargement of the peaks of the chromatogram and to the appereance of a shoulder. Although we were aware of this problem, we decided to perform the HPLC analysis keeping a high injection volume in order to be able to detect the longer chains, i.e. C22. However, we do not exclude a priori that these oscillations may due to some unknown degradation mechanism that is active in IPA and other solvents (in fact, this phenomenon occurs in almost all the solvents we used, except water).

4.2.2 TSC addition

A common method used to improve the stability of nanomaterials (such as metal nanoparticles or carbon nanotubes) is to dissolve a surfactant in the nanomaterial solution. One of the most widespread surfactant is trisodium citrate (TSC), which is an ionic surfactant.

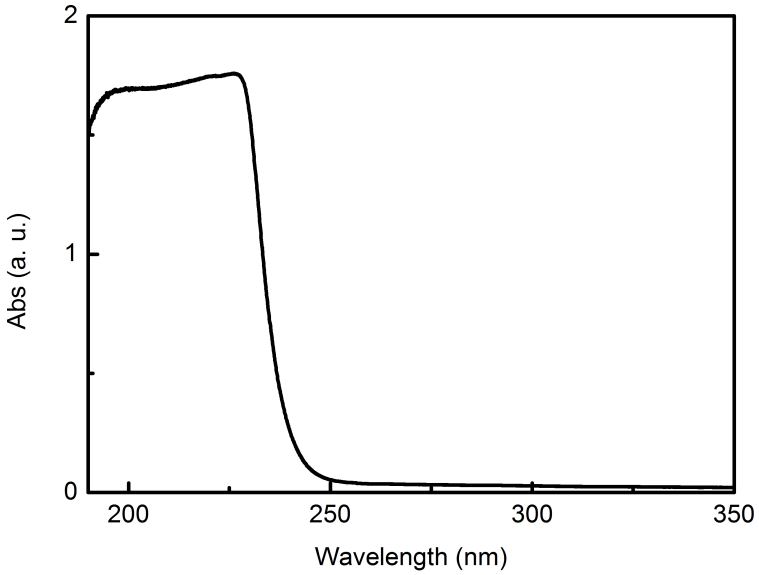

Figure 4.23: UV-Vis spectrum 10^{-6} M TSC solution

We decided to investigate its possble impact on polyynes stability performing two series of experiments in water using three concentrations each time, which were 10^{-1}, 10^{-3} and 10^{-6} M. In one case the TSC dissolution was made before the laser ablation while in the other it was performed after it. To check the solutions we were forced to use HPLC because in the UV-Vis spectrum the TSC absorption peak covers most of the polyynes signal (as can be seen in Fig. 4.23).

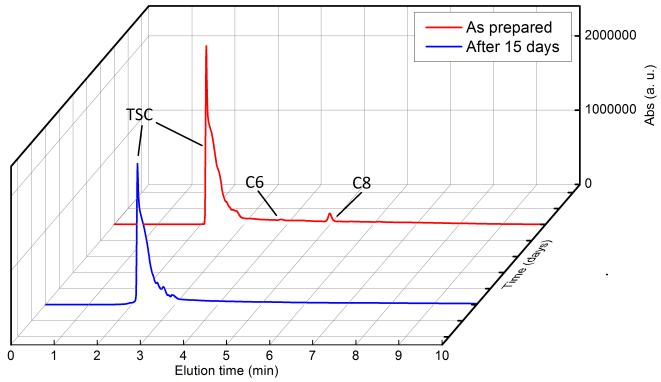

(a)

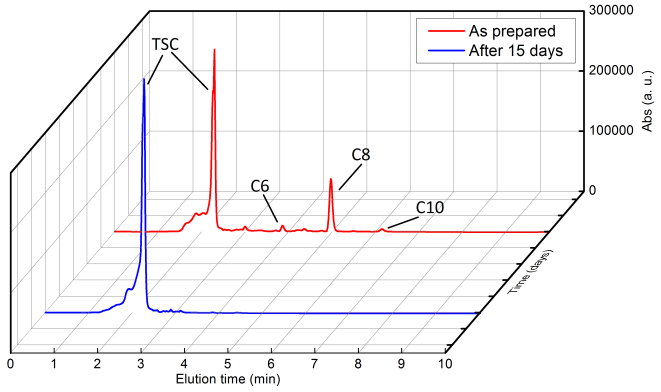

(b)

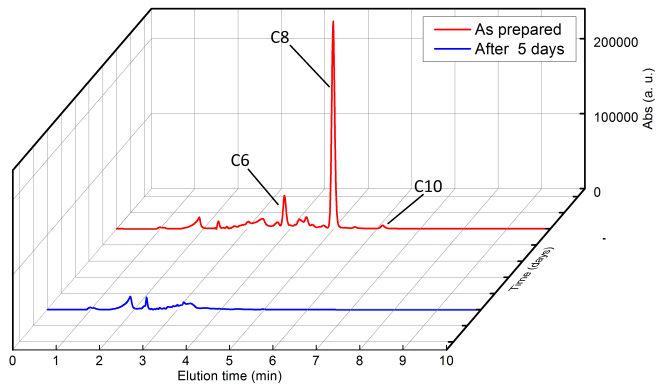

(c)

Figure 4.24: Chromatogram taken at 225 nm of polyynes solutions with TSC dissolved before the synthesis. In the figures are reported the results for, respectively, the case of 10^{-1} (a), 10^{-3} (b) and 10^{-6} M (c)

Considering first the case of TSC dissolution before PLAL, the chromatograms of the as prepared solutions for all the concentrations and after 15 days are shown in Fig. 4.24. In the case of 10^{-6} M, we decided to check the solution after just 5 days, instead of after 15 days, because of the very low TSC concentration. As can be seen in the chromatograms, there is no impact of TSC on polyynes stability, independently on the surfactant concentration used. In each cases, in fact, no peaks related to carbon chains are visbile after 15 days (or after 5 as in the 10^{-6} M solution). Because the surfactant was dissolved before the laser ablation, we may suppose that it could be dissociated or degraded by the laser. However, this is not the case, due to the fact that the TSC peak is present in the chromatogram, which means that the surfactant is still present in solution. The possible explanation can be either relative to the surfactant itself or to the fact that to be effective we must add it once the polyynes have been already synthesized. In order to test the latter hypothesis, we decided to perform another experiment in which the TSC concentrations were the same of the first study, but its addition to the polyynes mixture was made after the PLAL process.

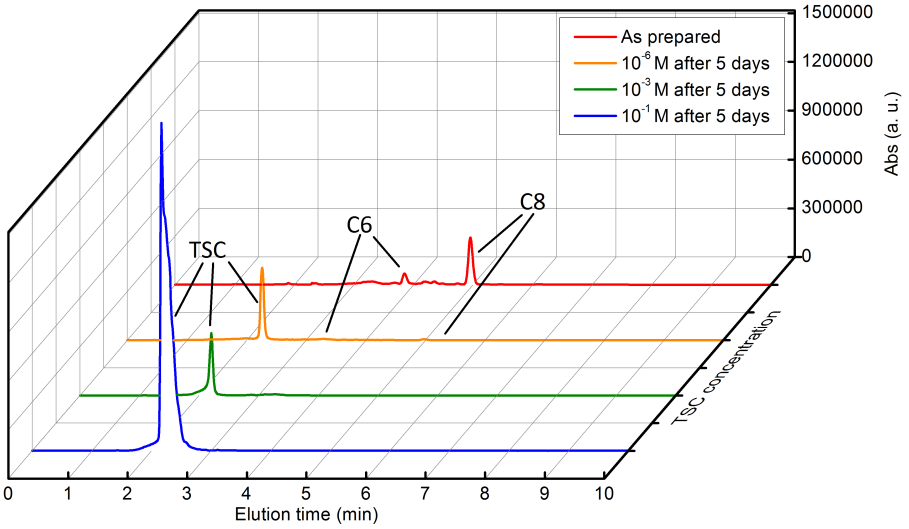

Figure 4.25: Chromatograms of polyynes mixture as prepared and after 5 days with three different TSC addition performed after PLAL

Therefore, we performed a laser ablation in liquid and then from the obtained polyynes mixture we prepared three samples to which add the surfactant at different concentrations (as can be seen in Fig. 4.25). After 5 days from the synthesis we checked the solutions and found a situation similar to the previous study, so TSC seems not to have an effect on

polyynes stability. Although, it was possible to detect polyynes peaks in the 10^{-6} M solution chromatogram (the ones related to C6 and C8), their concentration dropped over time while our aim was to keep the concentration constant over time. There are two possible explanations for these results. The first is that TSC, which is an ionic surfactant, is not suitable to improve polyynes stability due to the interaction it exploits to stabilize nanomaterials. The second hypothesis is that surfactants in general cannot enhance carbon chains stability. Indeed, they work with nanoparticles or carbon nanotubes because their size is significantly bigger than the surfactant one. So surfactants are able to adsorb on their surface and keep separate the nanomaterials avoiding their aggregation. In the case of polyynes, however, surfactants and carbon chains have almost the same size, so it is more difficult that the mechanism described above can work. However, we do not exclude that a different surfactant, maybe a non-ionic one, may provide a stability improvement to polyynes.

4.2.3 Solvent

The last factor studied to improve polyynes stability is the type of solvent in which the chains are dissolved in. We considered for this investigation all the solvents we have used to study the effect of different solvents on polyynes synthesis via PLAL (i.e. water, MeOH, EtOH, IPA, ACN). The reason behind the choice of investigating the impact of the solvent on polyynes stability is not just to find a solvent in which polyynes are more stable (because, anyway, in the solvents we studied polyynes degrade) but also to better understand the degradation of polyynes and which chemical environment is more favourable for their stability. We will first discuss the case of water and then we will focus on the organic solvents. Note that all the graphs reported were made using the same procedure used for building the graphs presented in the paragraph about temperature effect on stability (we considered chromatographic peaks area as quantitative index of of the presence of each species). In Fig. 4.26, it is reported the temporal evolution of polyynes concentration in water. As can be deduced looking at the graph, polyynes stability in water is quite low. In fact, after just 18 days there are no polyynes detected by our HPLC apparatus. It is interesting to underline that the only species capable to be present after 9 days are only C6 and C8, while C10 and C12 at that time were already degraded. In adddition, methyl-capped polyynes, present in very small concentration in water already after the synthesis, degrade much faster and there are no traces of them after just 9 days. This means that CH_3-capped polyynes in water are less stable than their respective H-terminated.

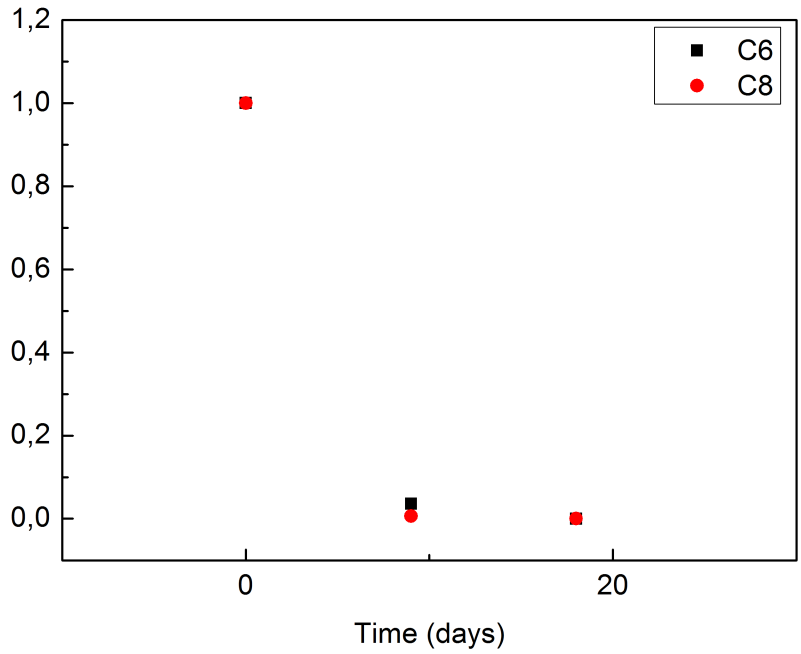

Figure 4.26: Polyynes stability in water. C10, C12 and methyl-capped polyynes degraded before the first check at 9 days from the synthesis

As preliminary study on the possible effectiveness of organic solvents on polyynes stability, we divided a polyynes solution in water into two samples: in one we added 200 μL of ACN to 1 mL of solution (which means that the final ACN concentration was 20% in volume), while in the other half we added the same volume of water. In this way the volume of the two samples was the same, which means that also their concentrations were the same. The solutions were checked after one week with UV-Vis spectroscopy and the results are displayed in Fig. 4.27. As can be easily observed, polyynes in the aqueous solution with acetonitrile were more stable than in pure water although the chains degradation seems to be unavoidable also in those conditions. This empirical observation is the reason for which we decided to investigate more deeply polyynes stability in other solvents.
Considering water as the reference, we wanted to improve this result and try to find a solvent able to provide a better stability to polyynes than water. Consequently, we started from some alcohols, i.e. methanol, ethanol and isopropanol. The results at 18 days after the synthesis are shown in Fig. 4.28.
It is quite clear that ethanol is the worst solvent, among the ones proposed, for the stabilization of polyynes in liquid. The concentrations of all the chains in that solvent shows a drop after 9 days and then a more

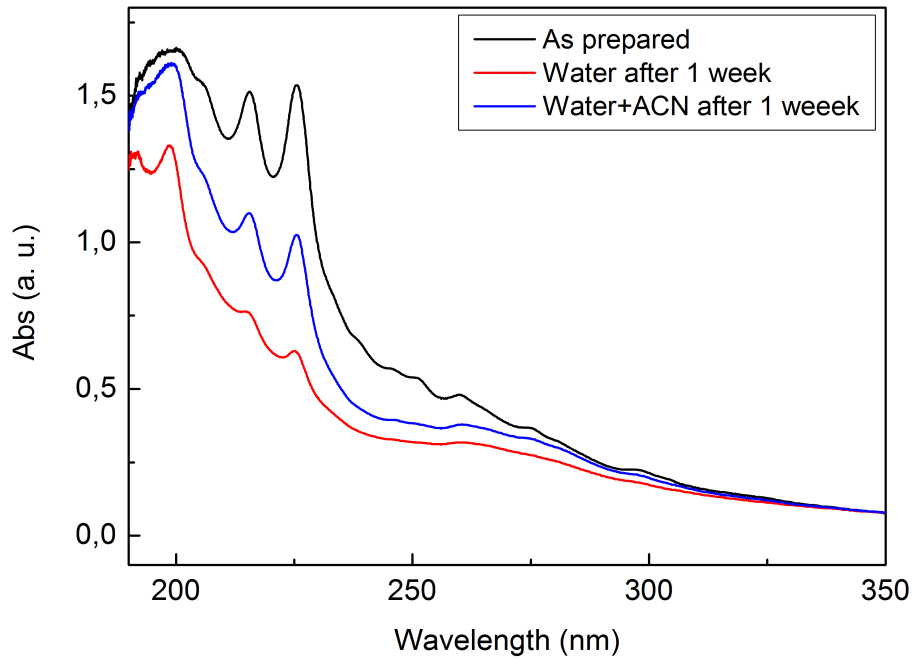

Figure 4.27: Comparison polyynes stability in water and in aqueous solution of ACN

slow degradation. It may be due to the fact that chains can interact among themselves, leading to a degradation by crosslinking. This can be favoured by a lower solubility of polyynes in ethanol, that results in their precipitation and degradation. Once the chains concentration is small enough, the degradation rate decreases because crosslinking effect becomes less important. This hypothesis, not confirmed by any evidence, requires also that the polyynes solubility should be different according to their length, due to the different degradation trends showed by chains with different length. Instead, polyynes in methanol and isopropanol show a much higher stability, as reported in the graph. A proof of this is that in methanol we are to detect polyynes up to C14 after 90 days from the ablation, while in IPA C16 was still present after the same amount of time. In ethanol, instead, all the chains were degraded after just 30 days. Methyl-capped polyynes are, in general, less stable than the H-capped ones and their concentrations in methanol display the same irregular trends they show in IPA. As, already discussed, this is probably due to the modifications of the chromaographic peaks over time. In methanol and isopropanol, these oscillations in the concentrations regard also some H-capped chains, as showed in Fig. 4.28. Another solvent, whose effect we wanted to investigate, was acetonitrile, mainly because we were interested

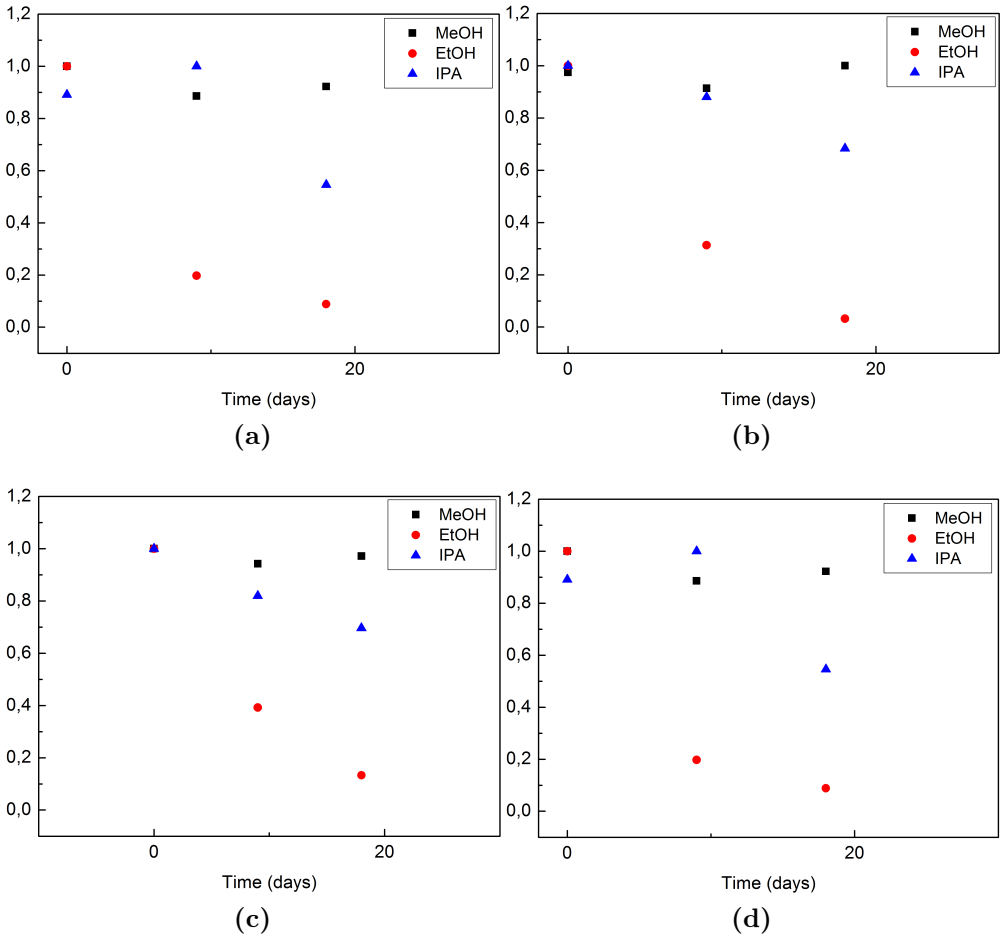

Figure 4.28: Comparison chromatographic peaks area trend over time of C6 (a), C8 (b), C10 (c), and C12 (d) in methanol, ethanol and isopropanol

in studying the stability of cyanopolyynes. Thise type of polyynes was formed only with this solvent (among the ones we used) so we perform a stability study similar to the ones conducted with water and alcohols. In Fig. 4.29, the trends over time of C6, C8, C10 and C12 concentrations in ACN are showed. As can be seen the degradation of carbon chains in this solvent is much slower with respect to the case of alcohols.
However, considering the results after 90 days (as we did for the alcohols case) the longer chain we were able to detect is C14, while in the case of IPA after the same time from the ablation we can still find C16. This may be due either to different properties of the solvents (although we did not succeed in individuating the property responsible for this behaviour) or to

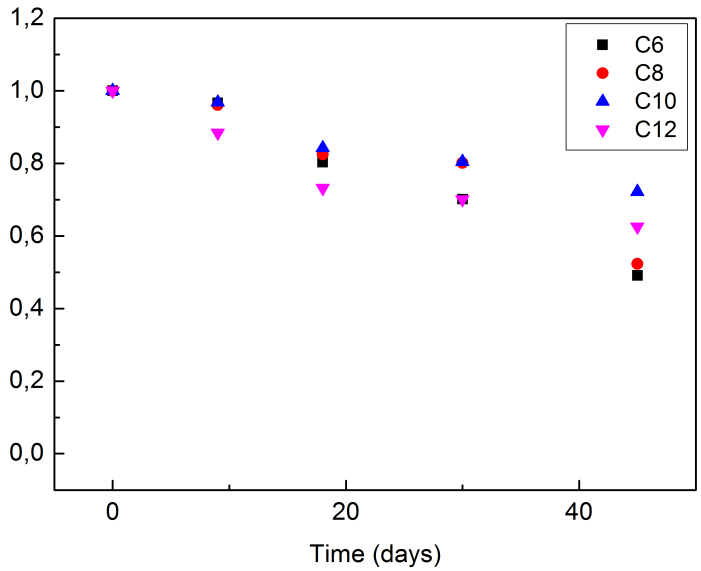

Figure 4.29: Stability of some selected polyynes in ACN

a partial evaporation of ACN (due to an inaccurate storage), which could have affected the results of our stability study. Considering the cyano and methyl-capped polyynes (whose concentration trend over time is displayed in Fig. 4.30), we can easily notice that cyanopolynes are species that degrade with the highest rate. Indeed, after 45 days there are no more traces of these compounds. Methylpolyynes, instead, are more resistant to degradation and in fact it is possible to detect methyl-capped chains up to $C14CH_3$ 90 days after the synthesis (as comparison, in methanol it was possible to detect $C12CH_3$ after the same time interval from the laser ablation).

Due to the results of the stability studies of IPA and ACN, we decided to perform another investigation mixing the two solvents, with a 1:1 volume ratio. Thus, we should be able to improve the stability of the chains, especially of the cyano-capped ones. However, the result of the solvent mixing is, opposite to our expectations, a decrease in the chains stability. In fact, as can be noticed in Fig 4.31, the rate of degradation is higher in the mixing than in the two pure solvents and this is true for all the chains, independently on their length or terminations. In particular, the most detrimental effect of the mixing is on the cyanopolyynes. Indeed, they degraded even before the first check performed after 9 days from their synthesis. Methyl-capped polyynes are negatively affected too. An evidence is the observation that at 90 days after the ablation is $C14CH_3$. Among the H-capped chains, instead, the longer chains detectable after

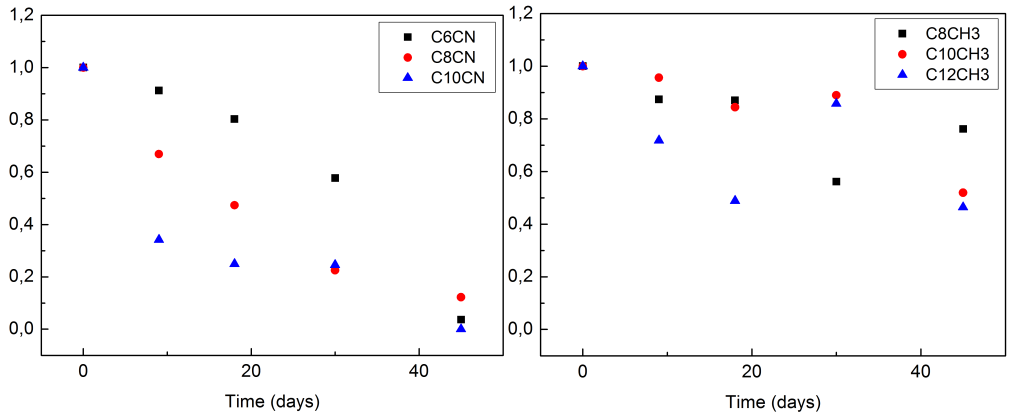

(a) (b)

Figure 4.30: Comparison chromatographic peaks area trend over time of cyanopolyynes (a) and methyl-capped polyynes in ACN

the same amount of time is C12. A possible explanation for this result are the interactions of polyynes with the different solvents and their dfferent solubilities. However, we are not able to formulate a more precise supposition.

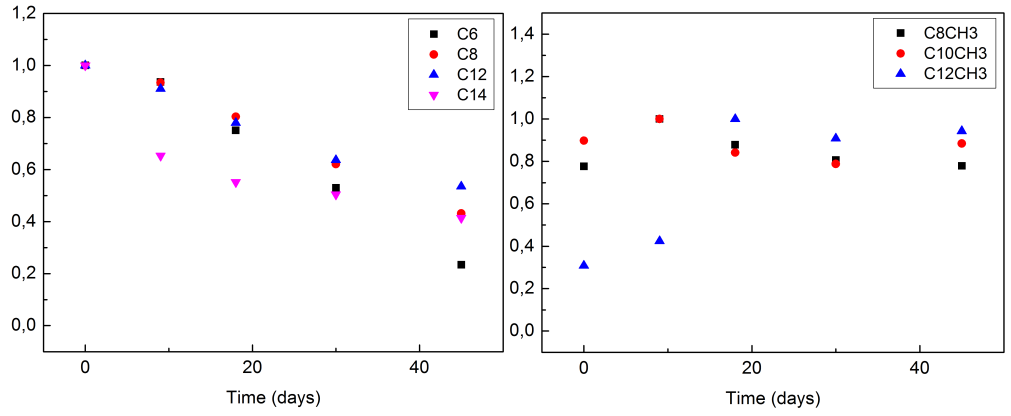

(a) (b)

Figure 4.31: Comparison chromatographic peaks area trend over time of H-capped (a) and methylpolyynes (b) in ACN-IPA mixing

We investigated the role of the solvent in the stability of polyynes. The obtained results showed that organic solvents improve their stability, if pure solvents are used. Although the long-time studies we have performed, which were never done before in any work in literature (to our knowledge

at least), there are still a lot of aspects of polyynes degradation that are not fully understood. Therefore further investigations are needed to clarify them.

Chapter 5

Conclusions and future perspectives

This thesis had two aims, the optimization of the PLAL process for the synthesis of polyynes and the study about the chains stability under different environmental conditions. Regarding the optimization of the synthesis process, we showed that is possible to improve the polyynes production by PLAL by uning accurately the laser ablation parameters. In particular, our results demonstrate that we could obtain higher concentrations using either a lower solvent volume or appropriate laser fluences and ablation times. It should be underlined that a further reduction of the solvent volume or a too high increase in the ablation time or in the laser fluence enhance the degradation of polyynes during their synthesis. Also the use of organic solvents allowed us to achieve higher polyynes concentrations, due to the laser induced dissociation of the solvent molecules that can provide additional carbon atoms for the chains growth. Moreover, the employment of organic solvents made us able to synthesize C22, whose formation was never reported in literature using the same solvents we employed for our experiments and a bulk graphite target. When organic solvents were used, it was also possible to detect methyl-capped polyynes and two species that we believe to be polyynes of that type, namely $C6CH_3$ and $C18CH_3$. This hypothesis is supported by the UV-Vis spectrum of the species, although it was not possible to collect and analyse them by SERS, because they were present in a very low concentrations. Other interesting results were the detection of methyl-capped polyynes after PLAL in water, whose presence was never indicated in other works. When acetonitrile was used, it was possible to detect the presence of cyano-polyynes up C12CN, confirming the results of other works. The achieving of all these results was possible due to our better understanding on how the PLAL process

works and on the critical issues regarding polyynes synthesis through this technique. Therefore, we can infer that we succeeded in optimizing the laser ablation process for the synthesis of the carbon chains. Although this, the comprehension of several aspects of laser ablation for polyynes production is still missing. For instance, other studies must be carried out to better understand the effect of the ablation time on the polyynes formation and a possible interconnection between this parameter and the laser fluence. Another open question regards the effect of the laser wavelength on polyynes synthesis, which is an aspect that we completely left apart but it has for sure deep consequences on the PLAL process. These issues and many others, such as the use of other solvents as medium in which perform the laser ablation, need to be investigated in order to exploit the PLAL technique in the best way.
However, the synthesis of polyynes was only part of our work. The other part of this thesis was aimed to the investigation of polyynes stability over time in different conditions. In particular, we conducted a first study on the effect of a decrease of the storage temperature. The results of this investigation show that decreasing the storage temperature slows down the degradation rate, although it is not sufficient to completely stop the degradation, at least at the temperatures we considered. So, in a future study the storage temperature may be decreased even further noting that, if freezing occurs, polyynes degradation is sped up (as we showed in the case of the water sample kept at -13 °C), probably because of the high temperature gradient during the melting phase (we need a liquid solution to perform the analysis after a certain time interval). We also demonstrate that the addition of a surfactant (TSC) has no impact on the degradation rate of polyynes. However, we suggest that other investigations should be done in order to clarify if other types of surfactant can have some positive effects on the carbon chains stability. The last factor considered for our stability studies was the solvent in which the chains were dissolved in. In particular, we found that organic solvents improve the polyynes stability. In fact, it was possible to detect polyynes signals even after 90 days from the synthesis. We also found out that the most stable chains are the one terminated by hydrogen atoms, while the ones with the lowest stability were the cyanopolyynes. Methyl-capped chains show an intermediate behaviour. The solvents that provided the highest stability were acetonitrile and isopropanol. If further studies will be done in future, we suggest to check the solutions after smaller time interval, especially at the beginning of the study. In this way, it should be possible to observe more in detail the degradation of polyynes and maybe find out which compounds are formed by their degradation. Anyway, the most desirable achievement remains

the synthesis, through a PLAL process, of stable polyynes (e.g. chains with stabilizing end groups such as phenyl groups). Although we were not able to completely avoid the degradation of the chains, we succeeded in achieving a higher stability of polyynes in many different environmental conditons, which is not a trivial result.

Bibliography

[1] Salisu Nasir et al. 'Carbon-based nanomaterials/allotropes: A glimpse of their synthesis, properties and some applications'. In: *Materials* 11.2 (2018), p. 295.

[2] Peter William Atkins, Julio De Paula, and James Keeler. *Atkins' physical chemistry*. Oxford university press, 2018.

[3] Fanghao Hu et al. 'Supermultiplexed optical imaging and barcoding with engineered polyynes'. In: *Nature methods* 15.3 (2018), p. 194.

[4] Franco Cataldo. *Polyynes: synthesis, properties, and applications*. CRC Press, 2005.

[5] Donald R Askeland and Pradeep P Phule. *The science and engineering of materials*. Springer, 2003.

[6] HO Pierson. 'Handbook of carbon, graphite, diamond and fullerenes. Properties, processing and applications, 1993'. In: *NY: William Andrew Publishing/Noyes* ().

[7] Peter Atkins and Tina Overton. *Shriver and Atkins' inorganic chemistry*. Oxford University Press, USA, 2010.

[8] Harold W Kroto et al. 'C60: Buckminsterfullerene'. In: *nature* 318.6042 (1985), pp. 162–163.

[9] Sumio Iijima. 'Helical microtubules of graphitic carbon'. In: *nature* 354.6348 (1991), p. 56.

[10] LV Radushkevich and VM Lukyanovich. 'About the structure of carbon formed by thermal decomposition of carbon monoxide on iron substrate'. In: *J. Phys. Chem.(Moscow)* 26 (1952), pp. 88–95.

[11] Kostya S Novoselov et al. 'Electric field effect in atomically thin carbon films'. In: *science* 306.5696 (2004), pp. 666–669.

[12] Philip Richard Wallace. 'The band theory of graphite'. In: *Physical Review* 71.9 (1947), p. 622.

[13] Andreas Hirsch. 'The era of carbon allotropes'. In: *Nature materials* 9.11 (2010), p. 868.

[14] Zaheen Ullah Khan, Ayesha Kausar, and Hidayat Ullah. 'A review on composite papers of graphene oxide, carbon nanotube, polymer/GO, and polymer/CNT: Processing strategies, properties, and relevance'. In: *Polymer-Plastics Technology and Engineering* 55.6 (2016), pp. 559–581.

[15] Somaia Said Abd El-Karim, Magdy Ibrahim El-Zahar, and Manal Mohamed Anwar. 'Nanotechnology in Cancer Diagnosis and Treatment'. In: *Journal of Pharmacy and Pharmacology* 3 (2015), pp. 299–315.

[16] Seunghun Hong and Sung Myung. 'Nanotube Electronics: A flexible approach to mobility'. In: *Nature nanotechnology* 2.4 (2007), p. 207.

[17] Prabhakar R Bandaru. 'Electrical properties and applications of carbon nanotube structures'. In: *Journal of nanoscience and nanotechnology* 7.4-5 (2007), pp. 1239–1267.

[18] Pradeep P Shanbogh and Nalini G Sundaram. 'Fullerenes revisited'. In: *Resonance* 20.2 (2015), pp. 123–135.

[19] Sun Kwok. 'Organic matter in space: from star dust to the Solar System'. In: *Astrophysics and Space Science* 319.1 (2009), pp. 5–21.

[20] Aleksei Mikhailovich Sladkov and Yu P Kudryavtsev. 'Polyynes'. In: *Russian Chemical Reviews* 32 (1963), pp. 229–243.

[21] Carlo Spartaco Casari et al. 'Carbon-atom wires: 1-D systems with tunable properties'. In: *Nanoscale* 8.8 (2016), pp. 4414–4435.

[22] Franco Cataldo et al. 'Simple synthesis of α, ω-diarylpolyynes part 1: Diphenylpolyynes'. In: *Journal of Macromolecular Science, Part A: Pure and Applied Chemistry* 47.8 (2010), pp. 739–746.

[23] Tomonari Wakabayashi et al. 'Isotope scrambling in the formation of cyanopolyynes by laser ablation of carbon particles in liquid acetonitrile'. In: *Carbon* 50.1 (2012), pp. 47–56.

[24] Andreea Spantulescu et al. 'Synthesis and characterization of cyclic alkyl tetraynes'. In: *Organic letters* 10.4 (2008), pp. 609–612.

[25] Carlo S Casari and Alberto Milani. 'Carbyne: from the elusive allotrope to stable carbon atom wires'. In: *MRS Communications* 8.2 (2018), pp. 207–219.

[26] Franco Cataldo. 'Stability of polyynes in air and their degradation by ozonolysis'. In: *polymer degradation and stability* 91.2 (2006), pp. 317–323.

[27] Franco Cataldo. 'Polyynes production in a solvent-submerged electric arc between graphite electrodes. III. chemical reactivity and stability toward air, ozone, and light'. In: *Fullerenes, Nanotubes and Carbon Nanostructures* 12.3 (2004), pp. 633–646.

[28] Franco Cataldo. 'Polyynes from Submerged Electric Arc. IV. Hydrogenation to Ene–Ynes'. In: (2004).

[29] Franco Cataldo. 'Storage stability of polyynes and cyanopolyynes in solution and the effect of ammonia or hydrochloric acid'. In: *Fullerenes, Nanotubes, and Carbon Nanostructures* 15.3 (2007), pp. 155–166.

[30] Seung-Keun Shin and Seung-Min Park. 'Preparation of polyynes by the laser ablation of graphite in water and organic solvents'. In: *Bulletin of the Korean Chemical Society* 33.2 (2012), pp. 597–600.

[31] Ryutaro Matsutani et al. 'Preparation of polyynes up to C22H2 by liquid-phase laser ablation and their immobilization into SiO2 gel'. In: *Carbon* 47.7 (2009), pp. 1659–1663.

[32] Kang An et al. 'Stability improvement of C8H2 and C10H2 embedded in poly (vinyl alcohol) films with adsorption on gold nanoparticles'. In: *Chemical Physics Letters* 637 (2015), pp. 71–76.

[33] Lei Shi et al. 'Confined linear carbon chains as a route to bulk carbyne'. In: *Nature materials* 15.6 (2016), p. 634.

[34] Roberto Pilot et al. 'A review on surface-enhanced Raman scattering'. In: *Biosensors* 9.2 (2019), p. 57.

[35] Hiroshi Tabata et al. 'Raman and surface-enhanced Raman scattering of a series of size-separated polyynes'. In: *Carbon* 44.15 (2006), pp. 3168–3176.

[36] Lloyd R Snyder, Joseph J Kirkland, and John W Dolan. *Introduction to modern liquid chromatography*. John Wiley & Sons, 2011.

[37] Franco Cataldo et al. 'One-pot synthesis and characterization of polyynes end-capped by biphenyl groups (α, ω-biphenylpolyynes)'. In: *Carbon* 126 (2018), pp. 232–240.

[38] Franco Cataldo et al. 'Synthesis, characterization, and modeling of naphthyl-terminated sp carbon chains: dinaphthylpolyynes'. In: *The Journal of Physical Chemistry B* 114.46 (2010), pp. 14834–14841.

[39] Wesley A Chalifoux and Rik R Tykwinski. 'Synthesis of extended polyynes: Toward carbyne'. In: *Comptes Rendus Chimie* 12.3-4 (2009), pp. 341–358.

[40] Wesley A Chalifoux and Rik R Tykwinski. 'Synthesis of polyynes to model the sp-carbon allotrope carbyne'. In: *Nature chemistry* 2.11 (2010), p. 967.

[41] Amir Hossein Sari, Arezoo Khazali, and Sara Sadat Parhizgar. 'Synthesis and characterization of long-CNTs by electrical arc discharge in deionized water and NaCl solution'. In: *International Nano Letters* 8.1 (2018), pp. 19–23.

[42] Hongkun Huang and Jiancheng Lai. 'Mechanism study of nanomaterial synthesis by pulsed laser ablation in liquid'. In: *Advanced Laser Processing and Manufacturing II*. Vol. 10813. International Society for Optics and Photonics. 2018, p. 1081318.

[43] Franco Cataldo. 'Synthesis of polyynes with electric arc Part 5: Detection of PAHs as minor products'. In: *Fullerenes, Nanotubes and Carbon Nanostructures* 13.1 (2005), pp. 21–30.

[44] Howard M Smith and AF Turner. 'Vacuum deposited thin films using a ruby laser'. In: *Applied Optics* 4.1 (1965), pp. 147–148.

[45] PP Patil et al. 'Pulsed-laser–induced reactive quenching at liquid-solid interface: Aqueous oxidation of iron'. In: *Physical review letters* 58.3 (1987), p. 238.

[46] Fumitaka Mafuné et al. 'Structure and stability of silver nanoparticles in aqueous solution produced by laser ablation'. In: *The Journal of Physical Chemistry B* 104.35 (2000), pp. 8333–8337.

[47] Changxin Chen, Wenzhe Chen, and Yafei Zhang. 'Synthesis of carbon nano-tubes by pulsed laser ablation at normal pressure in metal nanosol'. In: *Physica E: Low-dimensional Systems and Nanostructures* 28.2 (2005), pp. 121–127.

[48] Vincenzo Amendola and Moreno Meneghetti. 'What controls the composition and the structure of nanomaterials generated by laser ablation in liquid solution?' In: *Physical Chemistry Chemical Physics* 15.9 (2013), pp. 3027–3046.

[49] Danny Perez et al. 'Numerical study of the thermal ablation of wet solids by ultrashort laser pulses'. In: *Physical Review B* 77.1 (2008), p. 014108.

[50] R Fabbro et al. 'Physical study of laser-produced plasma in confined geometry'. In: *Journal of applied physics* 68.2 (1990), pp. 775–784.

[51] Carsten Momma et al. 'Short-pulse laser ablation of solid targets'. In: *Optics communications* 129.1-2 (1996), pp. 134–142.

[52] Daniel Werner et al. 'Femtosecond laser-induced size reduction of aqueous gold nanoparticles: In situ and pump- probe spectroscopy investigations revealing Coulomb explosion'. In: *The Journal of Physical Chemistry C* 115.17 (2011), pp. 8503–8512.

[53] Tetsuo Sakka et al. 'Laser ablation at the solid-liquid interface: transient absorption of continuous spectral emission by ablated aluminium atoms'. In: *Journal of Physics D: Applied Physics* 35.1 (2001), p. 65.

[54] Zijie Yan and Douglas B Chrisey. 'Pulsed laser ablation in liquid for micro-/nanostructure generation'. In: *Journal of Photochemistry and Photobiology C: Photochemistry Reviews* 13.3 (2012), pp. 204–223.

[55] Takeshi Tsuji et al. 'Microsecond-resolved imaging of laser ablation at solid–liquid interface: investigation of formation process of nano-size metal colloids'. In: *Applied surface science* 229.1-4 (2004), pp. 365–371.

[56] Tatiana E Itina. 'On nanoparticle formation by laser ablation in liquids'. In: *The Journal of Physical Chemistry C* 115.12 (2010), pp. 5044–5048.

[57] W Lauterborn et al. 'Experimental and theoretical bubble dynamics'. In: *Advances in chemical physics* 110 (1999), pp. 295–380.

[58] Vincenzo Amendola and Moreno Meneghetti. 'Laser ablation synthesis in solution and size manipulation of noble metal nanoparticles'. In: *Physical chemistry chemical physics* 11.20 (2009), pp. 3805–3821.

[59] William T Nichols, Takeshi Sasaki, and Naoto Koshizaki. 'Laser ablation of a platinum target in water. II. Ablation rate and nanoparticle size distributions'. In: *Journal of Applied Physics* 100.11 (2006), p. 114911.

[60] Philipp Wagener et al. 'Pulsed laser ablation of zinc in tetrahydrofuran: Bypassing the cavitation bubble'. In: *The Journal of Physical Chemistry C* 114.17 (2010), pp. 7618–7625.

[61] Fumitaka Mafuné et al. 'Formation of gold nanoparticles by laser ablation in aqueous solution of surfactant'. In: *The Journal of Physical Chemistry B* 105.22 (2001), pp. 5114–5120.

[62] Guowei Yang. *Laser ablation in liquids: principles and applications in the preparation of nanomaterials*. CRC Press, 2012.

[63] Kamal Abderrafi et al. 'Silicon nanocrystals produced by nanosecond laser ablation in an organic liquid'. In: *The Journal of Physical Chemistry C* 115.12 (2011), pp. 5147–5151.

[64] D Amans et al. 'Synthesis of oxide nanoparticles by pulsed laser ablation in liquids containing a complexing molecule: impact on size distributions and prepared phases'. In: *The Journal of Physical Chemistry C* 115.12 (2011), pp. 5131–5139.

[65] Jianming Zhang et al. 'Preparation of PtAu alloy colloids by laser ablation in solution and their characterization'. In: *The Journal of Physical Chemistry C* 116.24 (2012), pp. 13413–13420.

[66] GW Yang. 'Laser ablation in liquids: Applications in the synthesis of nanocrystals'. In: *Progress in Materials Science* 52.4 (2007), pp. 648–698.

[67] Dongsik Kim, Bukuk Oh, and Ho Lee. 'Effect of liquid film on near-threshold laser ablation of a solid surface'. In: *Applied surface science* 222.1-4 (2004), pp. 138–147.

[68] Sergey V Starinskiy, Yuri G Shukhov, and Alexander V Bulgakov. 'Laser-induced damage thresholds of gold, silver and their alloys in air and water'. In: *Applied Surface Science* 396 (2017), pp. 1765–1774.

[69] JR Heath et al. 'The formation of long carbon chain molecules during laser vaporization of graphite'. In: *Journal of the American Chemical Society* 109.2 (1987), pp. 359–363.

[70] Akihiro Wakisaka et al. 'Growth of carbon clusters. The simplest process, 2C 1 C 2, observed via spectrometry and chemical reaction'. In: *Journal of the Chemical Society, Faraday Transactions* 89.7 (1993), pp. 1001–1005.

[71] Masaharu Tsuji et al. 'Formation of hydrogen-capped polyynes by laser ablation of graphite particles suspended in solution'. In: *Chemical physics letters* 355.1-2 (2002), pp. 101–108.

[72] AA Zaidi et al. 'Femtosecond laser irradiation of liquid alkanes: Mechanism of polyyne formation'. In: *Chemical Physics Letters* 723 (2019), pp. 151–154.

[73] Ryutaro Matsutani et al. 'Preparation of long-chain polyynes of C28H2 and C30H2 by liquid-phase laser ablation'. In: *Journal of Photochemistry and Photobiology A: Chemistry* 240 (2012), pp. 1–4.

[74] Kohei Inoue et al. 'Preparation of long-chain polyynes of C24H2 and C26H2 by liquid-phase laser ablation in decalin'. In: *Carbon* 48.14 (2010), pp. 4209–4211.

[75] Ali Ramadhan et al. 'Synthesis of hydrogen-and methyl-capped long-chain polyynes by intense ultrashort laser pulse irradiation of toluene'. In: *Carbon* 118 (2017), pp. 680–685.

[76] Young Eun Park, Seung Keun Shin, and Seung Min Park. 'The physical effects on the formation of polyynes by laser ablation'. In: *Chemical Physics Letters* 568 (2013), pp. 112–116.

[77] Ryutaro Matsutani et al. 'Wavelength dependence of polyyne preparation by liquid-phase laser ablation using pellet targets'. In: *Chemical Communications* 47.20 (2011), pp. 5840–5842.

[78] Young Eun Park, Seung Keun Shin, and Seung Min Park. 'Power Dependence on Formation of Polyynes by Laser Ablation in Water'. In: *Bulletin of the Korean Chemical Society* 34.4 (2013), pp. 1039–1042.

[79] A Santagata et al. 'Carbon-based nanostructures obtained in water by ultrashort laser pulses'. In: *The Journal of Physical Chemistry C* 115.12 (2011), pp. 5160–5164.

[80] Seung Keun Shin, Jae Kyu Song, and Seung Min Park. 'Preparation of polyynes by laser ablation of graphite in aqueous media'. In: *Applied Surface Science* 257.12 (2011), pp. 5156–5158.

[81] Junwei Zhao et al. 'Synthesis of polyynes by intense femtosecond laser irradiation of SWCNTs suspended in methanol'. In: *Chemical Physics Letters* 682 (2017), pp. 96–100.

[82] Hiroshi Tabata, Minoru Fujii, and Shinji Hayashi. 'Laser ablation of diamond nanoparticles suspended in solvent: synthesis of polyynes'. In: *Chemical physics letters* 395.1-3 (2004), pp. 138–142.

[83] Michal J Wesolowski et al. 'Synthesis of Polymer-like Hydrogenated Amorphous Carbon by fs-pulsed Laser Induced Plasma Processing of Solid Hexane'. In: *Plasma Processes and Polymers* 9.7 (2012), pp. 701–708.

[84] AA Zaidi et al. 'Femtosecond laser ablation of solid methane'. In: *International Journal of Mass Spectrometry* 376 (2015), pp. 32–34.

[85] Ryutaro Matsutani et al. 'Preparation of long-chain polyynes C18H2 and C20H2 by laser ablation of pellets of graphite and perylene derivative in liquid phase'. In: *Carbon* 7.46 (2008), pp. 1103–1106.

[86] Y Sato et al. 'Synthesis of polyyne molecules from hexane by irradiation of intense femtosecond laser pulses'. In: *Carbon* 48.5 (2010), pp. 1673–1676.

[87] A Hu et al. 'Direct synthesis of polyyne molecules in acetone by dissociation using femtosecond laser irradiation'. In: *Carbon* 46.13 (2008), pp. 1823–1825.

[88] MJ Wesolowski et al. 'Polyyne synthesis and amorphous carbon nano-particle formation by femtosecond irradiation of benzene'. In: *Carbon* 49.2 (2011), pp. 625–630.

[89] Giuseppe Compagnini et al. 'Short polyyne chains produced by pulsed laser ablation of graphite in water'. In: *Carbon* 12.45 (2007), pp. 2456–2458.

[90] Giuseppe Compagnini et al. 'Spectroscopic study of polyynes obtained by laser ablation in liquids'. In: *Journal of Raman Spectroscopy: An International Journal for Original Work in all Aspects of Raman Spectroscopy, Including Higher Order Processes, and also Brillouin and Rayleigh Scattering* 39.2 (2008), pp. 177–181.

[91] Ryutaro Matsutani et al. 'Preparation of polyynes by liquid-phase laser ablation using different irradiation target materials and solvents'. In: *Carbon* 49.1 (2011), pp. 77–81.

[92] Young-Eun Park, Seung-Keun Shin, and Seung-Min Park. 'The Solvent Effects on the Formation of Polyynes by Laser Ablation'. In: *Bulletin of the Korean Chemical Society* 33.7 (2012), pp. 2439–2442.

[93] Natalia R Arutyunyan et al. 'Resonant Effects in SERS Spectra of Linear Carbon Chains'. In: *physica status solidi (b)* 255.1 (2018), p. 1700254.

[94] Kenji Hanamura et al. 'Surface-enhanced Raman scattering of size-selected polyynes (C8H2) adsorbed on silver colloidal nanoparticles'. In: *Chemical Physics Letters* 503.1-3 (2011), pp. 118–123.

[95] G Forte et al. 'The effects of liquid environments on the optical properties of linear carbon chains prepared by laser ablation generated plasmas'. In: *Applied Surface Science* 272 (2013), pp. 76–81.

[96] Franco Cataldo. 'Polyynes: a new class of carbon allotropes. About the formation of dicyanopolyynes from an electric arc between graphite electrodes in liquid nitrogen'. In: *Polyhedron* 23.11 (2004), pp. 1889–1896.

[97] Ian Smallwood. *Handbook of organic solvent properties*. Butterworth-Heinemann, 2012.

[98] K Sasaki, T Wakasaki, and K Kadota. 'Observation of continuum optical emission from laser-ablation carbon plumes'. In: *Applied surface science* 197 (2002), pp. 197–201.